ISSN 0040-6090
Published fortnightly

Vol. 178
Supplement

thin solid films

International Journal on the Science and Technology of Condensed Matter Films

Cumulative Indexes Volumes 166–178

Editor-in-chief:
J. N. Zemel

Elsevier Sequoia

TYPES OF CONTRIBUTIONS

- —Original papers not previously published.
- —Review articles.
- —Letters, 600–800 words.
- —Announcements, reports on conferences, news.

EDITOR-IN-CHIEF

J. N. Zemel, Center for Sensor Technologies, University of Pennsylvania, Philadelphia, PA 19104, U.S.A.

EDITORIAL BOARD

C. J. Adkins (Cambridge)
L. N. Aleksandrov (Novosibirsk)
D. E. Aspnes (Red Bank, NJ)
P. B. Barna (Budapest)
M. H. Brodsky (Yorktown Heights, NY)
R. F. Bunshah (Los Angeles, CA)
G. Deutscher (Tel Aviv)
P. J. Dobson (Oxford)
R. Grigorovici (Bucharest)
F. M. d'Heurle (Yorktown Heights, NY)
A. Hugot-Le Goff (Paris)
A. Kinbara (Tokyo)
O. Knotek (Aachen)
V. Litovchenko (Kiev)
A. Lopez-Otero (Stanford, CA)
H. Lüth (Aachen)
J. W. Mayer (Ithaca, NY)
J. H. van der Merwe (Pretoria)
S. Nakahara (Murray Hill, NJ)
M.-A. Nicolet (Pasadena, CA)
B. E. Nieuwenhuys (Leiden)
G. Ottaviani (Modena)
A. K. Pal (Calcutta)
G. Rasigni (Marseille)
J. R. Sambles (Exeter)
W. Scharff (Karl-Marx-Stadt)
M. Sugi (Tsukuba)
K. Tada (Tokyo)
R. H. Tredgold (Lancaster)
R. W. Vook (Syracuse, NY)
H. H. Wieder (San Diego, CA)

FREQUENCY

Two issues a month, 12 volumes in 1990.

SUBSCRIPTION INFORMATION

Subscription price for 1990 (Vols. 179–190): Sfr. 3780.— (approx. US$2392.—) incl. postage.

Issues are sent by surface mail after air delivery to Argentina, Australia, Brazil, Canada, China, Hong Kong, India, Israel, Japan, Malaysia, Mexico, New Zealand, Pakistan, Singapore, South Africa, South Korea, Taiwan, Thailand and the U.S.A. Airmail rates for other countries are available on request.

Subscription orders should be addressed to
ELSEVIER SEQUOIA S.A., P.O. Box 564, 1001 Lausanne 1, Switzerland.
Tel. (21) 20 73 81, Telex 450620 ELSA CH, Telefax (21) 235 444.

U.S. and Canadian customers may obtain information from
ELSEVIER SCIENCE PUBLISHING CO. INC., Attn: Journal Information Center,
655 Avenue of the Americas, New York, NY 10010, U.S.A.
Tel. (212) 633 3750, Telex 420 643 AEP UI, Telefax (212) 633 3990.

This journal is cited by the following Abstracting and/or Indexing Services:

- Metals Abstracts
- Chemical Abstracts
- Physics Abstracts
- Current Contents—Physical and Chemical Sciences
- Current Contents—Engineering, Technology and Applied Sciences
- Engineering Index
- Cambridge Scientific Abstracts
- Physikalische Berichte
- Science Citation Index
- Automatic Subject Citation Alert
- PASCAL (Centre National de la Recherche Scientifique)
- FIZ Karlsruhe

Thin Solid Films, *178* (1990) 1–11

Cumulative Author Index for Volumes 166–178

The volume numbers are given in bold-face type preceding the page numbers.

A

Abe, T., **178**, 313
Abelson, J. R., **171**, 217
Aboelfotoh, M. O., **176**, 173
Acharya, B. S., **171**, 277
Adriaansen, A. P. M., **169**, 241
Afonso, C. N., **167**, 57
Agarwal, V., **169**, 281
Agrawal, A., **169**, 257
Ahlroth, R., **166**, 113
Al-Jaroudi, M. Y., **170**, 293
Albella, J. M., **167**, 95; **175**, 49
Albrecht, O., **178**, 93, 171, 563
Aleksandrov, L. N., **171**, 235
Alexander, G. A., **177**, 95
Alexopoulos, P., **166**, 299
Almeida, J. B., **176**, 219
Alnot, P., **170**, 259
Anand, V., **166**, 163
Ance, C., **173**, 155
Ancelin, H., **176**, 151
Anderson, R. J., **166**, 345
Ando, E., **178**, 103
Araki, H., **169**, 187
Ariga, K., **178**, 465
Arisawa, S., **178**, 347
Armgarth, M., **177**, 77
Arnaud D'Avitaya, F., **174**, 285
Arndt, Th., **178**, 319
Asbury, D. A., **169**, 69
Ashok, S., **173**, L149
Atanassova, E., **169**, 43
Atilgan, I., **167**, 129
Atkinson, R., **173**, 175
Atmani, H., **177**, 239
Augelli, V., **170**, 163
van der Auweraer, M., **169**, 127
Azuma, M., **178**, 137, 165, 477

B

Baba, S., **167**, 299; **171**, 93
Baba, Y., **171**, 263
Bachmann, G., **174**, 149
Badoz, P. A., **174**, 285
Baklanov, M. R., **171**, 43
Balakrishnan, S., **166**, 121
Balandin, V. Yu, **171**, 235
Balk, P., **174**, 1
Ball, R. K., **176**, 55
Balland, B., **167**, 45
Bange, K., **175**, 185
Banno, T., **167**, 299
Baptista, G. B., **167**, 245
Barbottin, G., **167**, 45
Barboux, P., **167**, 67
Barden, P. E., **167**, 169
Barimani, A., **174**, 51
Barjenbruch, U., **172**, 123
Barna, P. B., **167**, 203
Barnaś, J., **175**, 317
Barraud, A., **175**, 73; **178**, 387, 499
Barriere, A. S., **170**, 259; **173**, 243
de Barros, B. A. S., Jr., **170**, 285
Barros Leite, C. V., **167**, 245; **170**, 285
Barsan, N., **171**, 53
Barthwal, S. K., **169**, 229
Barua, A. K., **167**, 121
Baszyński, J., **175**, 295
Batabyal, A. K., **169**, 79; **170**, 211
Bather, K.-H., **177**, 315
Bauer, E., **170**, 241
Baumgartner, H., **173**, 269
Baumvol, I. J. R., **170**, 285
Bayreuther, G., **175**, 311, 341
Beames, D. A., **166**, 171
Beamson, G., **172**, 269
Becker, U., **175**, 179
Belford, R. E., **173**, 129
Belgacem, S., **167**, 217
Belkacem, I. Y., **168**, 21
Belkouch, S., **174**, 203
Belu-Marian, A., **167**, 1; **168**, 1
Benes, E., **174**, 307, 323
Bengtson, A., **170**, 293
Benkacem, M., **172**, L65
Benmalek, M., **174**, 25
Bensch, W., **174**, 143
Beranger, G., **174**, 111
Berenguer, M., **167**, 45
Berg, J. M., **176**, 157; **178**, 261
Berg, S., **172**, 133, 241
Berger, S., **176**, 131
Bergmann, H. W., **174**, 33
Bernard, C., **177**, 189
Bernede, J. C., **168**, 249
Bernstein, P., **175**, 305
Bertault, D., **173**, 243
Berthold, W., **174**, 149
Berus, T., **172**, 71; **174**, 245
Bewilogua, K., **167**, 233
Bhatnagar, Y. K., **168**, 345
Bhattacharyya, A. B., **168**, 291
Bhattacharyya, R., **176**, 79
Bi, L.-S., **173**, 77
Bibo, A. M., **178**, 81
Bielle-Daspet, D., **175**, 43
Biesmans, G., **169**, 127
Bijeon, J. L., **177**, 49
Binasch, G., **175**, 317
Binst, L., **170**, 41
Birjega, M. I., **171**, 33

0040-6090/90/$3.50

© Elsevier Sequoia/Printed in The Netherlands

Biryukov, S. V., **176**, 227
Bischoff, B., **166**, 387
Blanchard-Desce, M., **178**, 387
Blanquet, E., **177**, 189
Blech, I., **176**, 131
Blom, H.-O., **172**, 133, 241
Blumstein, A., **178**, 243
den Boer, M., **178**, 233
Boher, P., **174**, 91; **175**, 161
Bohm, C., **178**, 511
Bolse, W., **174**, 139
Bolwin, K., **174**, 85
Boncheva, Z., **169**, 169
Bonosi, F., **178**, 271
Boone, J. L., **176**, 143
Boragno, C., **175**, 103
Bordignon, M., **168**, 61
Borowski, P., **173**, 287; **177**, 333
Bosland, P., **166**, 309
Boslooper, E. C., **177**, 17
Bottcher, H., **170**, 249
Boucherit, N., **174**, 111
Bouillaud, P., **176**, L161
Bouillon, F., **170**, 41
Boukezzata, M., **175**, 43
Bouldin, D. P., **166**, 55
Boulesteix, C., **170**, 107
Boulmer, J., **175**, 109
Boultadakis, S., **169**, 87
Bourgoin, J. P., **178**, 499
Boutaoui, N., **172**, 141
Boutry-Forville, A., **169**, 315
Bowers, D. H., **169**, 143
Brand, J. I., **166**, 139
Brauers, A., **174**, 1
Bremer, T., **175**, 235
Brennan, W. J., **172**, 269
Bresnock, F. J., **166**, 69
Brieu, M., **167**, 149
Briggs, A., **174**, 285
Brodie, D. E., **176**, 13
van den Broek, J. J., **172**, 51
Brotzen, F. R., **166**, 291
Bruno, P., **175**, 341
Bubeck, C., **178**, 483
Buchner, R., **168**, 35
Buchta, R., **168**, 325
Bucur, R. V., **171**, 367
Budach, W., **178**, 61
Budin, J. P., **175**, 109
Bunshah, R. F., **172**, 111
Burte, E. P., **168**, 41; **172**, L101

C

Cade, N. A., **178**, 125
Cailler, M., **168**, 193
Calsou, R., **167**, 195
Campos, P., **171**, 109
Canali, C., **176**, 187
Cantwell, G., **176**, 143
Caprile, C., **172**, L85
Cárabe, J., **174**, 239
Carim, A. H., **176**, L177
Carl, A., **174**, 225
Carlsson, J.-O., **172**, 81, 95; **176**, 263
Carnera, A., **176**, 187
Carter, C. B., **170**, 49
Catalina, F., **167**, 57
Caune, S., **174**, 289
Celis, J. P., **173**, 199
Cerny, R., **170**, 201, L55
Chai, X. D., **178**, 221, 535
Chaki, T. K., **168**, 207
Chandorkar, A. N., **169**, 117
Chandrasekhar, S., **169**, 205
Chang, C.-A., **166**, 97
Chang, C. Y., **173**, 149
Chang, E., **172**, 185
Chang, S. F., **172**, 185
Chao, C. H., **172**, 185
Chao, H., **169**, 179
Chaplanov, A. M., **168**, 363
Chapple-Sokol, J. D., **171**, 291
Charai, A., **171**, 343
Chatfield, C., **168**, 325
Chatterjee, P., **169**, 79; **170**, 211
Chaudanson, H., **174**, 111
Chaudhari, S. M., **171**, 335; **176**, 197
Chaudhuri, S., **176**, L183
de Chelle, F., **173**, 155
Chen, H. J., **178**, 221, 535
Chen, J., **178**, 233, 341
Chi, S. D., **172**, L91
Chopra, K. L., **169**, 281
Choquet, C., **167**, 45
Christoforou, N., **176**, 13
Chroboczek, J., **174**, 285
Chu, H. C., **173**, 149
Chu, P., **166**, 155
Chun, J. S., **166**, 37, 367; **169**, 57
Chung, D. W., **166**, 131, 181
Chybicki, M., **167**, 13
Claassen, W. A. P., **168**, 89
Claesson, P. M., **176**, 157; **178**, 261
Clarisse, C., **170**, L51
Coburn, J. W., **171**, 65
Cocke, D. L., **167**, 245
Cocking, J. L., **166**, 201
Coelho, M. A. N., **178**, 227
Coleman, L. B., **178**, 227
Colligon, J. S., **170**, 127
Comelli, G., **170**, 309
Conrad, J. R., **175**, L153
de Cooman, B. C., **170**, 49
Coquerel, G., **177**, 239
Cord, B., **175**, 287
Cordroch, W., **178**, 53
Corelli, J. C., **166**, 121
Corts, Th., **174**, 139
Cot, L., **173**, 83
Couch, N. R., **168**, 151
Coulon, J. F., **176**, 289
Couturier, G., **173**, 243
Crasemann, J. H., **175**, 261
Cross, B. J., **166**, 263
Csanady, A., **167**, 203
Cumberbatch, T. J., **167**, 169
Cuomo, J. J., **171**, 143
Curlee, R. M., **166**, 45

D

D'Olieslaeger, M., **173**, 199
Dacheva, E., **169**, 173
Dachraoui, M., **167**, 217; **170**, 171
Dallaire, S., **166**, 249
Damodara, Das, V., **172**, 167
Danchot, J. P., **176**, L157
Daniels, R. D., **166**, 235
Danroc, J., **166**, 309
Danto, Y., **170**, 71
Das, S. K., **175**, 221
Dath, J. P., **176**, L157
Datta, P. K. **168**, 221
Dawsey, J. R., **167**, 161
De, S. C., **167**, 121
Débarre, D., **175**, 109
Decher, G., **178**, 445
Decoster, D., **172**, L59
Delabouglise, G., **174**, 263
Delafond, J., **176**, L161
Delcambe, P., **170**, 41
Deline, V., **166**, 131, 181
Dembowski, J., **174**, 33
Denatale, J. F., **168**, 185
Deneuville, A., **174**, 203
Desbat, B., **170**, 259
Deschanvres, J. L., **174**, 263; **175**, 281
Deschler, M., **174**, 315
Deshpandey, C., **172**, 111

Despax, B., **168**, 81
Despujols, J., **168**, 11
Dewald, A. B., **166**, 349
Dhanavantri, C., **169**, 271; **170**, 1
Dhathathreyan, A., **178**, 53
Dhez, P., **175**, 151
Dimitrov, D., **169**, 43
Dimmler, B., **174**, 79
Dinca, G., **167**, 1; **168**, 1
Dinh, T., **176**, 13
Dinhut, J. F., **176**, L161
Diociaiuti, M., **173**, 67
Dirks, A. G., **172**, 51
Dixit, P. N., **176**, 79
Dixon, A. G., **168**, 281
Dobiasova, L., **170**, 201
Dodd, R. A., **175**, L153
Dodelet, J. P., **166**, 249
Doerr, H. J., **172**, 111
Dong, S., **178**, 227
Donley, M. S., **168**, 335
Donlon, W. T., **168**, 263
Dos Santos, M. P., **176**, 219
Draper, B. L., **166**, 45
Dubowik, J., **174**, 45
Duch, M. W., **166**, 171
Dudde, R., **175**, 85
Dulog, L., **175**, 95
Dultsev, F. N., **171**, 43
Dumas, M., **172**, L65
Dumpich, G., **174**, 225
Dupree, R., **173**, 209
Duquette, D. J., **177**, 207
Durand, J., **173**, 83
Durrant, J., **167**, 169
Dussert, C., **177**, 245
Dvurechenskii, A. V., **171**, 235

E

Eastman, L. F., **170**, 49
Edlinger, J., **175**, 207
Eguchi, K., **178**, 505
Egusa, S., **178**, 137, 165
Eibisch, B., **171**, 157
Elich, J. J. Ph., **177**, 17
Emiliani, G., **171**, 243
Endo, H., **178**, 355
Endres, G., **174**, 179
Enquist, F., **177**, 77
Era, M., **173**, L135; **178**, 351, 541
Erokhin, V. V., **178**, 433
Evetts, J. E., **173**, L129; **174**, 165

F

Fan, J., **178**, 525
Fang, Y. K., **169**, 51; **173**, 149; **176**, 91
Fantini, F., **172**, L85
Farnan, I., **173**, 209
Fattahallah, G. H., **169**, 235
Fedorenko, A. I., **173**, 225
Felder, E., **172**, 227
Feng, X., **178**, 341
Fenske, F., **168**, 51
Ferraton, J. P., **173**, 155
Ferreira, M. I. C., **176**, 219
Feurer, R., **167**, 195
Fiedler, R., **167**, 281
Fincher, C. R., **166**, 171
Fineman, J. P., **166**, 55
Finstad, T. G., **171**, 343
Fischer, J. E., **177**, 263
Fiske, T. G., **178**, 227
Fleischauer, P. D., **172**, L81
Flick, W., **166**, 15, 29; **173**, 217
Flietner, H., **168**, 51
Floch, H. G., **175**, 173
Flory, F., **170**, 107
Flouttard, J. L., **168**, 81
Fölsch, S., **172**, 123
Forty, A. J., **173**, 209
Francombe, M. H., **168**, 307
Franz, G., **169**, 105
Frauenheim, T., **171**, 157
Freire, Jr., F. L., **170**, 285
Frese, V., **174**, 1
Fritz, T., **170**, 249
Frost, R. L., **166**, 349
Fujihira, M., **178**, 281
Fujii, H., **168**, 103
Fujimoto, K., **169**, 249; **173**, L139
Fujimura, N., **167**, 187
Fujioka, H., **177**, 295
Fujiwara, H., **169**, 289; **176**, 255
Fukada, N., **173**, 253
Fukao, K., **171**, 359
Fukuda, K., **178**, 355, 361, 421, 439, 549
Fukui, Y., **176**, 165
Furuno, T., **178**, 459
Füßer, H.-J., **174**, 39

G

Gäbler, D., **168**, L43; **176**, 25
Gabrielli, G., **178**, 271
Gale, R. J., **166**, 291
Galindo, H., **170**, 227
Galindo, R., **170**, 107
Garcia-Castañeda, M., **176**, 69
Garland, C., **166**, 15
Garrett, P., **172**, 251
Garshcke, A., **169**, 159
Gasgnier, M., **176**, 111
Gasparotto, A., **176**, 187
Gau, J.-S., **176**, 309
Gavrilova, T. A., **171**, 43
Gawne, D. T., **166**, 375
Gealer, C. A., **166**, 83
Gebauer, M., **175**, 61
Geddes, N. J., **167**, 261; **168**, 151
Gemma, N., **178**, 137, 165, 477
Gendry, M., **173**, 83
Gessner, Th., **177**, 225
Gevers, G., **173**, 243
Gheeraert, E., **174**, 203
Ghosh, S. K., **166**, 359
Gierłowski, P., **174**, 249
Giessen, B. C., **167**, 141
Gill, S. S., **167**, 161
Gillet, M., **167**, 149
Gillet, R., **166**, 309
Gilormini, P., **172**, 227
Ginnai, T., **178**, 171
Gładyszewski, G., **170**, 99
Gobel, R., **169**, 159
Goebel, H., **174**, 5
Gogol, C. A., **171**, 171
Göpel, W., **175**, 95
Gordon, R. G., **171**, 291; **177**, 141
Gorman, G., **166**, 131, 181
Gotoh, Y., **178**, 281
Goudonnet, J. P., **177**, 49
Gouy, J. P., **172**, L59
Grammatica, S., **177**, 253
Granqvist, C. G., **173**, L123
Grant, J. T., **168**, 335
Greene, J. E., **169**, 299
Grigoriadis, P., **169**, 87
Grigoriew, H., **172**, L75
Grigorovici, R., **171**, 53
Grill, A., **173**, L109
Groeschl, M., **174**, 323
Grogan, Jr., A. L., **169**, 69
Grossman, E., **173**, L109
Grozdanov, I., **173**, 53
Grun, M., **175**, 179
Grünberg, P., **175**, 317
Grundy, M. J., **172**, 269
Grundy, P. J., **167**, 141
Guan, K., **168**, 231
Gudmundsson, B., **173**, 99
Guegan, H., **170**, 259; **173**, 243

Gunter, J. R., **167**, 203
Guo, B. Z., **178**, 27
Gupta, C. K., **176**, 197
Gupta, L., **176**, 33
Gurtler, K., **175**, 185
Gutiérrez, M. T., **174**, 239, 295
Gutmann, R., **175**, 201
Gzowski, O., **167**, 67

H

Haas, T. W., **168**, 335
Haberger, K., **168**, 35
Habermeier, H.-U., **174**, 185; **175**, 95
Habibi, H., **169**, 257
Hahn, J., **170**, 249
Haitjema, H., **169**, 1; **177**, 17
Hajto, E., **173**, 129
Hamamoto, K., **177**, 161
Hamilton, J. C., **166**, 345
Hammer, K., **171**, 157
Hammond, A. A., **167**, 269
Han, C. C., **176**, 187
Hanawa, T., **169**, 187
Hansen, P., **175**, 261
Hantsche, H., **175**, 185
Hanus, F. D., **170**, 227
Haque, A., **176**, 13
Hara, K., **169**, 289; **176**, 255
Hara, T., **177**, 9
Harada, Y., **178**, 305
Hardtdegen, H., **174**, 1
Hardtke, C., **175**, 61
Harker, A. B., **168**, 185
Haroutyunian, S. L., **170**, 321
Haroutyunian, V. A., **170**, 321
Harpalani, H. B., **166**, 235
Harper, J. M. E., **171**, 81
Harrington, A., **178**, 171
Hårsta, A., **176**, 263
Hasegawa, I., **173**, 235
Hashimoto, M., **167**, 223
Hashimoto, T., **169**, 289; **176**, 255
Hatwar, T. K., **166**, 359
Häupl, K., **174**, 105
Hayakawa, K., **178**, 519
Hayashi, H., **178**, 305
Hayashida, H., **177**, 9
Heckl, W. M., **173**, 269
Heckmann, K., **175**, 81
Heiland, W., **175**, 235
Heinitz, H.-J., **167**, 233
Heinrich, H., **171**, 271; **175**, 179
Helle, H., **178**, 197
Helmersson, C., **177**, 77
Helmersson, U., **169**, 299
Hensel, B., **174**, 179
Hensel, E., **168**, 51
Hentzell, H. T. G., **170**, 293
Henzler, M., **172**, 123
Hermel, H., **173**, L119
Hertel, P., **175**, 235
Hesto, P., **175**, 23
d'Heurle, F. M., **171**, 81, 343
Hill, R., **168**, 221
Hilton, M. R., **167**, L31; **172**, L81
Hiltunen, L., **166**, 149
Hingerl, K., **175**, 179
Hirai, Y., **178**, 519
Hirasaka, M., **167**, 85
Hirose, Y., **176**, 165
Hisamoto, K., **177**, L187
Hishiro, Y., **178**, 281
Hoffman, D. W., **171**, 5
Hoffmann, H., **174**, 45, 99; **175**, 273, 325
Hoflund, G. B., **169**, 69
Hofmann, L., **174**, 5
Holguin, E., **174**, 229
Holloway, P. H., **177**, 95
Hong, K., **178**, 233
Horache, E., **177**, 263
Horiuchi, T., **171**, 359
Hostalek, M., **174**, 1
Hou, J.-G., **173**, 77
Houdy, P., **174**, 91; **175**, 161; **176**, L177
Houghton, D., **173**, 185
Hövel, R., **174**, 1
Howard, J., **172**, 269
Howard, S. A., **176**, 143
Hu, Q. Y., **168**, 231
Hua, Y., **178**, 525
Huang, T., **166**, 131, 181
Huber, R., **174**, 301
Hugot-Le Goff, A., **174**, 111
Hulliger, J., **175**, 201
Hultman, L., **169**, 299
Hung, D. J., **178**, 203
Hussein, N. A. K., **170**, 127
Hutchings, I. M., **177**, 117
Hüttinger, M., **174**, 143
Hwang, C., **166**, 299
Hwang, H. L., **168**, 113

I

Ianno, N. J., **170**, 91
Ichikawa, Y., **173**, 253
Idczak, E., **173**, 163
Ignatiev, A., **172**, 19
van Ijzendoorn, L. J., **174**, 91
Ikeda, Y., **177**, 107
Ikegami, K., **178**, 157, 555
Ilyin, E. G., **178**, 433
Imazeki, S., **178**, 519
Inagaki, T., **178**, 233
Indrea, E., **171**, 367
Inglis, A. D., **173**, 185
Inoue, M., **177**, 295
Inoue, S., **173**, 235
Inoue, T., **166**, 1
Ionescu, R., **171**, 53
Ishida, H., **178**, 373
Ishii, T., **178**, 47, 109
Ishikawa, A., **172**, L97
Isobe, S., **171**, 263
Isomura, K., **178**, 351, 427
Ito, H., **178**, 313
Ito, T., **167**, 187
Ivanov, I., **168**, 239
Iwaki, M., **176**, 165
Iwamoto, M., **178**, 67
Iyechika, Y., **175**, 179

J

Jachimowicz, A., **168**, 157
Jacobson, B. E., **173**, 99
Jäger, D., **175**, 179
Jagner, M., **171**, 197
Jain, N., **166**, 163
Jain, R. K., **172**, 15
Jalochowski, M., **170**, 241
James, W. J., **177**, 271
Jang, D. H., **169**, 57
Janicki, A. J., **167**, 141
Jankowiak, L., **167**, 33
Jankowski, H., **175**, 335
Jansen, F., **177**, 253
Jansson, U., **172**, 81, 95
Jardinier-Offergeld, M., **170**, 41
Jark, W., **170**, 309
Jarvis, D. J., **167**, 261; **168**, 151
Jawalekar, S. R., **169**, 117
Jayaraj, M. K., **177**, 59
Jayarama Reddy, P., **174**, 233
Jelev, J., **168**, 239
Jeong, Y., **173**, 209
Jiang, Y., **178**, 535
Johnston, G. R., **166**, 201
Joiret, S., **174**, 111
Joliet, M. C., **170**, 227
Jones, J. P., **178**, 211
de Jong, A. F., **176**, L177

Joshi, N. V., **170**, 227
Joshi, R. V., **171**, 343
Joswig, H., **175**, 17
Joubert, J. C., **174**, 263; **175**, 281
Jouve, G., **168**, 21
Jung, G., **174**, 249
Jürgensen, H., **174**, 315

K

Kabbaj, M., **173**, 83
Kadam, P. B., **176**, 207
Kadlec, S., **167**, 107
Kaifu, K., **178**, 493
Kajiwara, T., **171**, 93
Kalkur, T. S., **170**, 185
Kalra, K. C., **177**, 35
Kalt, S., **174**, 185
Kamata, S., **178**, 399
Kamata, T., **178**, 305, 427
Kamiya, M., **169**, 289; **176**, 255
Kanaya, K., **167**, L27
Kanetkar, S. M., **171**, 335; **176**, 197
Karekar, R. N., **169**, 271; **170**, 1
Karim, A. A., **172**, 111
Karl, N., **175**, 85, 89
Karpuzov, D. S., **170**, 127
Karulkar, V. T., **169**, 205
Kashiwagi, M., **166**, 1
Kassabov, J., **169**, 43
Kassing, R., **174**, 57
Kasuga, T., **178**, 175, 183
Katircioğlu, B., **167**, 129
Kato, M., **178**, 313, 493
Kato, T., **178**, 37
Katyal, P, **177**, 35
Kawabata. Y.,**178**, 367, 413
Kawabe, H., **173**, 235
Kawada, H., **178**, 505
Kawai, T., **178**, 281
Kawamura, K., **178**, 493
Kazarian, E. M., **170**, 321
Kessler, J., **167**, 217
Kettunen, P., **166**, 255
Kahn, O. F. Z., **173**, 95
Kheyrandish, H., **170**, 127
Kiguchi, M., **169**, 323
Kikuchi, A., **171**, 93
Kim, H.-G., **171**, 251
Kim, I., **169**, 35
Kim J. G., **169**, 57
Kim, S. Y., **166**, 325
Kinbara, A., **167**, 299; **171**, 93
King, N., **166**, 121
Kinoshita, S,-I., **178**, 439
Kinsman, K. R., **166**, 83
Kiriakidis, G., **169**, 87
Kitada, M., **167**, L39
Kitahara, K., **178**, 361
Klingshirn, C., **175**, 179
Klinkhammer, F., **178**, 445
Knight, J. C., **177**, 117
Knolle, W. R., **168**, 123
Knotek, O., **174**, 51
Knuyt, G., **173**, 199
Kobayashi, K., **173**, 263; **178**, 381, 453
Kobayashi, Y., **168**, 133; **169**, 249
Koch, H., **168**, L43
Kodama, K., **174**, 63
Koezuka, H., **178**, 393
Kohl, C. D., **174**, 75
Kohler, H.-H., **175**, 81
Kohlhase, A., **175**, 17
Koike, Y., **178**, 473
Koinkar, V. N., **171**, 335
Kolawa, E., **166**, 15, 29, 63; **173**, 217
Kolodziej, A., **175**, 37
Komen, Y., **176**, 131
Konno, H., **175**, 329
Konno, M., **175**, 329
Konopka, A., **174**, 249
Konopka, J., **174**, 249
Konstantinova, A. F., **177**, 305
Köpfer, P., **174**, 255
Korin, E., **167**, 101
Körner, H., **175**, 55
Koshinaka, M., **168**, 103
Koster, H., **170**, 71
Koster, U., **174**, 11
Kourtev, J., **168**, 239
Kovalev, V. N., **177**, 181
Kreider, K. G., **176**, 73
Krishnaswamy, S. V., **168**, 307
Krokoszinski, H.-J., **175**, 241
Krusin-Elbaum, L., **169**, 17
Ku, Y. H., **172**, 1
Kubajewska, E., **175**, 299
Kubota, K., **168**, 133; **169**, 249; **173**, L139
Kuchar, F., **168**, 157
Kücher, P., **175**, 17
Kudo, T., **172**, L97
Kudryavtsev, Yu. V., **174**, 45
Kuhman, D., **177**, 253
Kuhn, H., **178**, 1
Kuisl, M., **177**, 231
Kula, W., **174**, 249
Kulak, A., **175**, 335
Kulisch, W., **174**, 57
Kulyasova, O. A., **171**, 235
Kumar, J., **178**, 243
Kumar, R., **170**, 15
Kumar, R. S., **178**, 243
Kumar, S. S., **178**, 243
Kumeda, M., **167**, L23
Kumehara, H., **178**, 175, 183
Kung, J. H., **173**, 149
Kunz, F. W., **168**, 263
Kuo, C. V., **173**, 59
Kurata, T., **178**, 393
Kurima, Y., **173**, 263
Kurita, S., **172**, 159
Kuroda, S.-I., **178**, 157, 555
Kuroyanagi, A., **176**, 247
Kurthen, C., **178**, 145
Kuwae, Y., **172**, 159
Kuzel, R., Jr., **170**, 201, L55
Kwong, D. L., **172**, 1
Kwor, R. Y., **170**, 185

L

Labrune, M., **175**, 305
Ladouceur, M., **166**, 249
Lagnel, F., **176**, 111
Lahav, M., **178**, 203
Lakshmi, P. J., **172**, 167
Lambert, M. R., **177**, 207
Landheer, D., **173**, 185
Lange, P., **174**, 159
Langlet, M., **174**, 263; **175**, 281
Larhrafi, M., **167**, 195
Larsson, T., **172**, 133, 241
Lassabatere, L., **172**, L65
Lau, S. S., **176**, 187
Laude, L. D., **170**, 227
Laurent, C., **170**, 235
Lebouvier, D., **172**, 227
Leciejewicz, J., **172**, L75
Lee, C. H., **173**, 59
Lee, C. L., **173**, 59
Lee, D., **166**, 163
Lee, G. H., **168**, 193
Lee, H.-Y., **171**, 251
Lee, J. J., **169**, 51
Lee, S. K., **172**, 1
Lee, V., **166**, 181
Lee, W. Y., **166**, 131, 181
Leech, P. W., **177**, 133
Lehn, J. M., **178**, 387
Leiserowitz, L., **178**, 203
Leja, E., **174**, 217

Lemperiere, G., **176**, 7
Lengeler, B., **174**, 5
Lepage, J., **172**, 197
Leppin, Ch., **174**, 155
Les, Z., **167**, 33
Leskela, M., **166**, 149
Leslie, J. D., **176**, 13
Levy-Clement, C., **169**, 315
Lewandowski, S. J., **174**, 249
Li, F. C., **178**, 53
Li, L. X., **172**, L91
Li, P., **166**, 273
Li, T. J., **178**, 221, 535
Li, Y., **178**, 525
Li, Z., **166**, 281
Li, Z.-M., **170**, 273
Liao, B., **176**, 309
Líbezný, M., **169**, 213
Lieb, K. P., **174**, 139
Ligonzo, T., **170**, 163
Lin, C. C., **171**, 323
Lin, C. L., **166**, 155
Lin, D. S., **168**, 221
Lin, H. T., **166**, 121
Lin, H. Y., **168**, 113
Lin, T., **173**, 39
Lin, T. J., **177**, 271
Lin, W. T., **173**, 149
Liou, Y., **172**, L91
Lippmann, T., **174**, 57
Lischka, K., **171**, 271
Lister, D. H., **171**, 313, 323
Littrell, D. M., **169**, 143
Liu, D. R., **173**, L115
Livage, J., **167**, 67
Llebaria, A., **177**, 245
Lo, J., **166**, 299
Logothetidis, S., **169**, 87
Lohe, C., **174**, 75
Lombaert, I., **170**, 71
Lombard, L., **166**, 309
Lommasson, T. C., **171**, 109
Lorriaux, J. L., **172**, L59
Loschek, R., **178**, 53
Lottiaux, M., **170**, 107
Lozano, L., **170**, 259
Luan, X., **166**, 281
Lubecka, M., **174**, 71
Luft, J., **175**, 213
Lugert, G., **175**, 311, 341
Lunstrom, I., **177**, 77
Luo, S., **166**, 273
Lupo, D., **178**, 403
Luth, H., **177**, 287
Lvov, Yu. M., **178**, 433
Lynn, K. G., **166**, 349

M

van den Meerakker, J. E. A. M., **173**, 139
Ma, E., **166**, 273
Maass, W., **175**, 287
Madar, R., **177**, 189
Mader, H., **175**, 1
Mader, W., **174**, 155
Madhusudhana Reddy, M. H., **169**, 117
Maekawa, E., **178**, 439
Magnus, B., **169**, 159
Magnussen, N., **167**, 245
Maheo, D., **176**, 7
Mahowald, M. A., **170**, 91
Mai, Q. X., **166**, 235
Majima, Y., **178**, 67
Makela, M., **166**, 149
Maksymowicz, A. Z., **170**, 191
Maksymowicz, L. J., **175**, 335
Malcolm, B. R., **178**, 17, 191
Maley, N., **171**, 217
Mall, R. P., **168**, 291
Malliet, B., **173**, 199
Manaila, R., **167**, 1; **168**, 1
Manaud, J. P., **170**, 71
Manda, E., **178**, 367, 413
Mansingh, A., **167**, L11; **176**, 33
Mantyla, T., **166**, 255
Mao, D., **173**, 39
Margolin, A. M., **176**, 227
Marinković, Ž., **176**, L173
Markevich, M. I., **168**, 363
Marmillion, N. P., **166**, 55
Marr-Leisy, D., **178**, 171
Marszalek, K., **175**, 227
Martin, D. D., **176**, 143
Martini, G., **178**, 271
Martino, G., **176**, 283
Marucco, J. F., **176**, 111
Masuhara, H., **169**, 323
Mathey, Y., **174**, 289
Mathuni, J., **174**, 39
Mathur, P. C., **170**, 15
Matsuda, H., **167**, L27; **178**, 313, 505
Matsuda, M., **168**, L47
Matsumoto, M., **178**, 367, 413
Matsushige, K., **171**, 359
Matthies, P., **172**, L101
Matts, Goho, S., **166**, 335
Matuda, N., **167**, 299
de Mauduit, B., **175**, 43
Mayer, J., **167**, 203
Maziewski, A., **175**, 299
Mbise, G., **173**, L123
McCune, R. C., **168**, 263
McDevitt, N. T., **168**, 335
McDonald, J. F., **166**, 121
McGee, S., **170**, 151
McGinn, P., **166**, 163
Mecea, V. M., **171**, 367
Mehra, R. M., **170**, 15
Meisels, R., **168**, 157
Meiser, S., **170**, 71
Mende, G., **168**, 51
Mendez, A. J., **176**, 1
Menon, C. S., **168**, 165
Mercadere, L., **175**, 43
Mertens, G., **174**, 185
Messier, R., **172**, L91
Metz, O., **175**, 81
Mezin, A., **172**, 197, 211
Mezzasalma, A. M., **176**, 283
Micocci, G., **172**, 179
Mikic, B., **167**, 101
Milewski, A., **175**, 335
Miller, D. R., **166**, 139
Milne, W. I., **168**, 345
Minami, T., **171**, 307; **176**, 277
Minamikawa, T., **167**, L23
Minari, N., **178**, 157
Misho, R. H., **169**, 235
Mitkova, M., **169**, 169
Mitra, S., **177**, 171
Mitra, U., **170**, 151
Mitreski, M., **167**, 309; **173**, 53
Mitsuya, M., **169**, 323
Miu, L., **168**, 1
Miura, A., **178**, 137, 165, 477
Miyairi, K., **177**, 1
Miyamoto, Y., **178**, 493
Miyano, K., **168**, 141
Miyasaka, H., **178**, 367
Miyashita, T., **168**, L47
Miyata, S., **178**, 175, 183
Miyauchi, S., **178**, 347
Mo, G. H., **172**, 19
Möbius, D., **178**, 53, 61, 221
Möbus, M., **175**, 89
Mochizuki, K., **174**, 63
Mogilevsky, L.Tu., **178**, 433
Mogilnikov, K. P., **171**, 43
Mohammed, M. A., **176**, 45
Mohan, S., **170**, 179; **172**, 45; **176**, 181
Möhwald, H., **173**, 269; **178**, 289

Mojtabai, F., **178**, 115
Molarius, J. M., **166**, 15, 29, 63
Molassioti, A., **174**, 1
Moldenhauer, W., **177**, 315
Momose, A., **178**, 519
Mondal, A., **176**, L183
Mondio, G., **176**, 283
Montalan, D., **170**, 235
Montero, I., **167**, 95; **175**, 49
Montes, S., **173**, 299
Morancho, R., **167**, 195
Morgan, D. V., **176**, 45
Morgan, H., **173**, L141, **178**, 73
Mori, A., **168**, 141
Morikawa, Y., **178**, 505
Morimoto, K., **178**, 103
Moritake, A., **167**, L27
Moriwaki, T., **178**, 393
Moriyama, K., **178**, 103
Morling, M., **177**, 69
Moser, M., **174**, 1
Mössner, C., **174**, 255
Motohiro, T., **172**, L71, L105
Motronea, M., **171**, 53
Mu, J., **178**, 341
Muhling, I., **171**, 157
Muller, H., **176**, 25
Muller, K.-H., **171**, 183; **174**, 117
Müller, M., **175**, 179
Murad, W. A., **169**, 235
Murali, K. R., **167**, L19
Murawski, L., **167**, 67
Murayama, T., **178**, 473
Muro, J., **178**, 109
Murray, P. T., **168**, 335
Murri, R., **170**, 163
Murthy, M. A., **176**, 181
Musil, J., **167**, 107; **170**, 201, L55
Musil, R., **169**, 159
Mutsukura, N., **176**, 289
Myers, A., **171**, 217

N

Nagamura, T., **178**, 399
Nagao, T., **178**, 473
Nagendra, C. L., **167**, 291
Nagpal, K. C., **168**, 291
Nahar, N. M., **172**, 19
Naik, V., **176**, 197
Naito, M., **178**, 519
Nakagiri, T., **178**, 505
Nakahara, H., **178**, 355, 361, 439, 549
Nakajima, H., **177**, 295
Nakamura, H., **167**, L39
Nakamura, T., **178**, 367, 413
Nakanishi, H., **178**, 313, 529
Nakanishi, K., **168**, 103; **172**. 159
Nakasaki, Y., **166**, 1
Nakatani, K., **167**, 85; **177**, 161
Nakayama, T., **173**, 253; **178**, 137, 165, 477
Nakayama, Y., **167**, 187
Nanto, H., **171**, 307; **176**, 277
Narasimha, Rao, K., **170**, 179; **176**, 181
Natarajan, B., **166**, 83
Nayak, B. B., **171**, 277
Nedev, N., **169**, 173
Neelakandan, K., **168**, 165
Neidhardt, A., **173**, 109
Nenasheva, L. A., **171**, 43
Nerger, D., **178**, 253
Neumann-Spallart, M., **169**, 315
Neureither, B., **175**, 67
Nicolet, M.-A., **166**, 15, 21, 29, 63; **173**, 217
Nieh, C. W., **166**, 15, 29
Nielsen, B., **166**, 349
Niewohner, L., **170**, 71
Nihoul, G., **170**, 107
Niinisto, L., **166**, 149
de Nijs, J. M. M., **173**, 1
Nikitas, P., **170**, 137
Nishi, H., **178**, 361
Nishitani, N., **177**, L187
Nistor, L. C., **167**, 1; **168**, 1
Nitsch, W., **178**, 145
Nivoit, M., **172**, 211
Nobutoki, H., **178**, 393
Nomura, R., **167**, L27
Noreika, A. J., **168**, 307
Norian, K. H., **167**, L35; **168**, 169, 353; **173**, L115
Norström, H., **168**, 325
Novak, F., **174**, 133
Novotny, I., **169**, 213
Nowak, S., **175**, 37
Nygren, S., **168**, 325
Nykanen, E., **166**, 149

O

O'Brien, P., **173**, 95
Ochiai, S., **178**, 453
Ocken, H., **171**, 313, 323
Oechsner, H., **174**, 5, 39, 133, 149, 255; **175**, 119
O'Keefe, T. J., **177**, 271
O'Neil, M., **172**, 269
Oelschig, S., **175**, 235
Oesterlein, R., **175**, 241
Ogale, S. B., **171**, 335; **176**, 197
Ogawa, K., **178**, 439
Ogawa, T., **178**, 399
Ohlídal, I., **169**, 213
Ohshima, K., **178**, 37
Ohst, H., **178**, 253
Ohtsuka, N., **174**, 63
Okada, S., **178**, 313
Okahata, Y., **178**, 465
Okamoto, H., **172**, L97
Okamoto, K., **169**, 289; **176**, 255
Okamoto, Y., **178**, 233
Okaniwa, H., **167**, 85; **177**, 161
Olcaytug, F., **168**, 157
Olive, G., **166**, 131
Oliveira, O. N., Jr., **173**, L141; **178**, 27, 73
Olsson, M., **172**, 81, 95
Oozono, Y., **178**, 351
Orihara, K., **178**, 459
Orlinov, V., **168**, 239
Orlowski, T. E., **166**, 335
Ortega, C., **167**, 95
Ortega, J., **174**, 295
Ortiz, C., **167**, 57
Östling, M., **168**, 325; **172**, 133
Osvald, G., **169**, 223
Oszwałdowski, M., **172**, 71; **174**, 245
Otsubo, S., **167**, L23
Ottaviani, M. F., **178**, 271
Owen, A. E., **173**, 129
Ozaki, H., **177**, 161; **178**, 305
Ozeki, M., **174**, 63

P

Paccagnella, A., **176**, 187
Pacia, N., **172**, 197, 211
Packwood, R., **173**, 185
Paez, M., **173**, 299
Page, T. F., **177**, 117
Pailharey, D., **174**, 289
Pal, A. K., **176**, L183
Palacin, S., **178**, 327, 387, 499
Palatnik, L. S., **173**, 225
Palleau, J., **177**, 189
Palmer, B. J., **177**, 141
Pamler, W., **174**, 143
Pan, E. T.-S., **166**, 63; **173**, 217
Pang, X., **178**, 525

Panitz, J. K. G., **166**, 45
Pankajakshan, V. S., **168**, 165
Panwar, B. S., **168**, 291
Panwar, O. S., **176**, 79
Paoletti, L., **173**, 67
Parent, L., **166**, 249
Park, C. D., **166**, 37
Park, H. L., **166**, 37
Park, Y. J., **166**, 367
Park, Y. W., **166**, 367
Parker, W. G., **168**, 151
Parsons, R. R., **170**, 273
Pastore, G., **173**, 299
Patel, B. H., **173**, 169
Patel, S. M., **173**, 169
Patnaik, B. K., **167**, 245
Patrykiejew, A., **173**, 13, 279, 287; **177**, 333
Patz, U., **175**, 287
Paulmier, D., **172**, 197
Pauty, M., **177**, 49
Paz de Araujo, C. A., **170**, 185
Peebles, D. E., **173**, 19
Peev, G., **169**, 173
Pellet, C., **175**, 23
Pelletier, E., **170**, 107
Penfold, A. S., **171**, 99
Penfold, J., **172**, 269
Perry, A. J., **166**, 191; **170**, 63; **171**, 197
Pertsch, P., **176**, 25
Peterson, I. R., **172**, 149; **178**, 81, 289, 445
Petersson, C. S., **168**, 325; **176**, 173
Petrov, I., **168**, 239; **169**, 299
Petty, M. C., **176**, 151
Picard, C., **174**, 209; **176**, 111
Picard-Lagnel, F., **174**, 209
Picozzi, P., **173**, 67
Piegari, A., **171**, 243
Pier, Th., **175**, 179
Pieraggi, B., **175**, 43
Pinarbasi, M., **171**, 217
Pisarkiewicz, T., **174**, 217, 277
Pitkanen, T. M., **166**, 113
Pitsch, M., **175**, 81
Pivin, J., **175**, 49
Plossu, C., **167**, 45
Plummer, H. K., Jr., **168**, 263
Pohl, L., **174**, 1
Poitevin, J. M., **176**, 7
Pokela, P. J., **166**, 113
Polak, M., **173**, L109
Pope, L. E., **173**, 19
Popescu-Pogrion, N., **171**, 33
Popovitz-Biro, R., **178**, 203
Porada, Z., **167**, L15; **175**, 249
Poulek, V., **170**, 201, L55
Poumellec, B., **174**, 209; **176**, 111
Pound, B. G., **171**, 313
Powrożnik, W., **174**, 71
Prasad, B., **172**, 15
Prasad, H. C., **167**, L7; **169**, 195; **176**, 99
Prass, W., **178**, 403
Priotton, J. J., **175**, 173
Pulker, H. K., **175**, 207

Q

Qian, S. W., **168**, 231
Quaranta, F. M., **175**, 255
Quinones, L., **167**, 245
Quirini, A., **176**, L167

R

Racheva, T., **169**, 173
Raczy, L., **172**, L59
Rajanna, K., **172**, 45
Raju, D. V. R., **176**, 207
Ramakrishnan, V., **170**, 35
Ramalingen, S., **166**, 387
Ramm, J., **175**, 207
Ramos, M. M. D., **176**, 219
Randhawa, H., **167**, 175
Rao, V. J., **176**, 207
Rasigni, G., **177**, 245
Rau, B., **167**, 233
Rauch, F., **175**, 185
Rauschenbach, B., **170**, 81; **175**, 295
Ray, S., **167**, 121
Ray, S., **169**, 229
Rayss, J., **173**, 13, 279
Redsten, A. M., **175**, L153
Regazzoni, G., **174**, 25
Regel, G. K., **174**, 1
Reich, R., **177**, 225
Reif, R., **167**, 101
Reigler, H., **178**, 511
Reim, W., **175**, 265
Reinhardt, H., **167**, L1
Reinhold, U., **173**, 109
Rekas, M., **174**, 269
Rella, R., **172**, 179
Renard, D., **175**, 341
Reniers, F., **170**, 41
Rettner, C. T., **166**, 181
Richardson, R. M., **172**, 269
Rieck, U., **167**, L35; **168**, 353
Rieger, J. H., **168**, 307
Ringsdorf, H., **178**, 227
Rio, F., **175**, 305
Ristov, M., **167**, 309; **173**, 53
Rivière, J. P., **176**, L161
Roas, B., **174**, 179
Robbins, W. P., **166**, 387
Robinet, S., **170**, L51
Robinson, I., **172**, 149; **178**, 125
Rockett, A., **171**, 109
Rohatgi, A., **166**, 349
Rohrmann, H., **175**, 273
Rolandi, R., **175**, 103
Röll, K., **175**, 149
Roman, Y. G., **169**, 241
Roos, J. R., **173**, 199
Rose, E., **168**, 35
Rosenmayer, C. T., **166**, 291
Rosenwaks, Y., **169**, 25
Roser, S. J., **172**, 269
Ross, C. A., **173**, L129
Rossi, M., **175**, 255
Rossnagel, S. M., **171**, 125, 143
Rost, M. C., **166**, 317
Rotberg, V. H., **166**, 191
Roth, S., **171**, 157; **175**, 95
Roux, H., **172**, 141
Roy, S. K., **169**, 205
Rubner, M. F., **178**, 233
Rudnik, P. J., **171**, 171
Ruiz, R., **166**, 63
Rupertus, V., **174**, 255
Russell, G. J., **168**, 221
Russell, T. P., **170**, 309
Ryan, J. G., **166**, 55
Rybicki, J., **167**, 13
Rydén, K. H., **168**, 325

S

Sadananda, K., **168**, 207
Saemann-Ischenko, G., **174**, 179
Safoula, G., **168**, 249
Sah, R. E., **167**, 255
Sainfort, P., **174**, 25
Saito, K., **178**, 157, 555
Saito, M., **178**, 157, 493, 555
Saito, S., **173**, L135; **178**, 351, 541
Saito, Y., **167**, 299
Saitta, G., **176**, 283
Salace, G., **168**, 11
Salem, J., **166**, 181
Salmeron, M., **167**, L31

Salzberger, U., **174**, 155
Sambles, J. R., **167**, 73, 261; **168**, 151; **172**, 27, 149; **178**, 125
Samuelson, L. A., **178**, 233, 243
Samula, J., **175**, 335
Samwer, K., **174**, 11
Sánchez, O., **175**, 49
Sánchez-Machet, H., **176**, 69
Sanders, J. H., **166**, 225
Šandrik, R., **169**, 223
Santucci, S., **173**, 67
Sasabe, H., **178**, 459
Sasaki, T. A., **171**, 263
Sathyalatha, K. C., **174**, 233
Sato, H., **171**, 307; **176**, 277
Satyanarayan, B. S., **176**, 79
Saulitis, J., **166**, 201
Saurenbach, F., **175**, 317
Savoy, R., **166**, 181
Sayer, M., **172**, 251
Schabowska-Osiowska, E., **167**, L15; **175**, 249
Schaffer, J. P., **166**, 349
Schalch, D., **167**, L1
Scharff, W., **171**, 157
Scharmann, A., **167**, L1
Scheib, M., **174**, 5
de Schepper, L., **173**, 199
Scheunemann, U., **178**, 403
Schiavulli, L., **170**, 163
Schier, H., **175**, 95
Schiller, C., **174**, 91; **175**, 161
Schiller, G., **174**, 85
Schilling, W., **175**, 61
Schirmer, G., **167**, 281
Schmatjko, K. J., **174**, 33
Schmeisser, D., **175**, 95
Schmid, M., **174**, 307
Schmidt, A., **175**, 179
Schmidt, E., **169**, 213; **174**, 323; **176**, 25
Schmitt, J. P. M., **174**, 193
Schneider, J., **178**, 227
Schneider, S., **174**, 11
Schnitzler, G., **175**, 85
Schnurnberger, W., **174**, 85
Scholz, F., **174**, 1
Schopper, H.-C., **178**, 253
Schreck, M., **175**, 89, 95
Schreiber, H., **177**, 315
Schreiber, H.-U., **175**, 29
Schreiner, W. H., **170**, 285
Schreiner, R. K., **174**, 315
Schrepp, W., **178**, 319
Schröder, H., **174**, 11
Schroeder, J., **175**, 287
Schroeter, E., **173**, 109
Schryer, D. R., **169**, 69
de Schryver, F. C., **169**, 127
Schuhmacher, B., **174**, 11
Schuller, K.-H., **175**, 287
Schultz, L., **174**, 179
Schulze, S., **167**, 233; **171**, 157
Schupp, H., **178**, 319
Schuster, K., **175**, 265
Schwebel, C., **175**, 23
Schweikert, E. A., **167**, 245
de Sedas, L., **177**, 95
Seeboth, A., **173**, L119
Seguelond, T., **173**, 243
Seguelong T., **170**, 259
Segui, Y., **170**, 235
Seifarth, H., **172**, 61
Seki, K., **178**, 529
Sekiguchi, T., **178**, 367
Sekiya, A., **178**, 373
Senet, E., **174**, 263
Sequeda, F., **166**, 131
Serbanescu, D., **167**, 1
Sernelius, Bo. E., **177**, 69
Serpinet, J., **173**, 13, 279
Seth, T., **176**, 79
Shackleton, C., **172**, 269
Shah, S. I., **166**, 171
Shah, V. V., **176**, 79
Shams El Din, A. M., **167**, 269
Shanbhogue, H. G., **170**, 27
Shanker, K., **177**, 95
Shapira, Y., **175**, 141
Shavit, E., **178**, 203
Shen, Y., **175**, 103
Sher, A., **169**, 25
Shibuya, Y., **168**, 103
Shima, S., **166**, 1
Shimizu, K., **173**, 263
Shimizu, T., **167**, L23
Shiozawa, T., **178**, 421
Shoji, T., **178**, 439
Siegmund, H., **174**, 323
Siejka, J., **167**, 95
van Silfhout, A., **173**, 1
Simanovskis, A. A., **177**, 181
Simić, V., **176**, L173
Sinadinovski, Gj., **167**, 309; **173**, 53
Singh, A. K., **168**, 207
Singh, K. C., **177**, 35
Singh, S. K., **171**, 277
Sinha, A. P. B., **176**, 197
Sisido, M., **178**, 355
Sitter, H., **171**, 271; **175**, 179
Skotheim, T. A., **178**, 233
Smardz, L., **175**, 295
Smith, G. B., **173**, L123
Snyder, P. G., **166**, 317
So, F. C. T., **166**, 15, 29; **173**, 217
Sobolewski, R., **174**, 249
Soderberg, S., **172**, 81, 95
Sohler, W., **175**, 191
Soininen, P., **166**, 149
Sokołowski, S., **173**, 287; **177**, 333
Somekh, R. E., **173**, L129; **174**, 165
Sommer, H., **170**, 81
Sommerfeldt, R., **175**, 235
Somorjai, G. A., **167**, L31
Sonoda, T., **171**, 307
Sorita, T., **177**, 295
Souag, N., **170**, 235
Specchiulli, G., **172**, L85
Spetz, A., **177**, 77
van der Spiegel, J., **177**, 263
Spindler, O., **175**, 67
Sproul, W. D., **171**, 171
Sreenivas, K., **172**, 251
Sridharan, K., **175**, L153
Srinivasan, D. R., **166**, 375
Srivastava, P. K., **176**, 33
Stals, L. M., **173**, 199
Stankiewicz, A., **175**, 299
Stapinski, T., **174**, 277
van Stappen, M., **173**, 199
Stark, J. P., **177**, 171
Stedile, F. C., **170**, 285
Steinberger, H., **168**, 35
Steinbrunn, A., **168**, 61
Steitz, R., **178**, 289, 445, 511
Stenzel, O., **171**, 157
Stetsenko, A. N., **173**, 225
Stirling, C. J. M., **178**, 27
Stobiecki, F., **174**, 45
Stobiecki, T., **174**, 45; **175**, 325
Stohr, J., **170**, 309
Stolt, L., **176**, 173
Stolyarova, S. V., **177**, 181
Strafford, K. N., **168**, 221
Strandberg, C. C., **166**, 191
Stridh, B., **172**, 81, 95
Strnad, J., **175**, 81
Stroeve, P., **178**, 227
Strumpler, R., **177**, 287
Suda, T., **176**, 247

Sugi, M., **178**, 157, 367, 555
Suguro, K., **166**, 1
Sun, C. Y., **168**, 113
Sundgren, J.-E., **169**, 299
Surowiak, Z., **176**, 227
Suryanarayanan, R., **175**, 221
Suzaki, Y., **173**, 235
Suzuki, K., **167**, 85; **177**, 161; **178**, 37
Suzuki, M.-A., **178**, 103
Suzuki, S., **178**, 393
Swann, C. P., **166**, 171
Sweeny, C. A., **167**, L35
Szklarski, Z., **174**, 269
Szuber, J., **170**, 219

T

Tachibana, H., **178**, 367, 413
Taga, Y., **172**, L71, L105
Tajima, K., **178**, 381
Takahashi, M., **178**, 381
Takahashi, S., **177**, 9
Takano, I., **171**, 263
Takaoka, K., **178**, 453
Takata, S., **171**, 307; **176**, 277
Takehara, K., **178**, 351, 427
Takei, W. J., **168**, 307
Takenaka, T., **178**, 281, 305, 427
Takimoto, K., **178**, 505
Talieh, H., **171**, 109
Tamai, N., **178**, 549
Tamizhmani, G., **169**, 315
Tamura, M., **178**, 373
Tanaka, H., **178**, 473
Tanaka, M., **178**, 367, 413
Tandon, J. L., **166**, 63
Tang, X. Y., **178**, 221
Taniguchi, H., **178**, 351, 427
Taniguchi, Y., **169**, 323
Tanoue, T., **170**, 49
Tatarchuk, B. J., **166**, 213, 225; **169**, 143
Tatti, S. R., **177**, 171
Tawada, Y., **173**, 253
Taylor, D. M., **173**, L141; **178**, 27, 73
Tazaki, M., **178**, 459
Temofonte, T. A., **168**, 307
Teodorescu, T., **167**, 1
Teodorescu, V., **168**, 1
Tepore, A., **172**, 179
Terada, S., **168**, 133
Thabti, A., **173**, 243
Tholomier, M., **172**, 141
Thomas, F. W., **174**, 323
Thomas, I. M., **175**, 173
Thomas, J. P., **176**, 111
Thomas, O., **171**, 343
Thomas, P. V., **170**, 35
Thompson, G. W., **173**, 209, 263
Thorn, G., **174**, 307, 323
Thornton, J. A., **171**, 5
Thuillard, M., **166**, 21
Thutupalli, G. K. M., **167**, 291; **170**, 27
Tian, K., **178**, 221
Tiller, H. J., **169**, 159
Tillin, M. D., **167**, 73; **172**, 27
Tochitsky, E. I., **168**, 363
Tomioka, Y., **178**, 519
Tondon, V. K., **169**, 229
Torres, J., **177**, 189
Tosa, M., **172**, 35; **177**, 107
Toth, L., **168**, 263
Tovazhnyansky, V. L., **173**, 225
Toyozawa, K., **178**, 399
Tran, L. T., **166**, 15, 21, 29
Tressaud, A., **170**, 259
Tripathi, S., **178**, 27
Tripathy, S. K., **178**, 233, 243
Tronin, A. Y., **177**, 305
Tsong, T. T., **172**, L91
Tsumura, A., **178**, 393
Tsutsui, T., **173**, L135; **178**, 351, 541
Turban, G., **176**, 289
Turtur, C., **175**, 341
Tvarožek, V., **169**, 213
Tyagi, A., **176**, 79
Tyagi, S. V. S., **169**, 229
Tyczkowski, J., **168**, 175

U

Uchida, W., **171**, 271
Uchil, J., **170**, 27
Uchimi, H., **178**, 549
Ufert, K.-D., **174**, 255
Uhlig, H., **168**, L43
Uhrmacher, M., **174**, 139
Ullmaier, H., **175**, 61
Ullman, J., **171**, 157
Ullrich, B., **168**, 157
Umbach, E., **175**, 85
Umemura, J., **178**, 281, 305, 427
Umezawa, K., **167**, 223
Unger, W., **177**, 225
Unruh, K. M., **166**, 171
Upadhyay, J. P., **167**, L7; **169**, 195; **176**, 99
Ushio, Y., **167**, 299
Uthanna, S., **174**, 233

V

Vahlas, C., **177**, 189
Vaidyan, V. K., **170**, 35
Valbusa, U., **175**, 103
Valentini, A., **175**, 255; **176**, L167
Vallabhan, C. P. G., **177**, 59
Valvoda, V., **167**, 107; **170**, 201
Vancu, A., **171**, 53
Vandevyver, M., **178**, 499
Vankar, V. D., **169**, 281
Varchenya, S. A., **177**, 181
Varhue, W. J., **169**, 179
Varnier, F., **170**, 107
Vasanelli, L., **175**, 255; **176**, L167
Vasant Kumar, C. V. R., **167**, L11
Vasileva, J., **169**, 43
Vasilyeva, L. L., **171**, 43
Vautier, C., **177**, 239
Vedam, K., **166**, 325
Vedel, J., **167**, 217; **170**, 171
Venezia, A., **166**, 63
Vengurlekar, A. S., **169**, 205
Venkatesan, M., **170**, 151
Venos, R., **174**, 99
Vepřek, S., **175**, 129
Verbeek, G., **169**, 127
Verschuere, B., **169**, 127
Vickholm, I., **178**, 197
Vilcot, J. P., **172**, L59
Vishwakarma, S. R., **167**, L7; **169**, 195; **176**, 99
Viswanathan, M., **167**, 291
Vodenicharov, C., **169**, 169
Vodenicharova, M., **169**, 169
Vogel, M., **171**, 157
Vogel, V., **178**, 53
Vohl, M., **175**, 317
Voigt-Martin, I., **178**, 289
Viogtmann, R., **177**, 315
de Vries, J. W. C., **167**, 25
Vuoristo, P., **166**, 255
Vyskočil, J., **167**, 107; **170**, 201

W

Wägli, P., **175**, 201
Wagner, W., **175**, 185
Wagner, G., **174**, 185

Wahlroos, J., **166**, 255
Waki, I., **178**, 519
Waldorf, J., **174**, 39
Wales, J. L. S., **166**, 375
Wang, B., **166**, 281
Wang, X., **178**, 525
Wang, Y. G., **173**, L149
Ward, L. P., **168**, 221
Ward, R. C., **172**, 269
Was, G., **166**, 191
Wassermann, E. F., **174**, 225
Watanabe, I., **178**, 233
Watanabe, K., **171**, 93
Watanabe, T., **178**, 175, 183
Webby, G. M., **178**, 211
Weber, B., **172**, 211
Weber, Th., **174**, 139
Wehrmann, R., **178**, 253
Wei, J. C. S., **166**, 15, 29
Wei, Q., **178**, 535
Weil, R., **169**, 35
Weiss, F., **174**, 263
Weiss, J., **174**, 155
Wen, L. S., **168**, 231
Wenda, J., **175**, 335
Wherry, D. C., **166**, 263
Whiting, J. S. S., **170**, 191
Wicks, G. W., **170**, 49
Wieder, H. H., **166**, 155
Wierenga, P. E., **172**, 51
Windbracke, W., **174**, 159
Window, B., **171**, 183
Wingen, G., **175**, 179
Winkler, S., **175**, 265
Wißmann, P., **174**, 105
Witt, A., **175**, 179
Woerlee, G. F., **169**, 1
Wolf, B., **168**, 71
Wolke, W., **177**, 225
Wood, G. C., **173**, 209, 263
Woollam, J. A., **166**, 317
Worzala, F. J., **175**, L153
Wu, B. C., **172**, 185
Wu, P. T., **173**, 149
Wu, T. W., **166**, 299
Wu, Y. L., **168**, 113
Wu, Z.-Q., **173**, 77
Wucher, A., **174**, 133
Wudy, E., **175**, 213
Wuttke, W., **173**, 109

X

Xu, X., **173**, L135; **178**, 541

Y

Yamada, T., **178**, 347
Yamamoto, H., **178**, 347
Yamamoto, K., **173**, 253
Yamamoto, R., **178**, 347
Yamanoue, A., **177**, 9
Yamazaki, I., **178**, 549
Yan, B., **173**, 39
Yang, C., **173**, 39
Yang, H. M., **176**, 91
Yang, K., **178**, 341
Yang, L. C., **171**, 109
Yang, M. H., **168**, 113
Yang, X. Q., **178**, 233
Yano, M., **177**, 161
Yarwood, J., **176**, 151
Yokoya, N., **167**, L23
Yonehara, H., **178**, 439
Yoneyama, M., **178**, 473
Yonezawa, Y., **167**, L23
Yoo, C. S., **168**, 281
Yoon, S.-G., **171**, 251
Yoshihara, K., **172**, 35; **177**, 107
Yoshii, K., **173**, 235
Yoshimura, S., **173**, L139
Yoshitake, M., **172**, 35
Yudasaka, M., **172**, 159
Yukami, N., **177**, L187
Yust, M., **176**, 73

Z

Zabinski, J. S., **166**, 213
Zagal, J. H., **173**, 299
Zakharchenko, I. N., **176**, 227
Zakrzewska, K., **174**, 217, 269
Zehe, A., **168**, 71
Zhang, J., **166**, 281
Zhao, X.-A., **173**, 217
Zhu, D. G., **176**, 151
Zhu, Z. Q., **178**, 221
Zhuang, Y. Z., **168**, 231
Ziani, A., **176**, 111
Ziemann, P., **174**, 301
Zies, G., **177**, 315
Zimmermann, U., **175**, 85
Zinn, W., **175**, 317
Zorn, G., **174**, 5
Zozulin, A. N., **178**, 433
Zubarev, Ye. N., **173**, 225
Zussman, A., **169**, 25

Cumulative Subject Index for Volumes 166–178

The volume numbers are given in bold-face type preceding the page numbers.

A

Abutted tails
Two types of hydrocarbon chain packing in Langmuir–Blodgett films: interdigitated and abutted tails, **178**, 433

Additive spreading solutions
Effects of additive spreading solutions to make stable monolayers, **178**, 47

Adhesion
Adhesion measurement of thin films on glass substrates, **171**, 93
Adhesion of fatty acid in Langmuir–Blodgett films, **178**, 347
Ambient-induced interface reactions and adhesion failure in the Ag/TlBr–TlI system, **177**, 181
A new concept of metal–resin adhesion using an intermediate layer of SiO_x–C, **169**, 159
Effect of surface precipitation of titanium carbide on adherence of alumina film on steels, **177**, 107

Adsorption kinetics
A new approach to adsorption kinetics on heterogeneous surfaces, **170**, 137

Aggregated structures
Control of aggregated structures in monolayers and multilayers by mixing at the molecular level of two azobenzene-linked amphiphiles, **178**, 541

Airless spraying
Preparation of copper indium disulphide films by airless spraying, **167**, 217

Alkanoic acid
Fluorescence characteristics, formation mechanism and chromophore association of ω-(1-pyrenyl)alkanoic acid films prepared by vacuum deposition, **169**, 323

Alkylammonium salts
Preparation of Langmuir–Blodgett films of long-chain alkylammonium salts, **178** 381

Alloying
Rapid IR lamp alloying of nickel-based ohmic contacts on n-GaAs, **167**, 161

Alumina
Structural chemistry of anodic alumina, **173**, 209

Aluminium
Al_3Ti formation of diffusion of aluminum through titanium, **166**, 21
Aluminium metallization of polyester and polypropylene films: properties and transmission electron microscopy microstructure investigations, **174**, 155
Aluminium nitride films made by low pressure chemical vapour deposition: preparation and properties, **169**, 241
Characterization of surface layers produced by ion implantation of nitrogen in bulk aluminum, **168**, 263
Chemical effect of CH_4^+ implantation into iron, nickel and aluminium thin films, **170**, 211
Chemical effect of N_2^+ implantation into iron, nickel and aluminium thin films, **169**, 79
Chemical stability of vanadium boride with aluminum, **166**, 29
A comparison of the step coverage of aluminum coatings produced by two sputter magnetron systems and a dual-beam ion system, **166**, 45
Composition of magnetron-sputtered aluminum alloy films, **173**, L115
Development of an Al_2O_3–Co selective absorber for solar collectors, **172**, 19
Effect of surface precipitation of titanium carbide on adherence of alumina films on steels, **177**, 107

0040-6090/90/$3.50

© Elsevier Sequoia/Printed in The Netherlands

Effect of V–O barriers in Cr–Si–O/V–O/Al thin film system, **177**, 315
Electrical resistivity and structural changes in amorphous $Ge_{1-x}Al_x$ thin films under thermal annealing, **167**, 57
Electrocolouring of anodized aluminium with copper: effect of porous and barrier oxide film thicknesses, **173**, 299
Epitaxial growth of WO_3 thin films on MgO and Al_2O_3, **168**, 133
Growth of GaAs and AlAs thin films by a new atomic layer epitaxy technique, **174**, 63
$In_{0.30}Al_{0.70}As/In_{0.30}Ga_{0.70}As$ quasi-insulating gate strained-layer field effect transistors grown by molecular beam epitaxy, **166**, 155
Interface reaction between sputter-deposited Al_2O_3 and stainless steels, **172**, 35
Intermetallic phase formation in aluminium and iron thin film systems, **167**, 203
The laser surface melting of aluminium–silicon-based alloys, **177**, 133
Mechanical behavior of aluminum and Al–Cu(2%) thin films, **166**, 291
Metal–organic vapour phase epitaxy: a thin film technology for large-scale production of high power GaAs/GaAlAs laser diodes, **175**, 213
Moisture patches in Al_2O_3/SiO_2 quarterwave reflectors studied by fringes of equal chromatic order like experiments, **168**, L43
Observations on aluminium diffusion and its effect on the specific contact resistance of Al/W/Si ohmic contact, **176**, 91
Oxidation studies of aluminium thin films by Raman spectroscopy, **170**, 35
Reduced aluminium electromigration in future integrated circuits—a problem of test procedure and threshold mechanisms, **175**, 29
Reflectivity of sputtered aluminum alloy films, **167**, L35
Scratch adhesion test of magnetron-sputtered copper coatings on aluminium substrates: effects of the surface preparation, **168**, 193
The structure and composition of contacts made of Al(2%Cu)–TiW films on amorphized (100) silicon, **176**, 131
Structure and properties of thin films of amorphous aluminium based alloys prepared by sputtering, **174**, 25
A surface plasmon–polariton study of the dielectric constants of reactive metals: aluminium, **167**, 73
Temperature and thickness dependence of the resistivity of thin polycrystalline aluminium, cobalt, nickel, palladium, silver and gold films, **167**, 25
Tungsten silicide barrier layers in aluminium ohmic contact systems, **177**, 9
Ultramicrohardness of aluminum and aluminum alloy thin films, **172**, 51
Amino acids
Langmuir–Blodgett films of long-chain derivatives of amino acid containing aromatic rings, **178**, 355
Ammonia
Structure and ammonia sensitivity of thin platinum or iridium gates in metal–oxide–silicon capacitors, **177**, 77
Amorphization
Phase sequence in the solid state amorphization reaction of metallic thin films, **174**, 11
Amphiphiles
Control of aggregated structures in monolayers and multilayers by mixing at the molecular level of two azobenzene-linked amphiphiles, **178**, 541
Langmuir–Blodgett films containing heterocycles: mixing of amphiphilic compounds, **178**, 351
Mixing at the molecular level of two designed azobenzene-linked amphiphiles at the air–water interface, **173**, L135
Monolayers and Langmuir–Blodgett films of amphiphilic cyanine dye with a mesogenic unit in the hydrophobic part: effect of matrix molecules, **178**, 367
Z-type films from diacetylene amphiphiles, **178**, 203
Anion incorporation
Influence of anion incorporation and argon implantation of substrate on ionic transport through anodic Nb_2O_5 films studied by X-ray photoelectron spectroscopy measurements, **168**, 21
X-ray photoelectron spectroscopy and Rutherford backscattering spectrometry study of anion incorporation in anodically grown films, **167**, 245
Anisotropy
Ellipsometric study of the optical anisotropy of lead arachidate Langmuir films, **177**, 305
In-plane anisotropy in Langmuir–Blodgett films of a copper phthalocyanine derivative, **178**, 439
Annealing
The annealing behaviour of electroless non-crystalline nickel phosphorus films, **169**, 229
Crystallization of amorphous silicon films using a multistep thermal annealing process, **167**, 101
Effects of ion implantation on the annealing

behaviour of amorphous germanium and gold bilayers, **173**, 77
Electrical resistivity and structural changes in amorphous $Ge_{1-x}Al_x$ thin films under thermal annealing, **167**, 57
Ti/Ni bilayers on silicon: sputter-induced intermixing, rapid thermal annealing and ternary silicide formation, **177**, 263
Anthracene
On the fluorescence of anthracene chromophores in Langmuir–Blodgett films, **169**, 127
Antimony
Capacitance–voltage measurements on a p-type InSb metal/insulator/semiconductor structure with Si_3N_4 as the insulator, **168**, 157
Crystallization of amorphous antimony layers on as-deposited ultrathin sublayers of silver, **167**, 223
Effect of hydrostatic pressure on resistivity of InSb thin films heavily doped with group VI elements, **174**, 245
Effect of tin doping on InSb thin films, **172**, 71
Electrical and optical properties of $Ge_{20}Sb_xSe_{80-x}$ thin films, **170**, 15
Ellipsometric investigation of the growth mode of antimony overlayers on GaAs(110), **177**, 287
Ion-beam-induced Sb–Si mixing, **170**, 127
A secondary ion mass spectrometry analysis of hydrogen reactions on disordered InSb(110) surfaces, **168**, 71
The structure of InAs/GaSb superlattices, **170**, 49
Antireflective coatings
Optimization study of titanium silica antireflective coatings in high efficiency silicon solar cells, **172**, 15
Argon
The effect of argon during the plasma-assisted chemical vapor deposition of TiN, **167**, L31
Influence of anion incorporation and argon implantation of substrate on ionic transport through anodic Nb_2O_5 films studied by X-ray photoelectron spectroscopy measurements, **168**, 21
Aromatic rings
Langmuir–Blodgett films of long-chain derivatives of amino acid containing aromatic rings, **178**, 355
Arsenic
Effect of encapsulation on the reaction between palladium and GaAs thin films, **166**, 63
The effect of oxygen adsorption on the electronic properties of the polar GaAs(111) surface after thermal cleaning in ultrahigh vacuum, **170**, 219
Ellipsometric investigation of the growth mode of antimony overlayers on GaAs(110), **177**, 287
An evaluation of some physical characteristics of $CdSnAs_2$ thin films, **176**, 207
Growth of GaAs and AlAs thin films by a new atomic layer epitaxy technique, **174**, 63
Improvements in the topography of AuGeNi-based ohmic contacts to n-GaAs, **176**, 55
$In_{0.30}Al_{0.70}As/In_{0.30}Ga_{0.70}$ as quasi-insulating gate strained-layer field effect transistors grown by molecular beam epitaxy, **166**, 155
Interdiffusion between some refractory metal silicides and GaAs, **169**, 223
Metal–organic vapour phase epitaxy: a thin film technology for large-scale production of high power GaAs/GaAlAs laser diodes, **175**, 213
Physical properties of arsenic-doped tin oxide thin films, **176**, 99
Physico-chemical characterization of thin films obtained by fluorination of GaAs under 5 bar of fluorine, **170**, 259
Quantitative comparison of a tungsten and a tantalum cracker cell for epitaxy with arsine, **174**, 75
Rapid IR lamp alloying of nickel-based ohmic contacts on n-GaAs, **167**, 161
The selective removal of the negative high-resolution photoresist system Ag–As–S, **173**, 129
Slow positron annihilation spectroscopy of heterojunctions and homojunctions of GaAs-based semiconductor thin films, **166**, 349
The structure of InAs/GaSb superlattices, **170**, 49
A study of Au/GaAs Schottky barriers with a cesiated interface, **173**, L149
Thermal stability of $TaSi_x$/n-GaAs metallizations, **176**, 187
Atomic layer epitaxy
Growth of GaAs and AlAs thin films by a new atomic layer epitaxy technique, **174**, 63
Atomic resolution
Atomic resolution with a new atomic force tip, **175**, 81
Auger depth profiles
Sputtering effects in Auger depth profiles of TiN thin films, **174**, 143
Auger electron spectroscopy
Auger electron spectroscopy study of low coverage palladium adsorption on Si(111), **172**, 141
Chemical bonding in microcrystalline Si:H:Cl films studied by ion-induced Auger electron spectroscopy, **173**, L109

Compositional analysis of lead titanate thin films by Auger electron spectroscopy and their electrical properties, **171**, 251
Determination of the composition of sputtered silicon oxynitride films by Auger electron spectroscopy and Rutherford backscattering spectrometry, **167**, L1
KVV Auger spectra of tetracyanoquinodimethane semiconducting films, **176**, 283
Modifications of InP(100) surfaces induced by electron beam during Auger measurement, **172**, L65.
Azobenzene
Control of aggregated structures in monolayers and multilayers by mixing at the molecular level of two azobenzene-linked amphiphiles, **178**, 541
Mixing at the molecular level of two designed azobenzene-linked amphiphiles at the air–water interface, **173**, L135

B

Barium
Characterization of a plasma-sprayed YBaCuO superconductor, **168**, 231
Characterization of ion-beam- and magnetron sputtered $YBa_2Cu_3O_{7-x}$ high T_c superconducting films by secondary neutral mass spectrometry depth profiling, **174**, 255
Effects of deposition conditions on the superconducting properties of r.f. and d.c. magnetron sputter-deposited $YBa_2Cu_3O_{7-x}$ films, **166**, 181
Growth and properties of $YBa_2Cu_3O_{7-x}$ superconducting thin films, **166**, 171
Growth of $BaTiO_3$–$SrTiO_3$ thin films by r.f. magnetron sputtering, **169**, 249
The influence of structure on the piezoelectric properties of $BaTiO_3$ and $(BaSr)TiO_3$ thin films with a diffuse phase transition, **176**, 227
Note on the heteroepitaxial growth of $Ba_{1-x}Sr_xTiO_3$ thin films on MgO, **173**, L139.
Optimization of rapid thermal processing to prepare superconducting Y–Ba–Cu–O thin films, **174**, 185
Photoluminescence of CdTe films grown on BaF_2 with PbTe buffer layers by hot-wall epitaxy, **171**, 271
Reactions of $YBa_2Cu_3O_{7-x}$ thin films on silicon substrates, **174**, 5
Superconducting properties of irradiation-induced effects in epitaxial YBaCuO thin films, **174**, 179
Thermally sprayed coatings of $YBa_2Cu_3O_{6+x}$, **166**, 163
Barrier coatings
Thermal cyclic response of yttria-stabilized zirconia/CoNiCr–AlY thermal barrier coatings, **172**, 185
Bismuth
Analysis of the interface of bismuth with polycrystalline selenium thin films, **168**, 249
Crystallization and melting of thin Bi_xSe_{1-x} layers, **177**, 239
Identification of interfacial structures in Bi–Ca-Sr-Cu-O thin film, **173**, 149
Blocking behaviour
On the blocking behaviour of mesa high voltage power devices passivated by semi-insulating polycrystalline silicon films, **168**, 41
Boron
Characterization of HfB_x films deposited by r.f. diode and r.f. magnetron sputtering, **166**, 131
Chemical stability of vanadium boride with aluminum, **166**, 29
Chemical vapour deposition of boron carbides. I: phase and chemical composition, **172**, 81
Chemical vapour deposition of boron carbides. II: morphology and microstructure, **172**, 95
Electrical properties of boron-doped hydrogenated amorphous silicon films prepared by glow discharge decomposition in dilute silane, **176**, 79
Modelling of reactive sputtering of titanium boride, **172**, 241
Reactive sputtering of titanium boride, **172**, 133
X-ray and electron microscopy study of amorphous boron nitride films, **172**, L75
Bubble formation
Microscopic bubble formation and collapse at liquid–solid interfaces during electrical powering of thin film structures, **166**, 335

C

Cadmium
Characterization of Langmuir–Blodgett films of cadmium stearate by Penning ionization electron spectroscopy, **178**, 305
A comparison of molecular beam epitaxy and ion-beam sputtering for growth of CdTe and HgCdTe films, **168**, 307
Comparison of thermal stability of Langmuir–Blodgett films of icosanoic acid and cadmium icosanoate, **178**, 453
A comparison of the sulfide–polysulfide and ferro–ferricyanide electrolytes in a photo-

electrochemical cell with electrochemically deposited CdSe films, **174**, 295
Electrical and photoconducting properties of vacuum evaporated pure and silver-doped CdSe films, **174**, 233
An electrochemical study of sprayed CdS and CdZnS films, **170**, 171
An evaluation of some physical characteristics of $CdSnAs_2$ thin films, **176**, 207
The grain growth of $CdS_{0.6}Se_{0.4}$ films, **177**, L187
Identification of interfacial structures in Bi–Ca–Sr–Cu–O thin film, **173**, 149
The influence of photoangular effect on dynamic characteristics of the current in CdS(Cu,Cl) thin films, **167**, L15
Interaction of metals with cadmium arachidate Langmuir–Blodgett films studied by X-ray photoelectron spectroscopy, **175**, 95
Metal–organic chemical vapour deposition of CdS onto (111) silicon substrates, **176**, 143
A new approach to the fabrication of cuprous sulphide–cadmium sulphide solar cells, **167**, 169
Photoangular effect in CdS(Cu,Cl) thin films, **175**, 249
Photoluminescence of CdTe films grown on BaF_2 with PbTe buffer layers by hot-wall epitaxy, **171**, 271
Physical properties of electrochemically deposited cadmium mercury telluride films, **169**, 315
Preparation of polycrystalline $Cd_{1-x}In_xCr_2Se_4$ thin films, **174**, 71
Properties of CdS:In thin films grown by ionized deposition, **176**, 247
Temperature-dependent electron diffraction studies of cadmium arachidate monolayers and multilayers, **178**, 511
Wave interference effects in liquid phase epitaxial layers of $Hg_{1-x}Cd_xTe$, **169**, 25

Caesium
A study of Au/GaAs Schottky barriers with a cesiated interface, **173**, L149

Capacitors
A metal/(organic bilayer)/metal capacitor, **168**, 151
Tantalum oxide films for monolithic capacitor applications, **176**, 45

Capillary waves
Detection of longitudinal waves in resonance with capillary waves at the air–water interface by energy transfer, **178**, 61

Capping layers
Optically matched capping layers for CO_2 laser recrystallization of polysilicon, **168**, 35

Carbon
Atomic structure of amorphous $Si_{1-x}C_x$ films prepared by r.f. sputtering, **173**, 235
The bond structures and properties of chemically vapour deposited amorphous SiC, **166**, 367
Characterization of plasma-deposited amorphous hydrogenated carbon films by neutron reflectivity, **172**, 269
Chemical vapour deposition of boron carbides. I: Phase and chemical composition, **172**, 81
Chemical vapour deposition of boron carbides. II: morphology and microstructure, **172**, 95
Crystallization of β-WC_{1-x} in W–C multilayers, **176**, L177
Effect of ion bombardment during growth on the electrical resistivity of magnetron-sputtered carbon films, **168**, 239
Electrical properties of carbon black–polyimide thick films, **168**, 169
Electronic structure of plasma-deposited amorphous Si–C alloy films, **168**, 175
Interface analysis of sputtered W–C, Rh–C and Ni–C multilayers for soft X-ray applications, **175**, 161
Mass spectrometric study of gas evolution from plasma-deposited fluoro-hydrogenated amorphous carbon films on heating, **167**, 255
Metal–insulator transition in thin granular palladium–carbon mixture films, **174**, 225
A new concept of metal–resin adhesion using an intermediate layer of SiO_x–C, **169**, 159
Optically matched capping layers for Co_2 laser recrystallization of polysilicon, **168**, 35
Preparation of amorphous i-C films by ion-assisted methods, **171**, 157
Properties of hydrogenated amorphous silicon carbide films prepared by plasma-enhanced chemical vapor deposition, **177**, 253
Reactive-magnetron-sputtered chromium carbide films, **169**, 281
Synthesis of gold–carbon composites by simultaneous sputtering and plasma polymerization of propane in r.f. capacitively coupled diode system (13.56 MHz), **168**, 81
The temperature dependence of electrical conduction in a discontinuous carbon film device between silver film electrodes, **169**, 187
Temperature influence on carbon ion implantation of iron, **170**, 81

Carboxylic acid
Forces between carboxylic acid layers in divalent salt solutions, **178**, 261

The stability of carboxylic acid Langmuir–Blodgett films as studied by the surface force technique, **176**, 157
Carotenoids
Well organized Langmuir–Blodgett films based on push–pull carotenoids, **178**, 387
Cathodic arc plasma deposition
Cathodic arc plasma deposition technology, **167**, 175
Ceramic beams
Ceramic beams and thin film growth, **166**, 139
Ceramics
Wear of Co–Ni thin film magnetic recording tape against metallic and ceramic surfaces, **166**, 375
Channel mobility
Influence of helium plasma UV radiation on the channel mobility and charges in $Si–SiO_2$ structures, **169**, 43
Charge carriers
Scattering of charge carriers in transparent and conducting thin oxide films with a non-parabolic conduction band, **174**, 217
Charge distribution
Control of interfacial equilibria by local charge distribution and average surface potential, **178**, 53
Chemical deposition
Physical properties of electrochemically deposited cadmium mercury telluride films, **169**, 315
Preparation and characterization of chemically deposited $CuInSe_2$ films, **167**, L19
Chemical vapour deposition
Aluminium nitride films made by low pressure chemical vapour deposition: preparation and properties, **169**, 241
The bond structures and properties of chemically vapour deposited amorphous SiC, **166**, 367
Chemical vapour deposition of boron carbides. I: phase and chemical composition, **172**, 81
Chemical vapour deposition of boron carbides. II: Morphology and microstructure, **172**, 95
The direct photochemical vapour deposition of SiO_2 from Si_2H_6 and N_2O_3 mixtures, **168**, 345
The effect of argon during the plasma-assisted chemical vapor deposition of TiN, **167**, L31
The effect of reactant gas composition on the plasma-enhanced chemical vapour deposition of TiN, **169**, 57
Experimental and thermodynamical investigation of selective low pressure chemical vapour deposition of tungsten using WC16 as tungsten source, **176**, 263
Factorial experimental investigation of plasma-enhanced chemical vapor deposition of silicon nitride thin films, **168**, 281
Formation of polymerized thiophene films by photochemical vapour deposition, **177**, 295
Garnet thin film deposited by a new chemical vapour deposition, **175**, 281
Hydrogen incorporation scheme in a-Si:H prepared by photochemical vapour deposition, **167**, L23
The influence of unsteady state plasma on the properties of a-Si:H films formed by glow discharge-chemical vapour deposition, **177**, 161
Kinetic model of morphological instabilities in chemical vapor deposition, **177**, 141
Metal–organic chemical vapour deposition of CdS onto (111) silicon substrates, **176**, 143
Novel organometallic starting materials for group III–V semiconductor metal–organic chemical vapour deposition, **174**, 1
On the use of zinc acetate as a novel precursor for the deposition of ZnO by low-pressure metal–organic chemical vapour deposition, **173**, 95
Oxynytride layers obtained by anodic oxidation of plasma-enhanced chemically vapour deposited Si_3N_4 films, **175**, 49
Plasma-enhanced chemical vapour deposition of silicon dioxide using tetraethoxysilane as silicon source, **174**, 57
Plasma-enhanced chemical vapor deposition of tungsten, **170**, 91
Preparation of graded-index thin films with specific index-profile by metal–organic chemical vapour deposition, **169**, 271
Properties of hydrogenated amorphous silicon carbide films prepared by plasma-enhanced chemical vapor deposition, **177**, 253
Selective low pressure chemical vapour deposition of tungsten: deposition kinetics, selectivity and film properties, **175**, 55
Structural and technological properties of heavily *in situ* phosphorus-doped low pressure chemically vapour deposited silicon films, **175**, 43
Structure and properties of metallic Sn–Zn alloy films prepared by plasma-enhanced metal-organic chemical vapor deposition, **177**, 271
Substrate-dependent growth of atmospheric pressure chemically vapor deposited silicon dioxide from dichlorosilane and oxygen, **171**, 291
A thermodynamic and experimental approach to $TaSi_2$ chemical vapour deposition, **177**, 189

Use of binuclear organometallic compounds in chemical vapour deposition, **167**, 195
Chlorine
Atomically thin epitaxial films of NaCl on germanium, **172**, 123
Crystallization of β-WC_{1-x} in W–C multilayers, **176**, L177
The influence of photoangular effect on dynamic characteristics of the current in CdS-(Cu,Cl) thin films, **167**, L15
Photoangular effect in CdS(Cu,Cl) thin films, **175**, 249
Photovoltaic characterization of amorphous hydrogenated and chlorinated silicon films, **170**, 163
Chromism
Surface-pressure-induced chromism in rhodamine monolayers, **178**, 473
Chromium
A chromium carbide phase with B1 structure in thin films prepared by ion plating, **167**, 233
Effect of V–O barriers in Cr–Si–O/V–O/Al thin film system, **177**, 315
Ellipsometric analysis of thin NiCr films, **169**, 213
An ellipsometric study of the effects of thickness and substrate on CoCr films, **170**, 273
Interdiffusion of an Au/Ni/Cr multilayer metallization on silicon substrates, **173**, 39
On the relations between the α-Cr and δ-Cr phases, **171**, 33
Preparation and optical properties of thin films of CrO_3 and Cr_2O_3 prepared by the method of chemical spray pyrolysis, **169**, 235
Preparation of polycrystalline $Cd_{1-x}In_xCr_2Se_4$ thin films, **174**, 71
Reactions of r.f.-sputtered chromium films with gallium and tin, **176**, L173
Reactive-magnetron-sputtered chromium carbide films, **169**, 281
A two-band model of conductivity to interpret chromium layer electron characteristics, **173**, 163
Chromophores
Fluorescence characteristics, formation mechanism and chromophore association of ω-(1-pyrenyl)alkanoic acid films prepared by vacuum deposition, **169**, 323
On the fluorescence of anthracene chromophores in Langmuir–Blodgett films, **169**, 127
Photochemical properties of mixed monolayer assemblies containing carbazolyl chromophores, **178**, 399
Cleanliness
Commonly used criteria for checking the cleanliness of Langmuir–Blodgett equipment and spreading solvents are not sufficient, **178**, 563
Cobalt
Characterisation of thin films of metallic molybdenum deposited onto a CoO(100) surface, **168**, 61
Development of an Al_2O_3–Co selective absorber for solar collectors, **172**, 19
Domain nucleation and wall movement in TbFeCo, **175**, 265
Effect of stress on the superconducting properties of $CoSi_2$ thin films, **174**, 285
Electrical resistivity of nanocrystalline FeCo thin films, **176**, L161
An ellipsometric study of the effects of thickness and substrate on CoCr films, **170**, 273
Magnetic aftereffects in ultrathin cobalt films with perpendicular anisotropy, **175**, 341
Resistivity, Hall effect and magnetoresistivity of amorphous iron and cobalt alloy films and their applications, **175**, 325
Solid state reaction in crystalline and amorphous Co–Zr multilayers, **174**, 45
Temperature and thickness dependence of the resistivity of thin polycrystalline aluminium, cobalt, nickel, palladium, silver and gold films, **167**, 25
Wear of Co–Ni thin film magnetic recording tape against metallic and ceramic surfaces, **166**, 375
Colloidal media
Optical coatings prepared from colloidal media, **175**, 173
Columnar grains
Well-defined columnar gains in iron films prepared on seed layers, **169**, 289
Columnar growth
Column growth in layers produced by vaporization, **167**, 281
High resolution studies of columnar growth in obliquely deposited metal films on glass, **173**, L123
Compression
An apparatus for the study of molecular monolayers compressed at the air–water interface with uniform shear, **178**, 191
Convective monolayer compression in channel flow: behaviour and transfer of soluble and insoluble films, **178**, 145
Surface pressure distribution of spread monolayers during compression, **178**, 165
Computer modelling
An evaluation of four computer modelling programs for Rutherford backscattering spectrometry analysis of oxidized surfaces, **166**, 201

Computer simulations
Structural evolution in continuous variation-of-incidence thin films: a computer simulation, **176**, 309
Condensation
Possibility of bose condensation of excitons in a size-quantized semiconductor disc, **170**, 321
Condensed films
Aspects of Langmuir trough design in relation to the study of molecular monolayers of polymers and condensed films, **178**, 17
Conductivity
Conductivity and optical absorption in amorphous gallium sulphide thin films, **172**, 179
Frequency-dependent conductivity in vanadium pentoxide gel, **167**, 67
The temperature dependence of electrical conduction in a discontinuous carbon film device between silver film electrodes, **169**, 187
Contact applications
Reactive-ion-etch-compatible metallization for partially covered contact applications, **166**, 55
Copper
Characterization of a plasma-sprayed YBaCuO superconductor, **168**, 231
Characterization of ion-beam- and magnetron sputtered $YBa_2Cu_3O_{7-x}$ high T_c superconducting films by secondary neutral mass spectrometry depth profiling, **174**, 255
Chemically deposited Cu_2O thin film as an oxygen pressure sensor, **167**, 309
Diode, r.f. sputtering of copper and copper oxide thin films and multilayers, **174**, 91
Effects of deposition conditions on the superconducting properties of r.f. and d.c. magnetron sputter-deposited $YBa_2Cu_3O_{7-x}$ films, **166**, 181
Electrical properties of copper-doped ZnTe films, **176**, L183
Electrocolouring of anodized aluminium with copper: effect of porous and barrier oxide film thicknesses, **173**, 299
Growth and properties of $YBa_2Cu_3O_{7-x}$ superconducting thin films, **166**, 171
Growth of $CuInSe_2$ by two magnetron sputtering techniques, **171**, 109
Identification of interfacial structures in Bi–Ca–Sr–Cu–O thin film, **173**, 149
The influence of photoangular effect on dynamic characteristics of the current in CdS-(Cu,Cl) thin films, **167**, L15
In-plane anisotropy in Langmuir–Blodgett films of a copper phthalocyanine derivative, **178**, 439
Laser-induced reaction in Cu–In–Se systems, **170**, 227
Mechanical behavior of aluminum and Al–Cu(2%) thin films, **166**, 291
A new approach to the fabrication of cuprous sulphide–cadmium sulphide solar cells, **167**, 169
On the growth of $CuInS_2$ thin films by three-source evaporation, **168**, 113
Optimization of rapid thermal processing to prepare superconducting Y–Ba–Cu–O thin films, **174**, 185
Photoangular effect in CdS(Cu,Cl) thin films, **175**, 249
Preparation and characterization of chemically deposited $CuInSe_2$ films, **167**, L19
Preparation of copper indium disulphide films by airless spraying, **167**, 217
Reactions of $YBa_2Cu_3O_{7-x}$ thin films on silicon substrates, **174**, 5
Reduction kinetics of thin and thick cupric oxide films at room temperature by hydrazine, **169**, 143
Scratch adhesion test of magnetron-sputtered copper coatings on aluminium substrates: effects of the surface preparation, **168**, 193
The structure and composition of contacts made of Al(2%Cu)–TiW films on amorphized (100) silicon, **176**, 131
The structure of copper layers obtained from electroless plating solutions with and without a polyoxyethylene compound, **173**, 139
Studying the interface of Au–Cu superlattices, **170**, 99
Superconducting properties of irradiation-induced effects in epitaxial YBaCuO thin films, **174**, 179
Surface accumulation and monolayer coverage during grain boundary diffusion in polycrystalline Cu/Ni bilayers, **174**, 99
Thermally sprayed coatings of $YBa_2Cu_3O_{6+x}$, **166**, 163
X-ray photoelectron spectroscopy study of lipid-free multilayer systems of copper phthalocyanine tetrasulphonate, **178**, 221
X-ray photoelectron spectroscopy study of the synthesis of copper sulphide in Langmuir–Blodgett films, **178**, 535
Coronene
Epitaxial growth of thin films of perylenetetracarboxylic dianhydride and coronene on NaCl(001), **175**, 89
Corrosion
Effect of laser nitridation on the electrochemical corrosion behaviour of 316 stainless steel, **176**, 197

Cracker cells
Quantitative comparison of a tungsten and a tantalum cracker cell for epitaxy with arsine, **174**, 75
Cracking
Statistical study of the cracking of coatings. I: theory, **172**, 197
Statistical study of the cracking of coatings. II: the case of molybdenum coatings, **172**, 211
Creep
Effects of CoCrAlY coating on microstructural stability and creep behaviour of a nickel-base superalloy, **168**, 207
Crystallization
Crystallization and melting of thin Bi_xSe_{1-x} layers, **177**, 239
Crystallization of amorphous silicon films using a multistep thermal annealing process, **167**, 101
Crystallization of amorphous antimony layers on as-deposited ultrathin sublayers of silver, **167**, 223
Optically matched capping layers for CO_2 laser recrystallization of polysilicon, **168**, 35
Recrystallization of silicon-on-insulator layers in pulsed nanosecond heating (model calculations), **171**, 235
A transmission electron microscopy study of the crystallization of ion-beam-mixed $Pd_{80}Si_{20}$ amorphous thin films, **167**, 141
A transmission electron microscopy study on the crystallization of amorphous Ni–P electroless deposited coatings, **166**, 273
Current-measuring techniques
Investigation of a fatty acid monolayer at the air–water interface using a current-measuring technique, **178**, 67

D

Data storage
Application of magnetic thin films for high-density data storage, **175**, 287
Densification
"Thermally stimulated area relaxations" of insoluble monolayers and densification of Langmuir–Blodgett films with "isobaric thermal treatment" of monolayers, **178**, 37
Depth profiling
Absolute depth profiling of thin film systems by low energy secondary neutral mass spectrometry, **174**, 133
N-*N*′-diarachidoylindigo
Characterization of *N*-*N*′-diarachidoylindigo transferred onto a surface acoustic wave device, **178**, 197
Dibutylindium thiolate
Preparation of transparent and conducting indium oxide films by solution pyrolysis of dibutylindium thiolate, **167**, L27
Dielectric breakdown
On the origin of the dielectric breakdown mechanism in plasma-polymerized hexamethyldisiloxane films, **170**, 235
Dielectric constants
A surface plasmon–polarition study of the dielectric constants of reactive metals: aluminium, **167**, 73
Dielectric islands
Polarizability of dielectric islands on a substrate, **173**, 175
Dielectric multilayers
High reflectance bands of some simple two-material dielectric multilayers, **167**, 33
Diffusion
Al_3Ti formation by diffusion of aluminum through titanium, **166**, 21
Comparison of the diffusion barrier properties of tungsten films prepared by hydrogen and silicon reduction of tungsten hexafluoride, **171**, 343
Interdiffusion between some refractory metal silicides and GaAs, **169**, 223
Observations on aluminium diffusion and its effect on the specific contact resistance of Al/W/Si ohmic contact, **176**, 91
Oxidation and diffusion in black chrome selective solar absorber coatings, **177**, 95
Reactively sputtered indium oxide diffusion barrier, **166**, 15
Surface accumulation and monolayer coverage during grain boundary diffusion in polycrystalline Cu/Ni bilayer, **174**, 99
Diffusion layers
A technique for determination of microhardness profiles in thin surface diffusion layer, **175**, L153
Digital image processing
Digital image processing for investigation of domain structure in garnet films, **175**, 299
Diodes
Preparation and properties of diodes on low-resistivity zinc phosphide films, **176**, 13
Disclination recombination kinetics
Disclination recombination kinetics in water-surface monolayers of 22-tricosenoic acid, **178**, 81
Domain nucleation
Domain nucleation and wall movement in TbFeCo, **175**, 265

Domain structure
Digital image processing for investigation of domain structure in garnet films, **175**, 299
Durability
Optical properties and durability of thin films deposited on vibrating substrates at ultrasonic frequencies, **170**, 27
Dyes
Determination of the optical constants of evaporated dye layers, **170**, 249
Monolayers and Langmuir–Blodgett films of amphiphilic cyanine dye with a mesogenic unit in the hydrophobic part: effect of matrix molecules, **178**, 367

E

Elastic properties
Residual stress in physically vapor deposited films: a study of deviations from elastic behavior, **171**, 197
Electret behaviour
Space charge and electret behaviour in anodic Ta_2O_5 films, **167**, 95
Electrical properties
Comparison of amorphous and crystalline $(Ti,Nb)O_2$ thin films: crystallization microstructure and electrical properties, **174**, 209
Compositional analysis of lead titanate thin films by Auger electron spectroscopy and their electrical properties, **171**, 251
Conducting defects in Langmuir–Blodgett films, **178**, 505
The effect of hydrogen dilution on the electrical properties of hydrogenated amorphous silicon, **169**, 179
Effect of oxygen on the electrical transport in RuO_2, **169**, 17
The effect of water quality on the electrical characteristics of Langmuir monolayers, **173**, L141
Electrical and optical properties of $Ge_{20}Sb_xSe_{80-x}$ thin films, **170**, 15
Electrical and photoconducting properties of vacuum evaporated pure and silver-doped CdSe films, **174**, 233
Electrical characteristics of Ti–Si(100) interfaces, **176**, 173
Electrical defect visualization in insulating Langmuir–Blodgett films, **178**, 499
Electrical properties of sprayed tin oxide layers, **177**, 17
Electrical properties of boron-doped hydrogenated amorphous silicon films prepared by glow discharge decomposition in dilute silane, **176**, 79
Electrical properties of carbon black–polyimide thick films, **168**, 169
Electrical properties of copper-doped ZnTe films, **176**, L183
Electrical resistivity of nanocrystalline FeCo thin films, **176**, L161
Humidity dependence of electrical properties of Si(phthalocyaninato) $(OH)_2$ deposited films, **172**, 159
Nickel silicide formation in electroless plated films on silicon: low temperature growth of Ni_3Si_2, morphology and electrical resistance, **171**, 277
Preparation and optical and electrical properties of co-evaporated $Pb_{1-x}Yb_xTe$ films, **175**, 221
Structural and electrical properties of epitaxial Pb/Ag superlattices, **170**, 241
Studies of electrical and optical properties of SnO_2: P films, **169**, 195
Electrochemical studies
An electrochemical study of sprayed CdS and CdZnS films, **170**, 171
Electrochromic devices
Magnetron-sputtered WO_3 films for electrochromic devices, **175**, 227
Electrochromic properties
Effect of heat treatment on the structure, composition and electrochromic properties of evaporated tungsten oxide films: I, **169**, 257
Electrocolouring
Electrocolouring of anodized aluminium with copper: effect of porous and barrier oxide film thicknesses, **173**, 299
Electrode coatings
Characterization of silver-doped perovskite- and spinel-type electrode coatings, **174**, 85
Electroless alloys
A transmission electron microscopy study on the crystallization of amorphous Ni–P electroless deposited coatings, **166**, 273
Structural changes induced by heating in electroless nickel–phosphorus alloys, **166**, 235
Electroless plating
The structure of copper layers obtained from electroless plating solutions with and without a polyoxyethylene compound, **173**, 139
Electromigration
On the validity of the resistometric technique in electromigration studies of narrow stripes, **172**, L85

Reduced aluminium electromigration in future integrated circuits—a problem of test procedure and threshold mechanisms, **175**, 29
A temperature gradient technique for measuring the activation energy for electromigration, **173**, L129
Electron beam induced currents
Electron beam induced current imaging applied to surface reaction study, **176**, L157
Electron beam resists
Characterization of an N-octadecylacrylamide Langmuir–Blodgett film for application as an electron beam resist, **168**, L47
Electron diffraction
A reflection high energy electron diffraction analysis of the orientation of the monoclinic subcell of 22-tricosenoic acid Langmuir–Blodgett bilayers as a function of the deposition pressure, **172**, 149
Temperature-dependent electron diffraction studies of cadmium arachidate monolayers and multilayers, **178**, 511
Electron mass
Effective electron mass in thin films of the Ge–Se–Ga system, **169**, 169
Electron microscopy
Microstructural properties and density dependence of the optical properties of microcrystalline silicon films by spectroscopic ellipsometry and electron microscopy, **169**, 87
X-ray and electron microscopy study of amorphous boron nitride films, **172**, L75
Electron spectroscopy
Characterization of Ta_2O_5 layers by electron spectroscopy for chemical analysis, Rutherford backscattering spectrometry nuclear reaction analysis and optical methods, **175**, 185
Interaction of metals with cadmium arachidate Langmuir–Blodgett films studied by X-ray photoelectron spectroscopy, **175**, 95
Electron spin resonance
Correlation between electron spin resonance and optical anisotropy in Langmuir–Blodgett films of a merocyanine dye, **178**, 555
Langmuir–Blodgett films of pure long-chain nitroxides, their mixtures and mixtures with stearic acid studied by electron spin resonance, **178**, 271
Electron tunnelling spectroscopy
Study of thin anodic SiO_2 layers on degenerate silicon by inelastic electron tunnelling spectroscopy, **168**, 11
Electronic properties
Electronic structure of plasma-deposited amorphous Si–C alloy films, **168**, 175
Hydrogenated amorphous silicon films deposited by reactive sputtering: the electronic properties, hydrogen bonding and microstructure, **171**, 217
The effect of oxygen adsorption on the electronic properties of the polar GaAs(111) surface after thermal cleaning in ultrahigh vacuum, **170**, 219
Electrophysical properties
The electrophysical properties of anodically grown silicon oxide films, **168**, 51
Elemental analysis
Elemental analysis of surfaces and thin films, **174**, 117
Ellipsometry
Analysis of tin dioxide coatings by multiple angle of incidence ellipsometry, **169**, 1
Ellipsometric analysis of thin NiCr films, **169**, 213
Ellipsometric investigation of the growth mode of antimony overlayers GaAs(110), **177**, 287
Ellipsometric study of low-temperature silicon surface cleaning during the process of reactive ionized cluster beam deposition, **168**, 103
An ellipsometric study of the effects of thickness and substrate on CoCr films, **170**, 273
Ellipsometric study of the optical anisotropy of lead arachidate Langmuir films, **177**, 305
Microstructural properties and density dependence of the optical properties of microcrystalline silicon films by spectroscopic ellipsometry and electron microscopy, **169**, 87
A novel derivative ellipsometric method for the study of the growth of thin films: titanium, **173**, 1
A simple ellipsometric method for the direct determination of the mean refractive index of non-absorbing graded-index thin films with linear index profile, **170**, 1
Simultaneous determination of dispersion relation and depth profile of thorium fluoride thin film by spectroscopic ellipsometry, **166**, 325
Variable angle spectroscopic ellipsometry: a non-destructive characterization technique for ultrathin and multilayer materials, **166**, 317
Encapsulation
Effect of encapsulation on the reaction between palladium and GaAs thin films, **166**, 63
Energy transfer
Detection of longitudinal waves in resonance

with capillary waves at the air–water interface by energy transfer, **178**, 61
Enzymes
On the formation of Langmuir–Blodgett films containing enzymes, **176**, 151
Epitaxy
Atomically thin epitaxial films of NaCl on germanium, **172**, 123
$In_{0.30}Al_{0.70}As/In_{0.30}Ga_{0.70}As$ quasi-insulating gate strained-layer field effect transistors grown by molecular beam epitaxy, **166**, 155
Initial growth and epitaxy of PVD TiN layers on austenitic steel, **173**, 199
Nitrides of titanium, niobium, tantalum and molybdenum grown as thin films by the atomic layer epitaxy method, **166**, 149
Ethanol
A tin oxide thin film sensor with high ethanol sensitivity, **169**, 51
Europium
Dielectric and optical properties of europium oxide films, **177**, 59
Evaporation
Deposition of stainless steel film using pulsed laser evaporation, **171**, 335
Deposition of stoichiometric MoS_2 thin films by pulsed laser evaporation, **168**, 335
Determination of the optical constants of evaporated dye layers, **170**, 249
The effect of heat treatment on the structural properties of electron-beam-evaporated SnO_2 films, **169**, 117
Effect of heat treatment on the structure, composition and electrochromic properties of evaporated tungsten oxide films: I, **169**, 257
Note on the origin of intrinsic stresses in films deposited via evaporation and sputtering, **171**, 81
Observation of molecular orientation in evaporated films of *n*-paraffins, **171**, 359
On the growth of $CuInS_2$ thin films by three-source evaporation, **168**, 113
Reactive evaporation of thin titanium nitride films in ultrahigh vacuum and their friction and wear behavior as a function of contact stress, **173**, 19
Excitons
Possibility of bose condensation of excitons in a size-quantized semiconductor disc, **170**, 321

F

Fatty acids
Adhesion of fatty acid in Langmuir–Blodgett films, **178**, 347
Investigation of a fatty acid monolayer at the air–water interface using a current-measuring technique, **178**, 67
Morphology in Langmuir–Blodgett multilayers of nitroaniline derivative–fatty acid mixtures, **178**, 493
Variations in the surface free energy of fatty acid Langmuir–Blodgett multilayers, **178**, 125
Fermi screening
Comparison of experimental and theoretical Fermi screening of charged impurities in degenerate semiconductors, **176**, 1
Ferric hydroxystearate
Deposition and structure of Langmuir–Blodgett films of ferric hydroxystearate, **178**, 341
Film transfer
Convective monolayer compression in channel flow: behaviour and transfer of soluble and insoluble films, **178**, 145
Fluorescence
Fluorescence characteristics, formation mechanism and chromophore association of ω-(1-pyrenyl)alkanoic acid films prepared by vacuum deposition, **169**, 323
On the fluorescence of anthracene chromophores in Langmuir–Blodgett films, **169**, 127
X-ray microfluorescence analyzer for multilayer metal films, **166**, 263
Fluorescence microscopic monitoring
A convection-free monolayer trough for fluoroescence microscopic monitoring of ultrathin organic films, **178**, 115
Fluorine
Comparison of the diffusion barrier properties of tungsten films prepared by hydrogen and silicon reduction of tungsten hexafluoride, **171**, 343
The deposition mechanisms and microstructures of tungsten films produced by silicon reduction of WF6, **166**, 37
Effect of addition of fluorine to phosphorus-doped tin oxide films, **167**, L7
Photoluminescence of CdTe films grown on $BaF_2$with PbTe buffer layers by hot-wall epitaxy, **171**, 271
Physico-chemical characterization of thin films obtained by fluorination of GaAs under 5 bar of fluorine, **170**, 259
Preparation and characterization of gallium(III) fluoride thin films, **173**, 243
Simultaneous determination of dispersion relation and depth profile of thorium fluoride thin film spectroscopic ellipsometry, **166**, 325

Thermal oxidation of silicon in O_2–SiF_4 mixtures, **169**, 173
Fourier transform IR spectroscopy
Orientation evaluation of polyion complex Langmuir–Blodgett films by Fourier transform IR transmission and reflection-absorption spectroscopy, **178**, 281
Molecular orientation in alternating Langmuir–Blodgett studied by Fourier transform IR transmission and reflection-absorption spectroscopy, **178**, 427
Fractals
The fractal aspects of *suminagashi* and marbling, **178**, 109

G

Gallium
Conductivity and optical absorption in amorphous gallium sulphide thin films, **172**, 179
Effect of encapsulation on the reaction between palladium and GaAs thin films, **166**, 63
The effect of oxygen adsorption on the electronic properties of the polar GaAs(111) surface after thermal cleaning in ultrahigh vacuum, **170**, 219
Effective electron mass in thin films of the Ge–Se–Ga system, **169**, 169
Ellipsometric investigation of the growth mode of antimony overlayers, on GaAs(110), **177**, 287
Growth of GaAs and AlAs thin films by a new atomic layer epitaxy technique, **174**, 63
Improvements in the topography of AuGeNi-based ohmic contacts to n-GaAs, **176**, 55
$In_{0.30}Al_{0.70}As/In_{0.30}Ga_{0.70}As$ quasi-insulating gate strained-layer field effect transistors grown by molecular beam epitaxy, **166**, 155
Interdiffusion between some refractory metal silicides and GaAs, **169**, 223
Metal–organic vapour phase epitaxy: a thin film technology for large-scale production of high power GaAs/GaAlAs laser diodes, **175**, 213
Physico-chemical characterization of thin films obtained by fluorination of GaAs under 5 bar of fluorine, **170**, 259
Preparation and characterization of gallium(III) fluoride thin films, **173**, 243
Rapid IR lamp alloying of nickel-based ohmic contacts on n-GaAs, **167**, 161
Reactions of r.f.-sputtered chromium films with gallium and tin, **176**, L173
Slow positron annihilation spectroscopy of heterojunctions and homojunctions of GaAs-based semi-conductor thin films, **166**, 349
The structure of InAs/GaSb superlattices, **170**, 49
A study of Au/GaAs Schottky barriers with a cesiated interface, **173**, L149
Thermal stability of $TaSi_x$/n-GaAs metallizations, **176**, 187
Garnet
Digital image processing for investigation of domain structure in garnet films, **175**, 299
Garnet thin film deposited by a new chemical vapour deposition, **175**, 281
Gas chromatography
Phase transitions in adsorbed layers. X: application of inverse gas chromatography to the determination of phase diagrams for monolayer films deposited on porous adsorbent surfaces, **173**, 13
Gas dilution
Inert gas dilution: an alternative technique to make layers for a-Si:H solar cells, **174**, 239
Gelatin
Gelatin films with embedded liquid crystals in the conoscopic ray, **173**, L119
Germanium
Atomically thin epitaxial films of NaCl on germanium, **172**, 123
Conductivity, dimensionality and morpholgy of co-sputtered Pb–Ge films, **173**, 185
Effective electron mass in thin films of the Ge–Se–Ga system, **169**, 169
Effects of ion implantation on the annealing behaviour of amorphous germanium and gold bilayers, **173**, 77
Electrical and optical properties of $Ge_{20}Sb_xSe_{80-x}$ thin films, **170**, 15
Electrical resistivity and structural changes in amorphous $Ge_{1-x}Al_x$ thin films under thermal annealing, **167**, 57
Improvements in the topography of AuGeNi-based ohmic contacts to n-GaAs, **176**, 55
Glass
Adhesion measurement of thin films on glass substrates, **171**, 93
High resolution studies of columnar growth in obliquely deposited metal films on glass, **173**, L123
Multilayer structure of metallic glass films in a variable saw delay line, **175**, 335
Glow discharge
Changes in the properties of glow-discharge-deposited microcrystalline silicon films with thickness, **167**, 121
Electrical properties of boron-doped hydrogenated amorphous silicon films prepared by glow discharge decomposition in dilute silane, **176**, 79

The influence of unsteady state plasma on the properties of a-Si:H films formed by glow discharge chemical vapour deposition, **177**, 161
Mass spectrometric studies of positive ions in r.f. glow discharges, **171**, 65
Physical properties and structure of carbon-rich a-SiC:H films prepared by r.f. glow discharge decomposition, **173**, 253
Gold
Characterization of gold layers selectively plated by a pulsed current, **169**, 105
The crystalline structure of ultrathin gold granular films, **173**, 67
Dynamical behavior of platinum and gold surfaces and thin films, **172**, L91
Effects of ion implantation on the annealing behaviour of amorphous germanium and gold bilayers, **173**, 77
Evidence for perpendicular magnetic anisotropy in Fe(110) epitaxial films in the monolayer range on gold, **175**, 311
Improvements in the topography of AuGeNi-based ohmic contacts to n-GaAs, **176**, 55
Interdiffusion of an Au/Ni/Cr multilayer metallization on silicon substrates, **173**, 39
The reliability of integrated circuits protected with Ti–W/Au bumps, **166**, 113
Studying the interface of Au–Cu superlattices, **170**, 99
A study of Au/GaAs Schottky barriers with a cesiated interface, **173**, L149
Synthesis of gold–carbon composites by simultaneous sputtering and plasma polymerization of propane in r.f. capacitively coupled diode system (13.56 MHz), **168**, 81
Graded-index films
Preparation of graded-index thin films with specific index-profile by metal–organic chemical vapour deposition, **169**, 271
A simple ellipsometric method for the direct determination of the mean refractive index of non-absorbing graded-index thin films with linear index profile, **170**, 1
Growth
Ceramic beams and thin film growth, **166**, 139
Growth and properties of $YBa_2Cu_3O_{7-x}$ superconducting thin films, **166**, 171
Growth rate
Effect of temperature rise on the growth rate of anodic SiO_2, **167**, 129

H

Hafnium
Characterization of HfB_x films deposited by r.f. diode and r.f. magnetron sputtering, **166**, 131
Hall effect
Resistivity, Hall effect and magnetoresistivity of amorphous iron and cobalt alloy films and their applications, **175**, 325
Hardness
The influence of substrate hardness on the response of TiN-coated steels to surface deformation, **177**, 117
Microhardness and microstructure of ion-beam-sputtered, nitrogen-doped NiFe films, **166**, 299
A technique for determination of microhardness profiles in thin surface diffusion layer, **175**, L153
Ultramicrohardness of aluminum and aluminum alloy thin films, **172**, 51
Heat treatment
Effects of heating on the molecular orientation of polymeric lipids, **178**, 227
Effects of heat treatment and ion doping of indium oxide, **173**, 59
Preparation of highly oriented Langmuir–Blodgett films: heat treatment of monolayers at the air–water interface, **168**, 141
Recrystallization of silicon-on-insulator layers in pulsed nanosecond heating (model calculations), **171**, 235
Helium
Influence of helium plasma UV radiation on the channel mobility and charges in $Si–SiO_2$ structures, **169**, 43
Heterocycles
Langmuir–Blodgett films containing heterocycles: mixing of amphiphilic compounds, **178**, 351
Hexamethyldisloxane
On the origin of the dielectric breakdown mechanism in plasma-polymerized hexamethyldisiloxane films, **170**, 235
Humidity
Humidity dependence of electrical properties of Si(phthalocyaninato)$(OH)_2$ deposited films, **172**, 159
Hydrazine
Reduction kinetics of thin and thick cupric oxide films at room temperature by hydrazine, **169**, 143
Hydrocarbon chain packing
Two types of hydrocarbon chain packing in Langmuir–Blodgett films: interdigitated and abutted tails, **178**, 433
Hydrogen
Comparison of the diffusion barrier properties

of tungsten films prepared by hydrogen and silicon reduction of tungsten hexafluoride, **171**, 343
Contributions of atomic hydrogen to the low temperature removal of traps at silicon oxide–silicon interfaces, **172**, L101
The effect of hydrogen dilution on the electrical properties of hydrogenated amorphous silicon, **169**, 179
Hydrogen incorporation scheme in a-Si:H prepared by photochemical vapour deposition, **167**, L23
A secondary ion mass spectrometry analysis of hydrogen reactions on disordered InSb(110) surfaces, **168**, 71
Hydrogen bonding
Hydrogenated amorphous silicon films deposited by reactive sputtering: the electronic properties, hydrogen bonding and microstructure, **171**, 217
Hydrostatic pressure
Effect of hydrostatic pressure on resistivity of InSb thin films heavily doped with group VI elements, **174**, 245
Hysteresis
Hysteresis effect in reactive r.f. sputtering and the adjustment of the set point for stoichiometric film deposition, **172**, 61

I

Icosanoic acid
Comparison of thermal stability of Langmuir–Blodgett films of icosanoic acid and cadmium icosanoate, **178**, 453
II–VI films
Linear and nonlinear optical properties of thin evaporated and epitaxial II–VI compound films, **175**, 179
III–V films
New aspects in modern production equipment for III–V processes, **174**, 315
Novel organometallic starting materials for group III–V semiconductor metal–organic chemical vapour deposition, **174**, 1
Studies of formation of thin metal films in III–V compound semiconductors, **175**, 141
Impurities
Impurity distribution of very thin permalloy films, **167**, L39
Indentation
A kinematic model for plastic indentation of a bilayer, **172**, 227
Indium
The anomalous photovoltaic effect in polycrystalline $AgInTe_2$ thin films, **173**, 169
Band gap narrowing and the band structure of tin-doped indium oxide films, **176**, 33
Capacitance–voltage measurements on a p-type InSb metal/insulator/semiconductor structure with Si_3N_4 as the insulator, **168**, 157
Deposition of tin-doped indium oxide films by a modified reactive magnetron sputtering process, **172**, 111
Effect of hydrostatic pressure on resistivity of InSb thin films heavily doped with group VI elements, **174**, 245
Effect of tin doping on InSb thin films, **172**, 71
Effects of heat treatment and ion doping of indium oxide, **173**, 59
Growth of $CuInSe_2$ by two magnetron sputtering techniques, **171**, 109
Heat treatment in hydrogen gas and plasma of transparent conducting oxide films such as ZnO, SnO_2 and indium tin oxide, **176**, 277
$In_{0.30}Al_{0.70}As/In_{0.30}Ga_{0.70}As$ quasi-insulating gate strained-layer field effect transistors grown by molecular beam epitaxy, **166**, 155
Indium tin oxide thin films for metallization in microelectronic devices, **170**, 151
Laser-induced reaction in Cu–In–Se systems, **170**, 227
Modifications of InP(100) surfaces induced by electron beam during Auger measurement, **172**, L65
On the growth of $CuInS_2$ thin films by three-source evaporation, **168**, 113
Optical dispersion in electron-beam-evaporated indium tin oxide thin films, **175**, 241
Preparation and characterization of chemically deposited $CuInSe_2$ films, **167**, L19
Preparation of copper indium disulphide films by airless spraying, **167**, 217
Preparation of polycrystalline $Cd_{1-x}In_xCr_2Se_4$ thin films, **174**, 71
Preparation of transparent and conducting indium oxide films by solution pyrolysis of dibutylindium thiolate, **167**, L27
Properties of CdS:In thin films grown by ionized deposition, **176**, 247
R.f.-sputtered indium tin oxide films on water-cooled substrates, **167**, L11
Reactively sputtered indium oxide diffusion barrier, **166**, 15
A secondary ion mass spectrometry analysis of hydrogen reactions on disordered InSb(110) surfaces, **168**, 71
The structure of InAs/GaSb superlattices, **170**, 49

Insulating films
Electrical defect visualization in insulating Langmuir–Blodgett films, **178**, 499
Integrated circuits
Advanced metallization of very-large-scale integration devices, **175**, 17
Reduced aluminium electromigration in future integrated circuits—a problem of test procedure and threshold mechanisms, **175**, 29
Integrated optics
Integrated optics in $LiNbO_3$, **175**, 191
Interdigitated tails
Two types of hydrocarbon chain packing in Langmuir–Blodgett films: interdigitated and abutted tails, **178**, 433
Interfacial equilibria
Control of interfacial equilibria by local charge distribution and average surface potential, **178**, 53
Interfacial structures
Identification of interfacial structures in Bi–Ca–Sr–Cu–O thin film, **173**, 149
Intermetallic phase formation
Intermetallic phase formation in aluminium and iron thin film systems, **167**, 203
Ion beam mixing
Ion-beam-induced Sb–Si mixing, **170**, 127
Ion-assisted methods
Preparation of amorphous i-C films by ion-assisted methods, **171**, 157
Ion bombardment
Effect of ion bombardment during growth on the electrical resistivity of magnetron-sputtered carbon films, **168**, 239
Film modification by low energy ion bombardment during deposition, **171**, 143
Microstructure modification of TiN by ion bombardment during reactive sputter deposition, **169**, 299
Preparation of TiN thin films by the dynamic mixing method using an N_2^+ ion beam of 1 keV, **171**, 263
Strain, ion bombardment and energetic neutrals in magnetron sputtering, **171**, 183
Ion deposition
Ion and plasma beam assisted thin film deposition, **175**, 119
Ion doping
Effects of heat treatment and ion doping of indium oxide, **173**, 59
Ion etching
A mechanistic study of SF_6 reactive ion etching of tungsten, **176**, 289
Ion implantation
Characterization of surface layers produced by ion implantation of nitrogen in bulk aluminum, **168**, 263
Chemical effect of CH_4^+ implantation into iron, nickel and aluminium thin films, **170**, 211
Chemical effect of N_2^+ implantation into iron, nickel and aluminium thin films, **169**, 79
Effects of ion implantation on the annealing behaviour of amorphous germanium and gold bilayers, **173**, 77
The influence of rapid thermal processing on the properties of $MoSi_2$ layers formed by using the ion implantation through metal technique, **177**, 225
Magnetic properties and defects in polycrystalline nickel films. II: effects of ion implantation, **168**, 1
Process of structure change in iron during titanium implantation, **176**, 165
Temperature influence on carbon ion implantation of iron, **170**, 81
Ion plating
A chromium carbide phase with B1 structure in thin films prepared by ion plating, **167**, 233
Properties of ion-plated Nb_2O_5 films, **175**, 207
Structure and preferred orientations in ion-plated niobium films and correlation of the substrate bias voltage with calculated strain energies, **168**, 221
Ionic contamination
Ionic contamination of thin films of silica by solutions of NaI and KCl, **167**, 45
Ionic transport
Influence of anion incorporation and argon implantation of substrate on ionic transport through anodic Nb_2O_5 films studied by X-ray photoelectron spectroscopy measurements, **168**, 21
Ionized deposition
Ellipsometric study of low-temperature silicon surface cleaning during the process of reactive ionized cluster beam deposition, **168**, 103
Properties of CdS:In thin films grown by ionized deposition, **176**, 247
Iridium
Structure and ammonia sensitivity of thin platinum or iridium gates in metal–oxide–silicon capacitors, **177**, 77
Iron
Chemical characterization of the deactivation and protection of FeTi thin films using complementary non-destructive techniques, **166**, 225
Chemical effect of CH_4^+ implantation into iron, nickel and aluminium thin films, **170**, 211

Chemical effect of N_2^+ implantation into iron, nickel and aluminium thin films, **169**, 79
A comparison of the sulfide–polysulfide and ferro–ferricyanide electrolytes in a photoelectrochemical cell with electrochemically deposited CdSe films, **174**, 295
Crystallographic investigation of the iron films deposited obliquely by sputtering, **176**, 255
Domain nucleation and wall movement in TbFeCo, **175**, 265
Electrical resistivity of nanocrystalline FeCo thin films, **176**, L161
Evidence for perpendicular magnetic anisotropy in Fe(110) epitaxial films in the monolayer range on gold, **175**, 311
The influence of titanium nitride sputter deposition temperature on surface-hardened 2.5% silicon iron, **170**, 293
Intermetallic phase formation in aluminium and iron thin film systems, **167**, 203
Magnetic properties of coupled α/γ-phase Fe–Ni films, **175**, 329
Microhardness and microstructure of ion-beam-sputtered, nitrogen-doped NiFe films, **166**, 299
Process of structure change in iron during titanium implantation, **176**, 165
Resistivity, Hall effect and magnetoresistivity of amorphous iron and cobalt alloy films and their applications, **175**, 325
Study of thin oxidation films in iron alloys by Raman spectroscopy, **174**, 111
Temperature influence on carbon ion implantation of iron, **170**, 81
Well-defined columnar grains in iron films prepared on seed layers, **169**, 289
Isobaric thermal treatment
"Thermally stimulated area relaxations" of insoluble monolayers and densification of Langmuir–Blodgett films with "isobaric thermal treatment" of monolayers, **178**, 37

J

J-aggregate formation
J-aggregate formation of long-chain merocyanine dye in various mixed monolayers and its exciton behaviour in Langmuir–Blodgett films, **178**, 549

K

Kerr observation
High-resolution Kerr observation of magnetic domains, **175**, 273

L

Laser-assisted processes
Laser-assisted processes in the microelectronic industry, **175**, 109
Laser diodes
Metal–organic vapour phase epitaxy: a thin film technology for large-scale production of high power GaAs/GaAlAs laser diodes, **175**, 213
Laser irradiation
Modification of surface films in metallic substrates by excimer laser irradiation, **174**, 33
Lateral conduction
Lateral conduction at a monolayer–water interface, **178**, 73
Lattice parameters
The relationship between residual stress, X-ray elastic constants and lattice parameters in TiN films made by physical vapor deposition, **170**, 63
Lead
Compositional analysis of lead titanate thin films by Auger electron spectroscopy and their electrical properties, **171**, 251
Conductivity, dimensionality and morpholgy of co-sputtered Pb–Ge films, **173**, 185
Ellipsometric study of the optical anisotropy of lead arachidate Langmuir films, **177**, 305
Photoluminescence of CdTe films grown in BaF_2 with PbTe buffer layers by hot-wall epitaxy, **171**, 271
Preparation and optical and electrical properties of co-evaporated $Pb_{1-x}Yb_xTe$ films, **175**, 221
Properties of d.c. magnetron-sputtered lead zirconate titanate thin films, **172**, 251
Structural and electrical properties of epitaxial Pb/Ag superlattices, **170**, 241
Lennard–Jones lattice gas
A two-dimensional Lennard–Jones lattice gas. I: ground state structures, **177**, 333
Lipids
Effects of heating on the molecular orientation of polymeric lipids, **178**, 227
Lateral surface potential distribution of a phospholipid monolayer, **173**, 269
Structural investigations on low-temperature-polymerized monolayers of a diacetylenic bronco lipid, **178**, 289
Liquid phase epitaxy
Growth of monocrystalline thin films of potassium–tantalate–niobate (KTN) by liquid-phase epitaxy, **175**, 201
Wave interference effects in liquid phase epitaxial layers of $Hg_{1-x}Cd_xTe$, **169**, 25

Lithium
Depth profiling of magnesium and titanium-doped $LiNbO_3$ waveguides, **175**, 235
Integrated optics in $LiNbO_3$, **175**, 191
Long-chain compounds
Langmuir–Blodgett films of pure long-chain nitroxides, their mixtures and mixtures with stearic acid studied by electron spin resonance, **178**, 271
Structural control and characterization in mixed and alternate Langmuir–Blodgett films of simple long-chain compounds, **178**, 421
Longitudinal waves
Detection of longitudinal waves in resonance with capillary waves at the air–water interface by energy transfer, **178**, 61

M

Magnesia
Electrical insulating properties of r.f.-sputtered magnesia coatings, **166**, 255
Magnesium
Depth profiling of magnesium and titanium-doped $LiNbO_3$ waveguides, **175**, 235
Epitaxial growth of WO_3 thin films on MgO and Al_2O_3, **168**, 133
Note on the heteroepitaxial growth of $Ba_{1-x}Sr_xTiO_3$ thin films on MgO, **173**, L139
Secondary electron emission studies on MgO films, **167**, 299
The sticking of magnesium on ω-tricosenoic acid multilayers deposited by the Langmuir–Blodgett technique, **167**, 261
Surface plasmon–polariton study of the dielectric function of magnesium, **172**, 27
Magnetic aftereffects
Magnetic affereffects in ultrathin cobalt films with perpendicular anisotropy, **175**, 341
Magnetic anisotropy
Evidence for perpendicular magnetic anisotropy in Fe(110) epitaxial films in the monolayer range on gold, **175**, 311
Magnetic properties and defects in polycrystalline nickel films. I: microstructure-related magnetic anisotropy, **167**, 1
Magnetic domains
High-resolution Kerr observation of magnetic domains, **175**, 273
Magnetic films
Application of magnetic thin films for high-density data storage, **175**, 287
Magnetic media
Temperature dependence of the critical radius of domains in rare earth transition metal alloys for magnetic media, **175**, 305
Magnetic properties
Magnetic properties and defects in polycrystalline nickel films. I: microstructure-related magnetic anisotropy, **167**, 1
Magnetic properties and defects in polycrystalline nickel films. II: effects of ion implantation, **168**, 1
Magnetic properties of coupled α/γ-phase Fe–Ni films, **175**, 329
Magnetic superlattices
Preparation and characterization of magnetic superlattices, **175**, 295
Magnetization
Influence of magnetization variation near the surface on spin wave modes, **170**, 191
Magnetoresistance
Spin waves and magnetoresistance in exchange coupled layered magnetic structures, **175**, 317
Magnetoresistivity
Resistivity, Hall effect and magnetoresistivity of amorphous iron and cobalt alloy films and their applications, **175**, 325
Magnetron deposition
New results in d.c. reactive magnetron deposition of TiN_x films, **167**, 107
Manganese
Strain-sensitive property of vacuum evaporated manganese films, **172**, 45
Marbling
The fractal aspects of *suminagashi* and marbling, **178**, 109
Mass spectrometry
Absolute depth profiling of thin film systems by low energy secondary neutral mass spectrometry, **174**, 133
Characterization of ion-beam- and magnetron sputtered $Yba_2Cu_3O_{7-x}$ high T_c superconducting films by secondary neutral mass spectrometry depth profiling, **174**, 255
Mass spectrometric studies of positive ions in r.f. glow discharges, **171**, 65
Mass spectrometric study of gas evolution from plasma-deposited fluoro-hydrogenated amorphous carbon films on heating, **167**, 255
Preparation of multinary thin films by mass spectrometer control, **174**, 79
A secondary ion mass spectrometry analysis of hydrogen reactions on disordered InSb(110) surfaces, **168**, 71
Mechanical properties
The mechanical properties of monocrystalline nickel electrodeposits, **169**, 35

Mercury
A comparison of molecular beam epitaxy and ion-beam sputtering for growth of CdTe and HgCdTe films, **168**, 307
Physical properties of electrochemically deposited cadmium mercury telluride films, **169**, 315
Wave interference effects in liquid phase epitaxial layers of $Hg_{1-x}Cd_xTe$, **169**, 25
Merocyanine dye
Correlation between electron spin resonance and optical anisotropy in Langmuir–Blodgett films of a merocyanine dye, **178**, 555
J-aggregate formation of long-chain merocyanine dye in various mixed monolayers and its exciton behaviour in Langmuir–Blodgett films, **178**, 549
Metallic glass films
Multilayer structure of metallic glass films in a variable saw delay line, **175**, 335
Metallization
Advanced metallization of very-large-scale integration devices, **175**, 17
Indium tin oxide thin films for metallization in microelectronic devices, **170**, 151
Reactive-ion-etching compatible metallization for partially covered contact applications, **166**, 55
Methacrylic acid
Fabrication of copoly(methacrylic acid–methylacrylate) Langmuir–Blodgett films using a moving-wall-type Langmuir–Blodgett trough, **178**, 175
Microbalance
On the possibility of thin film structure study with a quartz crystal microbalance, **171**, 367
Microdiffraction
Microdiffraction study of icosahedral nickel particles obtained by reduction of a salt in the liquid phase, **167**, 149
Microelectronics
Laser-assisted processes in the microelectronic industry, **175**, 109
Microstructures
Chemical vapour deposition of boron carbides. II: morphology and microstructure, **172**, 95
The deposition mechanisms and microstructures of tungsten films produced by silicon reduction of WF_6, **166**, 37
Microstructuring in semiconductor technology, **175**, 1
Mirrors
Scattering of light in TiO_2 layers of broad band mirrors, **176**, 25
Molecular beam epitaxy
A comparison of molecular beam epitaxy and ion-beam sputtering for growth of CdTe and HgCdTe films, **168**, 307
Molybdenum
Characterization of thin films of metallic molybdenum deposited onto a CoO(100) surface, **168**, 61
Deposition of stoichiometric MoS_2 thin films by pulsed laser evaporation, **168**, 335
Effects of neutral gas incorporation in molybdenum coatings produced by magnetron sputtering, **166**, 309
The influence of rapid thermal processing on the properties of $MoSi_2$ layers formed by using the ion implantation through metal technique, **177**, 225
Nitrides of titanium, niobium, tantalum and molybdenum grown as thin films by the atomic layer epitaxy method, **166**, 149
On the use of a brale indenter to evaluate the cross-sectional morphology of sputter deposited MoS_2 solid lubricant films, **172**, L81
Statistical study of the cracking of coatings. II: the case of molybdenum coatings, **172**, 211
Monte Carlo simulation
On the elemental dependence of the arrival rate of sputtered particles in the Monte Carlo simulation of the particle transport process in sputter deposition, **172**, L105
Morphology
Chemical vapour deposition of boron carbides. II: morphology and microstructure, **172**, 95
Conductivity, dimensionality and morphology of co-sputtered Pb–Ge films, **173**, 185
Kinetic model of morphological instabilities in chemical vapor deposition, **177**, 141
Morphology and structure of TiO_2 thin layers *vs.* thickness and substrate temperature, **170**, 107
Morphology in Langmuir–Blodgett multilayers of nitroaniline derivative–fatty acid mixtures, **178**, 493
Nickel silicide formation in electroless plated films on silicon: low temperature growth of Ni_3Si_2, morphology and electrical resistance, **171**, 277
On the use of a brale indenter to evaluate the cross-sectional morphology of sputter deposited MoS_2 solid lubricant films, **172**, L81

N

Neutron reflectivity
Characterization of plasma-deposited amorph-

ous hydrogenated carbon films by neutron reflectivity, **172**, 269

Nickel

The annealing behaviour of electroless non-crystalline nickel phosphorus films, **169**, 229

Chemical effect of CH_4^+ implantation into iron, nickel and aluminium thin films, **170**, 211

Chemical effect of N_2^+ implantation into iron, nickel and aluminium thin films, **169**, 79

Effects of CoCrAlY coating on microstructural stability and creep behaviour of a nickel-base superalloy, **168**, 207

Ellipsometric analysis of thin NiCr films, **169**, 213

Improvements in the topography of AuGeNi-based ohmic contacts to n-GaAs, **176**, 55

Interdiffusion of an Au/Ni/Cr multilayer metallization on silicon substrates, **173**, 39

Interface analysis of sputtered W–C, Rh–C and Ni–C multilayers for soft X-ray applications, **175**, 161

Magnetic properties and defects in polycrystalline nickel films: I: microstructure-related magnetic anisotropy, **167**, 1

Magnetic properties and defects in polycrystalline nickel films. II: effects of ion implantation, **168**, 1

Magnetic properties of coupled α/γ-phase Fe–Ni films, **175**, 329

The mechanical properties of monocrystalline nickel electrodeposits, **169**, 35

Microdiffraction study of icosahedral nickel particles obtained by reduction of a salt in the liquid phase, **167**, 149

Microhardness and microstructure of ion-beam-sputtered, nitrogen-doped NiFe films, **166**, 299

Nickel silicide formation in electroless plated films on silicon: low temperature growth of Ni_3Si_2, morphology and electrical resistance, **171**, 277

Rapid IR lamp alloying of nickel-based ohmic contacts on n-GaAs, **167**, 161

A spectroscopic study of nickel oxide films on polycrystalline nickel, **177**, 171

Structural changes induced by heating in electroless nickel–phosphorus alloys, **166**, 235

A study of electroless nickel coatings containing low phosphorus, **177**, 207

Surface accumulation and monolayer coverage during grain boundary diffusion in polycrystalline Cu/Ni bilayers, **174**, 99

Temperature and thickness dependence of the resistivity of thin polycrystalline aluminium, cobalt, nickel, palladium, silver and gold films, **167**, 25

Ti/Ni bilayers on silicon: sputter-induced intermixing, rapid thermal annealing and ternary silicide formation, **177**, 263

A transmission electron microscopy study on the crystallization of amorphous Ni–P electroless deposited coatings, **166**, 273

Wear of Co–Ni thin film magnetic recording tape against metallic and ceramic surfaces, **166**, 375

Niobium

Comparison of amorphous and crystalline $(Ti,Nb)O_2$ thin films: crystallization microstructure and electrical properties, **174**, 209

Depth profiling of magnesium and titanium-doped $LiNbO_3$ waveguides, **175**, 235

Growth of monocrystalline thin films of potassium–tantalate–niobate (KTN) by liquid-phase epitaxy, **175**, 201

Influence of anion incorporation and argon implantation of substrate on ionic transport through anodic Nb_2O_5 films studied by X-ray photoelectron spectroscopy measurements, **168**, 21

Integrated optics in $LiNbO_3$, **175**, 191

Mechanism for photosensitization of peroxo-polytungstic acid film by substitution of niobium or tantalum for a part of the tungsten, **172**, L97

Nitrides of titanium, niobium, tantalum and molybdenum growth as thin films by the atomic layer epitaxy method, **166**, 149

Preparation of amorphous thin films of $(Ti,V)O_2$ and $(Ti,Nb)O_2$ by r.f. sputtering, **176**, 111

Properties of ion-plated Nb_2O_5 films, **175**, 207

Structure and preferred orientations in ion-plated niobium films and correlation of the substrate bias voltage with calculated strain energies, **168**, 221

Nitrides

Aluminium nitride films made by low pressure chemical vapour deposition: preparation and properties, **169**, 241

Analysis of TiN by charged particle beams: nuclear reaction analysis, nuclear reaction broadening and Rutherford backscattering, **166**, 191

Capacitance–voltage measurements on a p-type InSb metal/insulator/semiconductor structure with Si_3N_4 as the insulator, **168**, 157

Correlation of refractive index and silicon content of silicon oxynitride films, **168**, 123

Determination of the composition of sputtered silicon oxynitride films by Auger electron spectroscopy and Rutherford backscattering spectrometry, **167**, L1
The effect of argon during the plasma-assisted chemical vapor deposition of TiN, **167**, L31
The effect of reactant gas composition on the plasma-enhanced chemical vapour deposition of TiN, **169**, 57
The effect of target power on the nitrogen partial pressure level and hardness of reactively sputtered titanium nitride coatings, **171**, 171
Factorial experimental investigation of plasma-enhanced chemical vapor deposition of silicon nitride thin films, **168**, 281
Growth and characterization of ZnO films deposited on a monolithic Si_3N_4–SiO_2–Si configuration, **168**, 291
The influence of substrate hardness on the response of TiN-coated steels to surface deformation, **177**, 117
The influence of titanium nitride sputter deposition temperature on surface-hardened 2.5% silicon iron, **170**, 293
Initial growth and epitaxy of PVD TiN layers on austenitic steel, **173**, 199
Microstructure modification of TiN by ion bombardment during reactive sputter deposition, **169**, 299
New results, in d.c. reactive magnetron deposition of TiN_x films, **167**, 107
Nitrides of titanium, niobium, tantalum and molybdenum grown as thin films by the atomic layer epitaxy method, **166**, 149
Position dependences in planar magnetron sputtering of TiN films, **173**, 109
Preparation and characterization of reactively sputtered silicon nitride thin films, **166**, 359
Preparation of TiN thin films by the dynamic mixing method using an N_2^+ ion beam of 1 keV, **171**, 263
Reactive evaporation of thin titanium nitride films in ultrahigh vacuum and their friction and wear behavior as a function of contact stress, **173**, 19
The relationship between residual stress, X-ray elastic constants and lattice parameters in TiN films made by physical vapor deposition, **170**, 63
Structure and properties of ion sulphocarbonitrided coatings on several structural steels, **166**, 281
ε-Ti_2N phase growth control in titanium nitride films, **170**, L55
Titanium nitridation in N_2 and NH_3 high frequency plasma, **173**, 83
X-ray analysis of heat-treated titanium nitride films, **170**, 201
X-ray and electron microscopy study of amorphous boron nitride films, **172**, L75
Nitroaniline
Morphology in Langmuir–Blodgett multilayers of nitroaniline derivative–fatty acid mixtures, **178**, 493
Nitrogen
Characterization of surface layers produced by ion implantation of nitrogen in bulk aluminium, **168**, 263
Chemical effect of N_2^+ implantation into iron, nickel and aluminium thin films, **169**, 79
The effect of target power on the nitrogen partial pressure level and hardness of reactively sputtered titanium nitride coatings, **171**, 171
Microhardness and microstructure of ion-beam-sputtered, nitrogen-doped NiFe films, **166**, 299
Preparation of TiN thin films by the dynamic mixing method using an N_2^+ ion beam of 1 keV, **171**, 263
Self-aligned $TiN_xO_y/TiSi_2$ contact formation, **172**, 1
Thermal stability of TiN films deposited onto silicon substrates, **176**, 7
Non-destructive techniques
Chemical characterization of the deactivation and protection of FeTi thin films using complementary non-destructive techniques, **166**, 225
Resonant low energy electrons and their impact on non-destructive depth profiling of thin film samples, **166**, 213
Variable angle spectroscopic ellipsometry: a non-destructive characterization technique for ultrathin and multilayer materials, **166**, 317
Non-linear optics
Structural investigations of Langmuir–Blodgett films of 2-docosylamino-5-nitropyridine, a new type of non-centrosymmetric multilayer for use in non-linear optics, **178**, 445
Novel organic molecules
Monolayer formation characteristics of novel organic molecules with non-linear optically active moieties, **178**, 243
Nuclear reaction analysis
Characterization of Ta_2O_5 layers by electron spectroscopy for chemical analysis, Rutherford backscattering spectrometry nuclear reaction analysis and optical methods, **175**, 185

O

Octadecanol
Phase transitions in adsorbed layers. XI: the condensed-solid to expanded-liquid transition in an *n*-octadecanol monolayer on a silica gel surface, **173**, 279

N-octadecylacrylamide
Characterization of an *N*-octadecylacrylamide Langmuir–Blodgett film for application as an electron beam resist, **168**, L47

Optical absorption
Conductivity and optical absorption in amorphous gallium sulphide thin films, **172**, 179
Thallium thin film oxidation investigated by an optical absorption method, **168**, 165

Optical anisotropy
Correlation between electron spin resonance and optical anisotropy in Langmuir–Blodgett films of a merocyanine dye, **178**, 555

Optical applications
Structural properties of ZnO films prepared by r.f. sputtering for optical applications, **175**, 255

Optical coatings
Optical coatings prepared from colloidal media, **175**, 173
Theoretical optical properties of polar semiconductors used as optical coatings for energy-efficient windows, **177**, 69

Optical constants
Determination of the optical constants of evaporated dye layers, **170**, 249

Optical dispersion
Optical dispersion in electron-beam-evaporated indium tin oxide thin films, **175**, 241

Optical excitation
Characterization of thermal and deposited thin oxide layers by longitudinal optical–transverse optical excitation in Fourier transform IR transmission measurements, **174**, 159

Optical filters
Tailored target approach to the deposition of gradient index optical filters, **168**, 185

Optical properties
Dielectric and optical properties of europium oxide films, **177**, 59
Electrical and optical properties of $Ge_{20}Sb_xSe_{80-x}$ thin films, **170**, 15
Influence of substrate temperature and post-deposition heat treatment on the optical properties of SiO_2 films, **170**, 179
Linear and nonlinear optical properties of thin evaporated and epitaxial II–VI compound films, **175**, 179
Microstructural properties and density dependence of the optical properties of microcrystalline silicon films by spectroscopic ellipsometry and electron microscopy, **169**, 87
Optical properties and durability of thin films deposited on vibrating substrates at ultrasonic frequencies, **170**, 27
Optical properties of electron-beam-evaporated TiO_2 films, **176**, 181
Optical properties of ZnO films deposited by r.f. sputtering on sapphire substrates, **176**, L167
Preparation and optical and electrical properties of co-evaporated $Pb_{1-x}Yb_xTe$ films, **175**, 221
Preparation and optical properties of thin films of CrO_3 and Cr_2O_3 prepared by the method of chemical spray pyrolysis, **169**, 235
Studies of electrical and optical properties of SnO_2:P films, **169**, 195
Theoretical optical properties of polar semiconductors used as optical coatings for energy-efficient windows, **177**, 69

Optical recording
Reversible optical recording on rare-earth–transition-metal disks, **175**, 261

Optically active moieties
Monolayer formation characteristics of novel organic molecules with non-linear optically active moieties, **178**, 243

Organic bilayers
A metal/(organic bilayer)/metal capacitor, **168**, 151

Organic films
Epitaxial growth and characterization of organic thin films on silicon, **175**, 85
Observation of molecular orientation in evaporated films of *n*-paraffins, **171**, 359

Organometallic compounds
Use of binuclear organometallic compounds in chemical vapour deposition, **167**, 195

Orientation
Effects of heating on the molecular orientation of polymeric lipids, **178**, 227
Minimal spanning tree: a new approach to quantifying the oriented growth of thin films, **177**, 245
Molecular orientation in alternating Langmuir–Blodgett films studied by Fourier transform IR transmission and reflection–absorption spectroscopy, **178**, 427
Observation of molecular orientation in evaporated films of *n*-paraffins, **171**, 359
Orientation evaluation of polyion complex Langmuir–Blodgett films by Fourier trans-

form IR transmission and reflection-absorption spectroscopy, **178**, 281
Structure and preferred orientations in ion-plated niobium films and correlation of the substrate bias voltage with calculated strain energies, **168**, 221
Vertical dipping method as a means of controlling the in-plane molecular orientation in Langmuir–Blodgett films, **178**, 157
Oxidation
Anodic oxidation of tantalum in aqueous electrolytes, **177**, 35
Oxidation and diffusion in black chrome selective solar absorber coatings, **177**, 95
Oxidation studies of aluminium thin films by Raman spectroscopy, **170**, 35
Thallium thin film oxidation investigated by an optical absorption method, **168**, 165
Thermal oxidation of silicon in O_2–SiF_4 mixtures, **169**, 173
Oxides
Analysis of tin dioxide coatings by multiple angle of incidence ellipsometry, **169**, 1
Band gap narrowing and the band structure of tin-doped indium oxide films, **176**, 33
Characterization of a plasma-sprayed YBaCuO superconductor, **168**, 231
Characterization of Ta_2O_5 layers by electron spectroscopy for chemical analysis, Rutherford backscattering spectrometry nuclear reaction analysis and optical methods, **175**, 185
Characterization of thermal and deposited thin oxide layers by longitudinal optical–transverse optical excitation in Fourier transform IR transmission measurements, **174**, 159
Characterization of thin films of metallic molybdenum deposited onto a CoO(100) surface, **168**, 61
Characterization of tin oxide thin films deposited by reactive sputtering, **170**, 285
A characterization study of a hydroxylated polycrystalline tin oxide surface, **169**, 69
Chemically deposited Cu_2O thin film as an oxygen pressure sensor, **167**, 309
Comparison of amorphous and crystalline $(Ti,Nb)O_2$ thin films: crystallization microstructure and electrical properties, **174**, 209
Contributions of atomic hydrogen to the low temperature removal of traps at silicon oxide–silicon interfaces, **172**, L101
Correlation of refractive index and silicon content of silicon oxynitride films, **168**, 123
Deposition of tin-doped indium oxide films by a modified reactive magnetron sputtering process, **172**, 111
Determination of the composition of sputtered silicon oxynitride films by Auger electron spectroscopy and Rutherford backscattering spectrometry, **167**, L1
Development of an Al_2O_3–Co selective absorber for solar collectors, **172**, 19
Dielectric and optical properties of europium oxide films, **177**, 59
Diode r.f. sputtering of copper and copper oxide thin films and multilayers, **174**, 91
The direct photochemical vapour deposition of SiO_2 from Si_2H_6 and N_2O_3 mixtures, **168**, 345
Doped silicon dioxide films from spin-on solutions, **177**, 231
Effect of addition of fluorine to phosphorus-doped tin oxide films, **167**, L7
The effect of heat treatment on the structural properties of electron-beam-evaporated SnO_2 films, **169**, 117
Effect of heat treatment on the structure, composition and electrochromic properties of evaporated tungsten oxide films: I, **169**, 257
Effect of oxygen on the electrical transport in RuO_2, **169**, 17
Effect of temperature rise on the growth rate of anodic SiO_2, **167**, 129
Effect of V–O barriers in Cr–Si–O/V–O/Al thin film system, **177**, 315
Effects of deposition conditions on the superconducting properties of r.f. and d.c. magnetron sputter-deposited $YBa_2Cu_3O_{7-x}$ films, **166**, 181
Effects of heat treatment and ion doping of indium oxide, **173**, 59
Electrical properties of sprayed tin oxide layers, **177**, 17
Electrocolouring of anodized aluminium with copper: effect of porous and barrier oxide film thicknesses, **173**, 299
The electrophysical properties of anodically grown silicon oxide films, **168**, 51
Elliptical blue patches growing in obliquely deposited WO_3 films, **172**, L71
Epitaxial growth of WO_3 thin films on MgO and Al_2O_3, **168**, 133
An evaluation of four computer modelling programs for Rutherford backscattering spectrometry analysis of oxidized surfaces, **166**, 201
Growth and characterization of ZnO films deposited on a monolithic Si_3N_4–SiO_2–Si configuration, **168**, 291
Growth and properties of $YBa_2Cu_3O_{7-x}$ superconducting thin films, **166**, 171

Growth of $BaTiO_3$–$SrTiO_3$ thin films by r.f. magnetron sputtering, **169**, 249
Heat treatment in hydrogen gas and plasma of transparent conducting oxide films such as ZnO, SnO_2 and indium tin oxide, **176**, 277
Identification of interfacial structures in Bi–Ca–Sr–Cu–O thin film, **173**, 149
Indium tin oxide thin films for metallization in microelectronic devices, **170**, 151
Influence of anion incorporation and argon implantation of substrate on ionic transport through anodic Nb_2O_5 films studied by X-ray photoelectron spectroscopy measurements, **168**, 21
Influence of electrode material on the photocurrent in tantalum pentoxide films, **177**, 1
Influence of helium plasma UV radiation on the channel mobility and charges in Si–SiO_2 structures, **169**, 43
Influence of oxides at metal electrode–amorphous silicon interface on solar cell characteristics, **167**, 85
The influence of structure on the piezoelectric properties of $BaTiO_3$ and (BaSr)TiO_3 thin films with a diffuse phase transition, **176**, 227
Influence of substrate and target temperatures on properties of transparent and conductive doped ZnO thin films prepared by r.f. magnetron sputtering, **171**, 307
Influence of substrate temperature and post-deposition heat treatment on the optical properties of SiO_2 films, **170**, 179
Interface reaction between sputter-deposited Al_2O_3 and stainless steels, **172**, 35
Mechanism of gas detection in polycrystalline thick film SnO_2 sensors, **171**, 53
Moisture patches in Al_2O_3/SiO_2 quarterwave reflectors studied by fringes of equal chromatic order like experiments, **168**, L43
Morphology and structure of TiO_2 thin layers, *vs.* thickness and substrate temperature, **170**, 107
A new concept of metal–resin adhesion using an intermediate layer of SiO_x–C, **169**, 159
Note on the heteroepitaxial growth of $Ba_{1-x}Sr_xTiO_3$ thin films on MgO, **173**, L139
On the use of zinc acetate as a novel precursor for the deposition of ZnO by low-pressure metal–organic chemical vapour deposition, **173**, 95
Optical dispersion in electron-beam-evaporated indium tin oxide thin films, **175**, 241
Optical properties of electron-beam-evaporated TiO_2 films, **176**, 181
Optical properties of ZnO films deposited by r.f. sputtering on sapphire substrates, **176**, L167
Optimization of rapid thermal processing to prepare superconducting Y–Ba–Cu–O thin films, **174**, 185
Oxide film formation and thickening on titanium in water, **167**, 269
Physical properties of arsenic-doped tin oxide thin films, **176**, 99
Plasma spraying of WO_3: structural characterization of the coatings, **166**, 249
Porous structure of SiO_2 films synthesized at low temperature and pressure, **171**, 43
Preparation and optical properties of thin films of CrO_3 and Cr_2O_3 prepared by the method of chemical spray pyrolysis, **169**, 235
Preparation of transparent and conducting indium oxide films by solution pyrolysis of dibutylindium thiolate, **167**, L27
Preparation of amorphous thin films of $(Ti,V)O_2$ and $(Ti,Nb)O_2$ by r.f. sputtering, **176**, 111
Properties of ion-plated Nb_2O_5 films, **175**, 207
R.f.-sputtered indium tin oxide films on water-cooled substrates, **167**, L11
Reactions of $YBa_2Cu_3O_{7-x}$ thin films on silicon substrates, **174**, 5
Reactive sputtering of RuO_2 films, **173**, 217
Reactively sputtered indium oxide diffusion barrier, **166**, 15
Reduction kinetics of thin and thick cupric oxide films at room temperature by hydrazine, **169**, 143
Scattering of charge carriers in transparent and conducting thin oxide films with a non-parabolic conduction band, **174**, 217
Scattering of light in TiO_2 layers of broad band mirrors, **176**, 25
Secondary electron emission studies on MgO films, **167**, 299
Self-aligned $TiN_xO_y/TiSi_2$ contact formation, **172**, 1
Space charge and electret behaviour in anodic Ta_2O_5 films, **167**, 95
A spectroscopic study of nickel oxide films on polycrystalline nickel, **177**, 171
Structural properties of ZnO films prepared by r.f. sputtering for optical applications, **175**, 255
Studies of electrical and optical properties of SnO_2:P films, **169**, 195
Substrate-dependent growth of atmospheric pressure chemically vapor deposited silicon dioxide from dichlorosilane and oxygen, **171**, 291
Superconducting properties of irradiation-

induced effects in epitaxial YBaCuO thin films, **174**, 179
Tantalum oxide films for monolithic capacitor applications, **176**, 45
Thermally sprayed coatings of $YBa_2Cu_3O_{6+x}$, **166**, 163
A tin oxide thin film sensor with high ethanol sensitivity, **169**, 51
Transmission electron microscopy examination of ultramicrotomed sections of tantalum and its anodic oxide films, **173**, 263
Yttrium oxide based metal–insulator–semiconductor structures on silicon, **170**, 185
Yttrium oxides in vacuum-plasma-sprayed CoNiCrAlY coatings, **173**, 99
Oxygen
Substrate-dependent growth of atmospheric pressure chemically vapor deposited silicon dioxide from dichlorosilane and oxygen, **171**, 291
The effect of oxygen adsorption on the electronic properties of the polar GaAs(111) surface after thermal cleaning in ultrahigh vacuum, **170**, 219
Thermal oxidation of silicon in O_2–SiF_4 mixtures, **169**, 173

P

Packaging
Coatings for strain compliance in plastic packages: opportunities and realities, **166**, 83
Focused electron and ion beam repair strategies for wafer-scale interconnections in thin film packaging, **166**, 121
Interface interactions relevant to packaging technology, **166**, 97
Process technology for packing applications, **166**, 69
Palladium
A transmission electron microscopy study of the crystallization of ion-beam-mixed $Pd_{80}Si_{20}$ amorphous thin films, **167**, 141
Anomalous low-temperature resistivity behavior of quench-condensed palladium films, **174**, 301
Auger electron spectroscopy study of low coverage palladium adsorption on Si(111), **172**, 141
Deposition and characterization of electroless palladium on austenitic stainless steel, **171**, 313
Effect of encapsulation on the reaction between palladium and GaAs thin films, **166**, 63
Metal–insulator transition in thin granular palladium–carbon mixture films, **174**, 225
Preparation and characterization of epitaxial films of silver, palladium and Ag–Pd alloys deposited by glow discharge sputtering. I: onto NaCl single-crystal substrates, **170**, 41
Temperature and thickness dependence of the resistivity of thin polycrystalline aluminium, cobalt, nickel, palladium, silver and gold films, **167**, 25
X-ray diffraction studies on thin palladium films epitaxially grown on Ag(1111), **174**, 105
Palmitic acid
Experimental study of the stability and metastability of palmitic acid, **178**, 93
Penning ionization electron spectroscopy
Characterization of Langmuir–Blodgett films of cadmium stearate by Penning ionization electron spectroscopy, **178**, 305
Perfluoroalkyl chains
Langmuir–Blodgett films of polyallylamine modified with long perfluoroalkyl chains by urea bonds, **178**, 373
Permalloy films
Impurity distribution of very thin permalloy films, **167**, L39
Peroxopolytungstic acid
Mechanism for photosensitization of peroxopolytungstic acid film by substitution of niobium or tantalum for a part of the tungsten, **172**, L97
Perylene
Epitaxial growth of thin films of perylenetetracarboxylic dianhydride and coronene on NaCl(001), **175**, 89
Phase sequence
Phase sequence in the solid state amorphization reaction of metallic thin films, **174**, 11
Phase transitions
The influence of structure on the piezoelectric properties of $BaTiO_3$ and $(BaSr)TiO_3$ thin films with a diffuse phase transition, **176**, 227
On the relations between the α-Cr and δ-Cr phases, **171**, 33
Phase transitions in adsorbed layers. X: application of inverse gas chromatography to the determination of phase diagrams for monolayer films deposited on porous adsorbent surfaces, **173**, 13
Phase transitions in adsorbed layers. XI: the condensed-solid to expanded-liquid transition in an *n*-octadecanol monolayer on a silica gel surface, **173**, 279

Phase transitions in adsorbed layers. XII: a two-dimensional van der Waal's fluid with softened repulsive interactions, **173**, 287
Phosphorus
The annealing behaviour of electroless non-crystalline nickel phosphorus films, **169**, 229
Effect of addition of fluorine to phosphorus-doped tin oxide films, **167**, L7
Modifications of InP(100) surfaces induced by electron beam during Auger measurement, **172**, L65
Preparation and properties of diodes on low-resistivity zinc phosphide films, **176**, 13
Structural and technological properties of heavily *in situ* phosphorus-doped low pressure chemically vapour deposited silicon films, **175**, 43
Structural changes induced by heating in electroless nickel–phosphorus alloys, **166**, 235
Studies of electrical and optical properties of SnO_2:P films, **169**, 195
A study of electroless nickel coatings containing low phosphorus, **177**, 207
A transmission electron microscopy study on the crystallization of amorphous Ni–P electroless deposited coatings, **166**, 273
Photoangular effect
Photoangular effect in CdS(Cu,Cl) thin films, **175**, 249
The influence of photoangular effect on dynamic characteristics of the current in CdS(Cu,Cl) thin films, **167**, L15
Photochemical properties
Photochemical properties of mixed monolayer assemblies containing carbazolyl chromophores, **178**, 399
Photocurrents
Influence of electrode material on the photocurrent in tantalum pentoxide films, **177**, 1
Photoelectrochemical cells
A comparison of the sulfide–polysulfide and ferro–ferricyanide electrolytes in a photoelectrochemical cell with electrochemically deposited CdSe films, **174**, 295
Photoluminescence
Photoluminescence of CdTe films grown on BaF_2 with PbTe buffer layers by hot-wall epitaxy, **171**, 271
Photoreceivers
0.8 μm wavelength integrated photoreceiver: improvement using a special heteroepitaxy suitable for high electron mobility transistor fabrication, **172**, L59
Photoresists
The selective removal of the negative high-resolution photoresist system Ag–As–S, **173**, 129
Photosensitization
Mechanism for photosensitization of peroxo-polytungstic acid film by substitution of niobium or tantalum for a part of the tungsten, **172**, L97
Photovoltaic characterization
Photovoltaic characterization of amorphous hydrogenated and chlorinated silicon films, **170**, 163
Photovoltaic effect
The anomalous photovoltaic effect in polycrystalline $AgInTe_2$ thin films, **173**, 169
Phthalocyanines
Humidity dependence of electrical properties of Si(phthalocyaninato)$(OH)_2$ deposited films, **172**, 159
In-plane anisotropy in Langmuir–Blodgett films of a copper phthalocyanine derivative, **178**, 439
Langmuir–Blodgett films of octa-alkyl phthalocyanines, **178**, 361
A new method for measuring refractive index and thickness of Langmuir–Blodgett films of ttb–$PcSiCl_2$, **178**, 525
Semiconductive properties of diphthalocyanine thin films, **170**, L51
X-ray photoelectron spectroscopy study of lipid-free multilayer systems of copper phthalocyanine tetrasulphonate, **178**, 221
Physical vapour deposition
Initial growth and epitaxy of PVD TiN layers on austenitic steel, **173**, 199
The relationship between residual stress, X-ray elastic constants and lattice parameters in TiN films made by physical vapor deposition, **170**, 63
Residual stress in physically vapor deposited films: a study of deviations from elastic behavior, **171**, 197
Planarization
In situ planarization of intermetal dielectrics: process steps, degree of planarization and film properties, **175**, 67
Plasma beams
Generation of surface layers and microstructures with a low energy plasma beam source, **174**, 39
Plasma deposition
Characterization of plasma-deposited amorphous hydrogenated carbon films by neutron reflectivity, **172**, 269

Controversies in the suggested mechanisms of plasma-induced deposition of silicon from silane, **175**, 129
Electronic structure of plasma-deposited amorphous Si–C alloy films, **168**, 175
Ion and plasma beam assisted thin film deposition, **175**, 119
Magnetron plasma deposition processes, **171**, 125
Mass spectrometric study of gas evolution from plasma-deposited fluoro-hydrogenated amorphous carbon films on heating, **167**, 255
Plasma-enhanced deposition of amorphous silicon at temperatures between 300 and 500 °C, **168**, 89
Plasma polymerization
Synthesis of gold–carbon composites by simultaneous sputtering and plasma polymerization of propane in r.f. capacitively coupled diode system (13.56 MHz), **168**, 81
Plasma spraying
Characterization of a plasma-sprayed YBaCuO superconductor, **168**, 231
Plasma spraying of WO_3: structural characterization of the coatings, **166**, 249
Yttrium oxides in vacuum-plasma-sprayed CoNiCrAlY coatings, **173**, 99
Plasmon–polariton studies
A surface plasmon–polariton study of the dielectric constants of reactive metals: aluminium, **167**, 73
Surface plasmon–polariton study of the dielectric function of magnesium, **172**, 27
Plastics
Coatings for strain compliance in plastic packages: opportunities and realities, **166**, 83
Platinum
Dynamical behavior of platinum and gold surfaces and thin films, **172**, L91
Electronic characterization of new c-Si/a-Si:H/Pt thin film devices, **174**, 203
Silicide formation in the Pt/a-Si:H system, **167**, 187
Structure and ammonia sensitivity of thin platinum or iridium gates in metal–oxide–silicon capacitors, **177**, 77
Polarizability
Polarizability of dielectric islands on a substrate, **173**, 175
Polyallylamine
Langmuir–Blodgett films of polyallylamine modified with long perfluoroalkyl chains by urea bonds, **178**, 373
Polyamides
Structure and properties of Langmuir–Blodgett films made from polyamides, **178**, 403
Polydiacetylene
Studies on Langmuir–Blodgett films fabricated from the monolayers containing polydiacetylene and polythiophene derivatives, **178**, 393
Polyester
Aluminium metallization of polyester and polypropylene films: properties and transmission electron microscopy microstructure investigations, **174**, 155
Polyesters and polyurethanes as prepolymerized materials for Langmuir–Blodgett films: preparation and characterization of multilayers, **178**, 253
Polyheterocycles
Langmuir–Blodgett films of polyheterocycles: a study with synchrotron radiation techniques, **178**, 233
Polyimide
Electrical properties of carbon black–polyimide thick films, **168**, 169
Polyion complexes
Orientation evaluation of polyion complex Langmuir–Blodgett films by Fourier transform IR transmission and reflection–absorption spectroscopy, **178**, 281
Polymers
Aspects of Langmuir trough design in relation to the study of molecular monolayers of polymers and condensed films, **178**, 17
Formation of polymerized thiophene films by photochemical vapour deposition, **177**, 295
Langmuir–Blodgett monolayers from preformed polymerized surfactants containing styrene, **175**, 103
A microstructural study of oriented polymer–zinc diethyldithiocarbamate thin films, **168**, 353
Polyoxyethylene
The structure of copper layers obtained from electroless plating solutions with and without a polyoxyethylene compound, **173**, 139
Polypropylene
Aluminium metallization of polyester and polypropylene films: properties and transmission electron microscopy microstructure investigations, **174**, 155
Polythiophene
Studies on Langmuir–Blodgett films fabricated from the monolayers containing polydiacetylene and polythiophene derivatives, **178**, 393
Polyurethanes
Polyesters and polyurethanes as prepolymer-

ized materials for Langmuir–Blodgett films: preparation and characterization of multilayers, **178**, 253

Porous structure
Porous structure of SiO_2 films synthesized at low temperature and pressure, **171**, 43

Positron annihilation spectroscopy
Slow positron annihilation spectroscopy of heterojunctions and homojunctions of GaAs-based semiconductor thin films, **166**, 349

Potassium
Growth of monocrystalline thin films of potassium–tantalate–niobate (KTN) by liquid-phase epitaxy, **175**, 201

Precursors
On the use of zinc acetate as a novel precursor for the deposition of ZnO by low-pressure metal–organic chemical vapour deposition, **173**, 95

Pressure drop
In situ measurement of the pressure drop in a Langmuir–Blodgett film during fast deposition, **178**, 171

Propane
Synthesis of gold–carbon composites by simultaneous sputtering and plasma polymerization of propane in r.f. capacitively coupled diode system (13.56 MHz), **168**, 81

Pulsed current plating
Characterization of gold layers selectively plated by a pulsed current, **169**, 105

Pyrolysis
High T_c superconducting films obtained by pyrolysis of an ultrasonically deposited gel, **174**, 263
Preparation and optical properties of thin films of CrO_3 and Cr_2O_3 prepared by the method of chemical spray pyrolysis, **169**, 235
Preparation of transparent and conducting indium oxide films by solution pyrolysis of dibutylindium thiolate, **167**, L27

Q

Quartz
On the possibility of thin film structure study with a quartz crystal microbalance, **171**, 367
Progress in monitoring thin film thickness by use of quartz crystals, **174**, 307
Swelling behaviour and stability of Langmuir–Blodgett films deposited on a quartz crystal microbalance in a water phase, **178**, 465

R

Radionuclides
Thin films to impede the incorporation of radionuclides in austenitic stainless steels, **171**, 323

Raman spectroscopy
Dependence of polarized surface-enhanced resonance Raman spectrum of Langmuir–Blodgett monolayer film on the incident light angle, **178**, 529
Oxidation studies of aluminium thin films by Raman spectroscopy, **170**, 35
Study of thin oxidation films on iron alloys by Raman spectroscopy, **174**, 111

Rare earth metals
Reversible optical recording on rare-earth–transition-metal disks, **175**, 261
Temperature dependence of the critical radius of domains in rare earth transition metal alloys for magnetic media, **175**, 305

Reaction kinetics
Reaction kinetics in tungsten/barrier metal/silicon systems, **166**, 1

Reduction kinetics
Reduction kinetics of thin and thick cupric oxide films at room temperature by hydrazine, **169**, 143

Reflectance bands
High reflectance bands of some simple two-material dielectric multilayers, **167**, 33

Reflectivity
Reflectivity of sputtered aluminum alloy films, **167**, L35

Reflectors
High efficiency front and rear surface silver reflectors, **167**, 291
Moisture patches in Al_2O_3/SiO_2 quarterwave reflectors studied by fringes of equal chromatic order like experiments, **168**, 430

Refractive index
Correlation of refractive index and silicon content of silicon oxynitride films, **168**, 123
An iterative and consistent method for the complex refraction index calculation of absorbent thin films, **176**, 69
A new method for measuring refractive index and thickness of Langmuir–Blodgett films of ttb–$PcSiCl_2$, **178**, 525
A simple ellipsometric method for the direct determination of the mean refractive index of non-absorbing graded-index thin films with linear index profile, **170**, 1
Static refractive index of hydrogenated amorphous and polycrystalline silicon between 293 K and 973 K, **173**, 155

Temperature, light intensity and microstructure dependence of the refractive index of polycrystalline silicon films, **169**, 205
Reliability
The reliability of integrated circuits protected with Ti–W/Au bumps, **166**, 113
Resistivity
Effect of ion bombardment during growth on the electrical resistivity of magnetron-sputtered carbon films, **168**, 239
Resistivity, Hall effect and magnetoresistivity of amorphous iron and cobalt alloy films and their applications, **175**, 325
Resistometric technique
On the validity of the resistometric technique in electromigration studies of narrow stripes, **172**, L85
Resonant low energy electrons
Resonant low energy electrons and their impact on non-destructive depth profiling of thin film samples, **166**, 213
Rhodamine
Surface-pressure-induced chromism in rhodamine monolayers, **178**, 473
Rhodium
Interface analysis of sputtered W–C, Rh–C and Ni–C multilayers for soft X-ray applications, **175**, 161
Ruthenium
Effect of oxygen on the electrical transport in RuO_2, **169**, 17
Reactive sputtering of RuO_2 films, **173**, 217
Rutherford backscattering spectrometry
Analysis of TiN by charged particle beams: nuclear reaction analysis, nuclear reaction broadening and Rutherford backscattering, **166**, 191
Characterization of Ta_2O_5 layers by electron spectroscopy for chemical analysis, Rutherford backscattering spectrometry, nuclear reaction analysis and optical methods, **175**, 185
Determination of the composition of sputtered silicon oxynitride films by Auger electron spectroscopy and Rutherford backscattering spectrometry, **167**, L1
An evaluation of four computer modelling programs for Rutherford backscattering spectrometry analysis of oxidized surfaces, **166**, 201
X-ray photoelectron spectroscopy and Rutherford backscattering spectrometry study of anion incorporation in anodically grown films, **167**, 245

S

Sapphire
Optical properties of ZnO films deposited by r.f. sputtering on sapphire substrates, **176**, L167
Scanning electron microscopy
Direct observation of the surface structure of Langmuir–Blodgett films with scanning electron microscopy, **178**, 477
Schottky barriers
A study of Au/GaAs Schottky barriers with a cesiated interface, **173**, L149
Scratch adhesion tests
Scratch adhesion test of magnetron-sputtered copper coatings on aluminium substrates: effects of the surface preparation, **168**, 193
Second harmonic generation
Optical second harmonic generation as a probe of interface composition and structure, **166**, 345
Secondary electron emission
Secondary electron emission studies on MgO films, **167**, 299
Seed layers
Well-defined columnar grains in iron films prepared on seed layers, **169**, 289
Selenium
Analysis of the interface of bismuth with polycrystalline selenium thin films, **168**, 249
A comparison of the sulfide–polysulfide and ferro–ferricyanide electrolytes in a photoelectrochemical cell with electrochemically deposited CdSe films, **174**, 295
Crystallization and melting of thin Bi_xSe_{1-x} layers, **177**, 239
Effective electron mass in thin films of the Ge–Se–Ga system, **169**, 169
Electrical and optical properties of $Ge_{20}Sb_xSe_{80-x}$ thin films, **170**, 15
Electrical and photoconducting properties of vacuum evaporated pure and silver-doped CdSe films, **174**, 233
Growth of $CuInSe_2$ by two magnetron sputtering techniques, **171**, 109
Laser-induced reaction in Cu–In–Se systems, **170**, 227
The grain growth of $CdS_{0.6}Se_{0.4}$ films, **177**, L187
Preparation and characterization of chemically deposited $CuInSe_2$ films, **167**, L19
Preparation of polycrystalline $Cd_{1-x}In_xCr_2Se_4$ thin films, **174**, 71
Thermoelectric power of $Se_{20}Te_{80}$ alloy thin films: temperature and size effects, **172**, 167
Semiconductors
Comparison of experimental and theoretical

Fermi screening of charged impurities in degenerate semiconductors, **176**, 1

Sensors

Chemically deposited Cu_2O thin film as an oxygen pressure sensor, **167**, 309

Insert-mounted thin film sensors for real-time monitoring of tool conditions, **166**, 387

Mechanism of gas detection in polycrystalline thick film SnO_2 sensors, **171**, 53

Sensor for the detection of the incident point of an electron beam, **174**, 323

Thin oxide films as gas sensors, **174**, 269

A tin oxide thin film sensor with high ethanol sensitivity, **169**, 51

Shear

An apparatus for the study of molecular monolayers compressed at the air–water interface with uniform shear, **178**, 191

Silica

Phase transitions in adsorbed layers. XI: the condensed-solid to expanded-liquid transition in an *n*-octadecanol monolayer on a silica gel surface, **173**, 279

Silicon

Amorphous silicon deposition: industrial and technical challenges, **174**, 193

Atomic structure of amorphous $Si_{1-x}C_x$ films prepared by r.f. sputtering, **173**, 235

Auger electron spectroscopy study of low coverage palladium adsorption on Si(111), **172**, 141

The bond structures and properties of chemically vapour deposited amorphous SiC, **166**, 367

Capacitance–voltage measurements on a p-type InSb metal/insulator/semiconductor structure with Si_3N_4 as the insulator, **168**, 157

Changes in the properties of glow-discharge-deposited microcrystalline silicon films with thickness, **167**, 121

Characteristics of hydrogenated amorphous silicon thin film transistors fabricated by d.c. magnetron sputtering, **175**, 37

Chemical bonding in microcrystalline Si:H:Cl films studied by ion-induced Auger electron spectroscopy, **173**, L109

Comparison of the diffusion barrier properties of tungsten films prepared by hydrogen and silicon reduction of tungsten hexafluoride, **171**, 343

Comparison of the properties of $TiSi_2$ films obtained by silicon and titanium co-sputtering and by composite target sputtering, **170**, 71

Contributions of atomic hydrogen to the low temperature removal of traps at silicon oxide–silicon interfaces, **172**, L101

Controversies in the suggested mechanisms of plasma-induced deposition of silicon from silane, **175**, 129

Correlation of refractive index and silicon content of silicon oxynitride films, **168**, 123

Crystallization of amorphous silicon films using a multistep thermal annealing process, **167**, 101

Determination of the composition of sputtered silicon oxynitride films by Auger electron spectroscopy and Rutherford backscattering spectrometry, **167**, L1

The deposition mechanisms and microstructures of tungsten films produced by silicon reduction of WF_6, **166**, 37

The direct photochemical vapour deposition of SiO_2 from Si_2H_6 and N_2O_3 mixtures, **168**, 345

Doped silicon dioxide films from spin-on solutions, **177**, 231

The effect of hydrogen dilution on the electrical properties of hydrogenated amorphous silicon, **169**, 179

Effect of stress on the superconducting properties of $CoSi_2$ thin films, **174**, 285

Effect of temperature rise on the growth rate of anodic SiO_2, **167**, 129

Effect of V–O barriers in Cr–Si–O/V–O/Al thin film system, **177**, 315

Electrical characteristics of Ti–Si(100) interfaces, **176**, 173

Electrical properties of boron-doped hydrogenated amorphous silicon films prepared by glow discharge decomposition in dilute silane, **176**, 79

Electronic characterization of new c-Si/a-Si:H/Pt thin film devices, **174**, 203

Electronic structure of plasma-deposited amorphous Si–C alloy films, **168**, 175

The electrophysical properties of anodically grown silicon oxide films, **168**, 51

Ellipsometric study of low-temperature silicon surface cleaning during the process of reactive ionized cluster beam deposition, **168**, 103

Epitaxial growth and characterization of organic thin films on silicon, **175**, 85

Factorial experimental investigation of plasma-enhanced chemical vapor deposition of silicon nitride thin films, **168**, 281

Growth and characterization of ZnO films deposited on a monolithic Si_3N_4–SiO_2–Si configuration, **168**, 291

Humidity dependence of electrical properties of

Si(phthalocyaninato) $(OH)_2$ deposited films, **172**, 159
Hydrogen incorporation scheme in a-Si:H prepared by photochemical vapour deposition, **167**, L23
Hydrogenated amorphous silicon films deposited by reactive sputtering: the electronic properties, hydrogen bonding and microstructure, **171**, 217
Inert gas dilution: an alternative technique to make layers for a-Si:H solar cells, **174**, 239
Influence of helium plasma UV radiation on the channel mobility and charges in $Si–SiO_2$ structures, **169**, 43
The influence of rapid thermal processing on the properties of $MoSi_2$ layers formed by using the ion implantation through metal technique, **177**, 225
Influence of substrate temperature and post-deposition heat treatment on the optical properties of SiO_2 films, **170**, 179
The influence of titanium nitride sputter deposition temperature on surface-hardened 2.5% silicon iron, **170**, 293
Interdiffusion between some refractory metal silicides and GaAs, **169**, 223
Interdiffusion of an Au/Ni/Cr multilayer metallization on silicon substrates, **173**, 39
Ion-beam-induced Sb–Si mixing, **170**, 127
Ionic contamination of thin films of silica by solutions of NaI and KCl, **167**, 45
The laser surface melting of aluminium–silicon-based alloys, **177**, 133
Metal–organic chemical vapour deposition of CdS onto (111) silicon substrates, **176**, 143
Microstructural properties and density dependence of the optical properties of microcrystalline silicon films by spectroscopic ellipsometry and electron microscopy, **169**, 87
Moisture patches in Al_2O_3/SiO_2 quarterwave reflectors studied by fringes of equal chromatic order like experiments, **168**, L43
A new concept of metal–resin adhesion using an intermediate laver of SiO_x–C, **169**, 159
Nickel silicide formation in electroless plated films on silicon: low temperature growth of Ni_3Si_2, morphology and electrical resistance, **171**, 277
Observations on aluminium diffusion and its effect on the specific contact resistance of Al/W/Si ohmic contact, **176**, 91
On the blocking behaviour of mesa high voltage power devices passivated by semi-insulating polycrystalline silicon films, **168**, 41
Optically matched capping layers for CO_2 laser recrystallization of polysilicon, **168**, 35
Optimization study of titanium silica anti-reflective coatings in high efficiency silicon solar cells, **172**, 15
Oxynytride layers obtained by anodic oxidation of plasma-enhanced chemically vapour deposited Si_3N_4 films, **175**, 49
Photovoltaic characterization of amorphous hydrogenated and chlorinated silicon films, **170**, 163
Physical and electrical properties of yttria-stabilized zirconia epitaxial thin films deposited by ion beam sputtering on silicon, **175**, 23
Physical properties and structure of carbon-rich a-SiC:H films prepared by r.f. glow discharge decomposition, **173**, 253
Plasma-enhanced chemical vapour deposition of silicon dioxide using tetraethoxysilane as silicon source, **174**, 57
Plasma-enhanced deposition of amorphous silicon at temperatures between 300 and 500 °C, **168**, 89
Porous structure of SiO_2 films synthesized at low temperature and pressure, **171**, 43
Preparation and characterization of reactively sputtered silicon nitride thin films, **166**, 359
Properties of hydrogenated amorphous silicon carbide films prepared by plasma-enhanced chemical vapor deposition, **177**, 253
Reaction kinetics in tungsten/barrier metal/silicon systems, **166**, 1
Reactions of $YBa_2Cu_3O_{7-x}$ thin films on silicon substrates, **174**, 5
Recrystallization of silicon-on-insulator layers in pulsed nanosecond heating (model calculations), **171**, 235
Self-aligned $TiN_xO_y/TiSi_2$ contact formation, **172**, 1
Silicide formation in the Pt/a-Si:H system, **167**, 187
Static refractive index of hydrogenated amorphous and polycrystalline silicon between 293 K and 973 K, **173**, 155
Stress relaxation in tantalum silicide films by particle bombardment, **175**, 61
Structural and technological properties of heavily *in situ* phosphorus-doped low pressure chemically vapour deposited silicon films, **175**, 43
Study of thin anodic SiO_2 layers on degenerate silicon by inelastic electron tunnelling spectroscopy, **168**, 11
Substrate-dependent growth of atmospheric pressure chemically vapor deposited silicon

dioxide from dichlorosilane and oxygen, **171**, 291
Temperature, light intensity and microstructure dependence of the refractive index of polycrystalline silicon films, **169**, 205
Thermal degradation of $TiSi_2$/poly-Si gate electrodes, **168**, 325
Thermal oxidation of silicon in O_2–SiF_4 mixtures, **169**, 173
Thermal stability of $TaSi_x$/n-GaAs metallizations, **176**, 187
Thermal stability of TiN films deposited onto silicon substrates, **176**, 7
A thermodynamic and experimental approach to $TaSi_2$ chemical vapour deposition, **177**, 189
Ti/Ni bilayers on silicon: sputter-induced intermixing, rapid thermal annealing and ternary silicide formation, **177**, 263
A transmission electron microscopy study of the crystallization of ion-beam-mixed $Pd_{80}Si_{20}$ amorphous thin films, **167**, 141
Tungsten silicide barrier layers in aluminium ohmic contact systems, **177**, 9
Ytrrium oxide based metal–insulator–semiconductor structures on silicon, **170**, 185

Silver
Ambient-induced interface reactions and adhesion failure in the Ag/TlBr–TlI system, **177**, 181
The anomalous photovoltaic effect in polycrystalline $AgInTe_2$ thin films, **173**, 169
Characterization of silver-doped perovskite- and spinel-type electrode coatings, **174**, 85
Crystallization of amorphous antimony layers on as-deposited ultrathin sublayers of silver, **167**, 223
Electrical and photoconducting properties of vacuum evaporated pure and silver-doped CdSe films, **174**, 233
High efficiency front and rear surface silver reflectors, **167**, 291
A method for determining shape and volume of ellipsoidal silver particles from absorbance measurements, **177**, 49
Preparation and characterization of epitaxial films of silver, palladium and Ag–Pd alloys deposited by glow discharge sputtering. I: onto NaCl single-crystal substrates, **170**, 41
The selective removal of the negative high-resolution photoresist system Ag–As–S, **173**, 129
Structural and electrical properties of epitaxial Pb/Ag superlattices, **170**, 241
Surface decoration of Langmuir–Blodgett films with evaporated silver islands, **178**, 483
Temperature and thickness dependence of the resistivity of thin polycrystalline aluminium, cobalt, nickel, palladium, silver and gold films, **167**, 25
The temperature dependence of electrical conduction in a discontinuous carbon film device between silver film electrodes, **169**, 187
X-ray diffraction studies on thin palladium films epitaxially grown on Ag(1111), **174**, 105

Sodium
Atomically thin epitaxial films of NaCl on germanium, **172**, 123

Solar absorber coatings
Oxidation and diffusion in black chrome selective solar absorber coatings, **177**, 95

Solar cells
A new approach to the fabrication of cuprous sulphide–cadmium sulphide solar cells, **167**, 169
Influence of oxides at metal electrode–amorphous silicon interface on solar cell characteristics, **167**, 85

Solar collectors
Development of an Al_2O_3–Co selective absorber for solar collectors, **172**, 19

Space charge behaviour
Space charge and electret behaviour in anodic Ta_2O_5 films, **167**, 95

Spectrophotometric measurement
Analysis of inhomogeneous thin films by spectrophotometric measurements, **171**, 243

Spin waves
Influence of magnetization variation near the surface on spin wave modes, **170**, 191
Spin waves and magnetoresistance in exchange coupled layered magnetic structures, **175**, 317

Spiropyrans
Molecular arrangements of photochromic spiropyrans on a subphase, **178**, 103

Sputtering
Atomic structure of amorphous $Si_{1-x}C_x$ films prepared by r.f. sputtering, **173**, 235
Characteristics of hydrogenated amorphous silicon thin film transistors fabricated by d.c. magnetron sputtering, **175**, 37
Characterization of HfB_x films deposited by r.f. diode and r.f. magnetron sputtering, **166**, 131
Characterization of ion-beam- and magnetron sputtered $YBa_2Cu_3O_{7-x}$ high T_c superconducting films by secondary neutral mass spectrometry depth profiling, **174**, 255
Characterization of tin oxide thin films deposited by reactive sputtering, **170**, 285

Comparison of the properties of $TiSi_2$ films obtained by silicon and titanium co-sputtering and by composite target sputtering, **170**, 71

A comparison of molecular beam epitaxy and ion-beam sputtering for growth of CdTe and HgCdTe films, **168**, 307

A comparison of the step coverage of aluminum coatings produced by two sputter magnetron systems and a dual-beam ion system, **166**, 45

Composition of magnetron-sputtered aluminum alloy films, **173**, L115

Crystallographic investigation of the iron films deposited obliquely by sputtering, **176**, 255

Deposition of tin-doped indium oxide films by a modified reactive magnetron sputtering process, **172**, 111

Diode r.f. sputtering of copper and copper oxide thin films and multilayers, **174**, 91

Early days of magnetron sputtering—an enigma, **171**, 99

Effect of ion bombardment during growth on the electrical resistivity of magnetron-sputtered carbon films, **168**, 239

The effect of target power on the nitrogen partial pressure level and hardness of reactively sputtered titanium nitride coatings, **171**, 171

Effects of deposition conditions on the superconducting properties of r.f. and d.c. magnetron sputter-deposited $YBa_2Cu_3O_{7-x}$ films, **166**, 181

Effects of neutral gas incorporation in molybdenum coatings produced by magnetron sputtering, **166**, 309

Electrical insulating properties of r.f.-sputtered magnesia coatings, **166**, 255

Growth of $BaTiO_3$–$SrTiO_3$ thin films by r.f. magnetron sputtering, **169**, 249

Growth of $CuInSe_2$ by two magnetron sputtering techniques, **171**, 109

Hydrogenated amorphous silicon films deposited by reactive sputtering: the electronic properties, hydrogen bonding and microstructure, **171**, 217

Hysteresis effect in reactive r.f. sputtering and the adjustment of the set point for stoichiometric film deposition, **172**, 61

Influence of substrate and target temperatures on properties of transparent and conductive doped ZnO thin films prepared by r.f. magnetron sputtering, **171**, 307

The influence of titanium nitride sputter deposition temperature on surface-hardened 2.5% silicon iron, **170**, 293

Interface reaction between sputter-deposited Al_2O_3 and stainless steels, **172**, 35

Magnetron-sputtered WO_3 films for electrochromic devices, **175**, 227

Microhardness and microstructure of ion-beam-sputtered, nitrogen-doped NiFe films, **166**, 299

Microstructure modification of TiN by ion bombardment during reactive sputter deposition, **169**, 299

Modelling of reactive sputtering of titanium boride, **172**, 241

Note on the origin of intrinsic stresses in films deposited via evaporation and sputtering, **171**, 81

On spinodal decomposition in magnetron-sputtered (Ti,Zr) nitride and carbide thin films, **174**, 51

On the elemental dependence of the arrival rate of sputtered particles in the Monte Carlo simulation of the particle transport process in sputter deposition, **172**, L105

On the use of a brale indenter to evaluate the cross-sectional morphology of sputter deposited MoS_2 solid lubricant films, **172**, L81

Optical properties of ZnO films deposited by r.f. sputtering on sapphire substrates, **176**, L167

Physical and electrical properties of yttria-stabilized zirconia epitaxial thin films deposited by ion beam sputtering on silicon, **175**, 23

Position dependences in planar magnetron sputtering of TiN films, **173**, 109

Preparation and characterization of epitaxial films of silver, palladium and Ag–Pd alloys deposited by glow discharge sputtering. I: onto NaCl single-crystal substrates, **170**, 41

Preparation and characterization of reactively sputtered silicon nitride thin films, **166**, 359

Preparation of amorphous thin films of $(Ti,V)O_2$ and $(Ti,Nb)O_2$ by r.f. sputtering, **176**, 111

Properties of d.c. magnetron-sputtered lead zirconate titanate thin films, **172**, 251

R.f.-sputtered indium tin oxide films on water-cooled substrates, **167**, L11

Reactions of r.f.-sputtered chromium films with gallium and tin, **176**, L173

Reactive sputtering of RuO_2 films, **173**, 217

Reactive sputtering of titanium boride, **172**, 133

Reactive-magnetron-sputtered chromium carbide films, **169**, 281

Reactively sputtered indium oxide diffusion barrier, **166**, 15

Reflectivity of sputtered aluminum alloy films, **167**, L35

Scratch adhesion test of magnetron-sputtered copper coatings on aluminium substrates: effects of the surface preparation, **168**, 193
The sputter deposition of superconducting ceramics, **174**, 165
Sputtering effects in Auger depth profiles of TiN thin films, **174**, 143
Sputtering of TiN coatings during ion beam mixing, **174**, 139
Strain, ion bombardment and energetic neutrals in magnetron sputtering, **171**, 183
Structural properties of ZnO films prepared by r.f. sputtering for optical applications, **175**, 255
Structure and properties of thin films of amorphous aluminium based alloys prepared by sputtering, **174**, 25
Synthesis of gold–carbon composites by simultaneous sputtering and plasma polymerization of propane in r.f. capacitively coupled diode system (13.56 MHz), **168**, 81
Thin film deposition by magnetron sputtering and determination of some physical parameters, **176**, 219
Ti/Ni bilayers on silicon: sputter-induced intermixing, rapid thermal annealing and ternary silicide formation, **177**, 263

Stability
Chemical stability of vanadium boride with aluminum, **166**, 29
Effects of CoCrAlY coating on microstructural stability and creep behaviour of a nickel-base superalloy, **168**, 207
Experimental study of the stability and metastability of palmitic acid, **178**, 93
Swelling behaviour and stability of Langmuir–Blodgett films deposited on a quartz crystal microbalance in a water phase, **178**, 465

Stearic acid
Langmuir–Blodgett films of pure long-chain nitroxides, their mixtures and mixtures with stearic acid studied by electron spin resonance, **178**, 271

Steel
Deposition and characterization of electroless palladium on austenitic stainless steel, **171**, 313
Deposition of stainless steel film using pulsed laser evaporation, **171**, 335
Effect of laser nitridation on the electrochemical corrosion behaviour of 316 stainless steel, **176**, 197
Effect of surface precipitation of titanium carbide on adherence of alumina film on steels, **177**, 107
The influence of substrate hardness on the response of TiN-coated steels to surface deformation, **177**, 117
Initial growth and epitaxy of PVC TiN layers on austenitic steel, **173**, 199
Interface reaction between sputter-deposited Al_2O_3 and stainless steels, **172**, 35
Structure and properties of ion sulphocarbonitrided coatings on several structural steels, **166**, 281
Thin films to impede the incorporation of radionuclides in austenitic stainless steels, **171**, 323

Step coverage
A comparison of the step coverage of aluminum coatings produced by two sputter magnetron systems and a dual-beam ion system, **166**, 45

Strain
Coatings for strain compliance in plastic packages: opportunities and realities, **166**, 83
Dislocation mechanisms of epitaxial strain relaxation in Ta/V multilayer films, **173**, 225
Strain, ion bombardment and energetic neutrals in magnetron sputtering, **171**, 183
Strain-sensitive property of vacuum evaporated manganese films, **172**, 45

Strain energies
Structure and preferred orientations in ion-plated niobium films and correlation of the substrate bias voltage with calculated strain energies, **168**, 221

Stress
Effect of stress on the superconducting properties of $CoSi_2$ thin films, **174**, 285
Note on the origin of intrinsic stresses in films deposited via evaporation and sputtering, **171**, 81
Reactive evaporation of thin titanium nitride films in ultrahigh vacuum and their friction and wear behavior as a function of contact stress, **173**, 19
The relationship between residual stress, X-ray elastic constants and lattice parameters in TiN films made by physical vapor deposition, **170**, 63
Residual stress in physically vapor deposited films: a study of deviations from elastic behavior, **171**, 197
Stress relaxation in tantalum silicide films by particle bombardment, **175**, 61
Stress-related effects in thin films, **171**, 5

Strontium
Identification of interfacial structures in Bi–Ca–Sr–Cu–O thin film, **173**, 149
The influence of structure on the piezoelectric

properties of $BaTiO_3$ and $(BaSr)TiO_3$ thin films with a diffuse phase transition, **176**, 227
Note on the heteroepitaxial growth of $Ba_{1-x}Sr_xTiO_3$ thin films on MgO, **173**, L139
Structural changes
Electrical resistivity and structural changes in amorphous $Ge_{1-x}Al_x$ thin films under thermal annealing, **167**, 57
Styrene
Langmuir–Blodgett monolayers from preformed polymerized surfactants containing styrene, **175**, 103
Substrate surface
Influence of substrate surface on Langmuir–Blodgett multilayers, **178**, 459
Sulphide acids
Characterization of Langmuir monolayers and Langmuir–Blodgett-deposited multilayers of ω-functionalized sulphide acids, **178**, 27
Sulphur
Characterization of Langmuir monolayers and Langmuir–Blodgett-deposited multilayers of ω-functionalized sulphide acids, **178**, 27
Chemical deposition of tin(II) sulphide thin films, **173**, 53
A comparison of the sulfide–polysulfide and ferro–ferricyanide electrolytes in a photoelectrochemical cell with electrochemically deposited CdSe films, **174**, 295
Conductivity and optical absorption in amorphous gallium sulphide thin films, **172**, 179
Deposition of stoichiometric MoS_2 thin films by pulsed laser evaporation, **168**, 335
An electrochemical study of sprayed CdS and CdZnS films, **170**, 171
The grain growth of $CdS_{0.6}Se_{0.4}$ film, **177**, L187
The influence of photoangular effect on dynamic characteristics of the current in CdS(Cu, Cl) thin films, **167**, L15
Metal–organic chemical vapour deposition of CdS onto (111)silicon substrates, **176**, 143
A new approach to the fabrication of cuprous sulphide–cadmium sulphide solar cells, **167**, 169
On the growth of $CuInS_2$ thin films by three-source evaporation, **168**, 113
On the use of a brale indenter to evaluate the cross-sectional morphology of sputter deposited MoS_2 solid lubricant films, **172**, L81
Photoangular effect in CdS(Cu,Cl) thin films, **175**, 249
Preparation of copper indium disulphide films by airless spraying, **167**, 217
Properties of CdS:In thin films grown by ionized deposition, **176**, 247
The selective removal of the negative high-resolution photoresist system Ag–As–S, **173**, 129
X-ray photoelectron spectroscopy study of the synthesis of copper sulphide in Langmuir–Blodgett films, **178**, 535
Suminagashi
The fractal aspects of *suminagashi* and marbling, **178**, 109
Superconductors
Characterization of a plasma-sprayed YBaCuO superconductor, **168**, 231
Characterization of ion-beam- and magnetron sputtered $YBa_2Cu_3O_{7-x}$ high T_c superconducting films by secondary neutral mass spectrometry depth profiling, **174**, 255
Deposition and properties of high critical temperature superconducting ceramic thin films, **174**, 249
Destruction of the two-dimensional mixed state in superconducting cylindrical thin films, **174**, 229
Effect of stress on the superconducting properties of $CoSi_2$ thin films, **174**, 285
Effects of deposition conditions on the superconducting properties of r.f. and d.c. magnetron sputter-deposited $YBa_2Cu_3O_{7-x}$ films, **166**, 181
Growth and properties of $YBa_2Cu_3O_{7-x}$ superconducting thin films, **166**, 171
High T_c superconducting films obtained by pyrolysis of an ultrasonically deposited gel, **174**, 263
Optimization of rapid thermal processing to prepare superconducting Y–Ba–Cu–O thin films, **174**, 185
Reactions of $YBa_2Cu_3O_{7-x}$ thin films on silicon substrates, **174**, 5
The sputter deposition of superconducting ceramics, **174**, 165
Superconducting properties of irradiation-induced effects in epitaxial YBaCuO thin films, **174**, 179
Thermally sprayed coatings of $YBa_2Cu_3O_{6+x}$, **166**, 163
Superlattices
Novel superlattice composed of crystalline monolayers and amorphous monolayers, **178**, 313
Structural and electrical properties of epitaxial Pb/Ag superlattices, **170**, 241
The structure of InAs/GaSb superlattices, **170**, 49

Studying the interface of Au–Cu superlattices, **170**, 99
Supermolecular engineering
Supermolecular engineering by the Langmuir–Blodgett method, **175**, 73
Supermolecular engineering in Langmuir–Blodgett films, **178**, 327
Surface acoustic waves
Characterization of *N*-*N'*-diarachidoylindigo transferred onto a surface acoustic wave device, **178**, 197
Surface decoration
Surface decoration of Langmuir–Blodgett films with evaporated silver islands, **178**, 483
Surface force technique
The stability of carboxylic acid Langmuir–Blodgett films as studied by the surface force technique, **176**, 157
Surface free energy
Variations in the surface free energy of fatty acid Langmuir–Blodgett multilayers, **178**, 125
Surface potential
Control of interfacial equilibria by local charge distribution and average surface potential, **178**, 53
Surface pressure
Improvement of Langmuir–Blodgett film structure by dynamic surface pressure control, **178**, 137
Surface pressure distribution of spread monolayers during compression, **178**, 165
Swelling behaviour
Swelling behaviour and stability of Langmuir–Blodgett films deposited on a quartz crystal microbalance in a water phase, **178**, 465
Synchrotron radiation techniques
Langmuir–Blodgett films of polyheterocycles: a study with synchrotron radiation techniques, **178**, 233

T

Tantalum
Anodic oxidation of tantalum in aqueous electrolytes, **177**, 35
Characterization of Ta_2O_5 layers by electron spectroscopy for chemical analysis, Rutherford backscattering spectrometry nuclear reaction analysis and optical methods, **175**, 185
Dislocation mechanisms of epitaxial strain relaxation in Ta/V multilayer films, **173**, 225
Growth of monocrystalline thin films of potassium–tantalate–niobate (KTN) by liquid-phase epitaxy, **175**, 201
Influence of electrode material on the photocurrent in tantalum pentoxide films, **177**, 1
Mechanism for photosensitization of peroxopolytungstic acid film by substitution of niobium or tantalum for a part of the tungsten, **172**, L97
Nitrides of titanium, niobium, tantalum and molybdenum grown as thin films by the atomic layer epitaxy method, **166**, 149
Quantitative comparison of a tungsten and a tantalum cracker cell for epitaxy with arsine, **174**, 75
Space charge and electret behaviour in anodic Ta_2O_5 films, **167**, 95
Stress relaxation in tantalum silicide films by particle bombardment, **175**, 61
Tantalum oxide films for monolithic capacitor applications, **176**, 45
Thermal stability of $TaSi_x$/n–GaAs metallizations, **176**, 187
A thermodynamic and experimental approach to $TaSi_2$ chemical vapour deposition, **177**, 189
Transmission electron microscopy examination of ultramicrotomed sections of tantalum and its anodic oxide films, **173**, 263
Tellurium
A comparison of molecular beam epitaxy and ion-beam sputtering for growth of CdTe and HgCdTe films, **168**, 307
Deposition and characterization of $ZrTe_x$ thin films, **174**, 289
Electrical properties of copper-doped ZnTe films, **176**, L183
Photoluminescence of CdTe films grown on BaF_2 with PbTe buffer layers by hot-wall epitaxy, **171**, 271
Physical properties of electrochemically deposited cadmium mercury telluride films, **169**, 315
Preparation and optical and electrical properties of co-evaporated $Pb_{1-x}Yb_xTe$ films, **175**, 221
The anomalous photovoltaic effect in polycrystalline $AgInTe_2$ thin films, **173**, 169
Thermoelectric power of $Se_{20}Te_{80}$ alloy thin films: temperature and size effects, **172**, 167
Wave interference effects in liquid phase epitaxial layers of $Hg_{1-x}Cd_xTe$, **169**, 25
Terbium
Domain nucleation and wall movement in TbFeCo, **175**, 265
Thallium
Ambient-induced interface reactions and adhesion failure in the Ag/TlBr–TlI system, **177**, 181

Thallium thin film oxidation investigated by an optical absorption method, **168**, 165
Thermal degradation
Thermal degradation of $TiSi_2$/poly-Si gate electrodes, **168**, 325
Thermal desorption
Thermal desorption of Langmuir–Blodgett monolayers, **178**, 211
Thermal spraying
Thermally sprayed coatings of $YBa_2Cu_3O_{6+x}$, **166**, 163
Thermal stability
Comparison of thermal stability of Langmuir–Blodgett films of icosanoic acid and cadmium icosanoate, **178**, 453
Thermal stability of $TaSi_x$/n-GaAs metallizations, **176**, 187
Thermal stability of TiN films deposited onto silicon substrates, **176**, 7
Thermally stimulated area relaxation
"Thermally stimulated area relaxations" of insoluble monolayers and densification of Langmuir–Blodgett films with "isobaric thermal treatment" of monolayers, **178**, 37
Thermocouples
Transparent thin film thermocouple, **176**, 73
Thermoelectric power
Thermoelectric power of $Se_{20}Te_{80}$ alloy thin films: temperature and size effects, **172**, 167
Thermopower measurements
Influence of gas atmosphere on thermopower measurements in tin oxide thin films, **174**, 277
Thickness monitoring
Progress in monitoring thin film thickness by use of quartz crystals, **174**, 307
Thiocarbaminates
Self-assembled and Langmuir–Blodgett films of thiocarbaminates: a comparative study, **178**, 319
Thiophene
Formation of polymerized thiophene films by photochemical vapour deposition, **177**, 295
Thorium
Simultaneous determination of dispersion relation and depth profile of thorium fluoride thin film by spectroscopic ellipsometry, **166**, 325
Tin
Analysis of tin dioxide coatings by multiple angle of incidence ellipsometry, **169**, 1
Band gap narrowing and the band structure of tin-doped indium oxide films, **176**, 33
Characterization of tin oxide thin films deposited by reactive sputtering, **170**, 285
A characterization study of a hydroxylated polycrystalline tin oxide surface, **169**, 69
Chemical deposition of tin(II) sulphide thin films, **173**, 53
Deposition of tin-doped indium oxide films by a modified reactive magnetron sputtering process, **172**, 111
Destruction of the two-dimensional mixed state in superconducting cylindrical tin films, **174**, 229
Effect of addition of fluorine to phosphorus-doped tin oxide films, **167**, L7
The effect of heat treatment on the structural properties of electron-beam-evaporated SnO_2 films, **169**, 117
Effect of tin doping on InSb thin films, **172**, 71
An evaluation of some physical characteristics of $CdSnAs_2$ thin films, **176**, 207
Heat treatment in hydrogen gas and plasma of transparent conducting oxide films such as ZnO, SnO_2 and indium tin oxide, **176**, 277
Indium tin oxide thin films for metallization in microelectronic devices, **170**, 151
Influence of gas atmosphere on thermopower measurements in tin oxide thin films, **174**, 277
Mechanism of gas detection in polycrystalline thick film SnO_2 sensors, **171**, 53
Optical dispersion in electron-beam-evaporated indium tin oxide thin films, **175**, 241
Physical properties of arsenic-doped tin oxide thin films, **176**, 99
R.f.-sputtered indium tin oxide films on water-cooled substrates, **167**, L11
Reactions of r.f.-sputtered chromium films with gallium and tin, **176**, L173
Structure and properties of metallic Sn–Zn alloy films prepared by plasma-enhanced metal-organic chemical vapor deposition, **177**, 271
Studies of electrical and optical properties of SnO_2:P films, **169**, 195
A tin oxide thin film sensor with high ethanol sensitivity, **169**, 51
Titanium
Al_3Ti formation by diffusion of aluminum through titanium, **166**, 21
Analysis of TiN by charged particle beams: nuclear reaction analysis, nuclear reaction broadening and Rutherford backscattering, **166**, 191
Chemical characterization of the deactivation and protection of FeTi thin films using complementary non-destructive techniques, **166**, 225
Comparison of amorphous and crystalline $(Ti,Nb)O_2$ thin films: crystallization micro-

structure and electrical properties, **174**, 209
Comparison of the properties of $TiSi_2$ films obtained by silicon and titanium co-sputtering and by composite target sputtering, **170**, 71
Compositional analysis of lead titanate thin films by Auger electron spectroscopy and their electrical properties, **171**, 251
Depth profiling of magnesium and titanium-doped $LiNbO_3$ waveguides, **175**, 235
The effect of argon during the plasma-assisted chemical vapor deposition of TiN, **167**, L31
The effect of reactant gas composition on the plasma-enhanced chemical vapour deposition of TiN, **169**, 57
Effect of surface precipitation of titanium carbide on adherence of alumina film on steels, **177**, 107
The effect of target power on the nitrogen partial pressure level and hardness of reactively sputtered titanium nitride coatings, **171**, 171
Electrical characteristics of Ti–Si(100) interfaces, **176**, 173
ε-Ti_2N phase growth control in titanium nitride films, **170**, L55
Growth of $BaTiO_3$–$SrTiO_3$ thin films by r.f. magnetron sputtering, **169**, 249
The influence of structure on the piezoelectric properties of $BaTiO_3$ and $(BaSr)TiO_3$ thin films with a diffuse phase transition, **176**, 227
The influence of substrate hardness on the response of TiN-coated steels to surface deformation, **177**, 117
The influence of titanium nitride sputter deposition temperature on surface-hardened 2.5% silicon iron, **170**, 293
Initial growth and epitaxy of PVD TiN layers on austenitic steel, **173**, 199
Microstructure modification of TiN by ion bombardment during reactive sputter deposition, **169**, 299
Modelling of reactive sputtering of titanium boride, **172**, 241
Morphology and structure of TiO_2 thin layers, *vs.* thickness and substrate temperature, **170**, 107
New results in d.c. reactive magnetron deposition of TiN_x films, **167**, 107
Nitrides of titanium, niobium, tantalum and molybdenum grown as thin films by the atomic layer epitaxy method, **166**, 149
Note on the heteroepitaxial growth of $Ba_{1-x}Sr_xTiO_3$ thin films on MgO, **173**, L139
A novel derivative ellipsometric method for the study of the growth of thin films: titanium, **173**, 1
On spinodal decomposition in magnetron-sputtered (Ti,Zr) nitride and carbide thin films, **174**, 51
Optical properties of electron-beam-evaporated TiO_2 films, **176**, 181
Optimization study of titanium silica anti-reflective coatings in high efficiency silicon solar cells, **172**, 15
Oxide film formation and thickening on titanium in water, **167**, 269
Position dependences in planar magnetron sputtering of TiN films, **173**, 109
Preparation of TiN thin films by the dynamic mixing method using an N_2^+ ion beam of 1 keV, **171**, 263
Preparation of amorphous thin films of $(Ti,V)O_2$ and $(Ti,Nb)O_2$ by r.f. sputtering, **176**, 111
Process of structure change in iron during titanium implantation, **176**, 165
Properties of d.c. magnetron-sputtered lead zirconate titanate thin films, **172**, 251
Reactive evaporation of thin titanium nitride films in ultrahigh vacuum and their friction and wear behavior as a function of contact stress, **173**, 19
Reactive sputtering of titanium boride, **172**, 133
The relationship between residual stress, X-ray elastic constants and lattice parameters in TiN films made by physical vapor deposition, **170**, 63
The reliability of integrated circuits protected with Ti–W/Au bumps, **166**, 113
Scattering of light in TiO_2 layers of broad band mirrors, **176**, 25
Self-aligned $TiN_xO_y/TiSi_2$ contact formation, **172**, 1
Sputtering effects in Auger depth profiles of TiN thin films, **174**, 143
Sputtering of TiN coatings during ion beam mixing, **174**, 139
The structure and composition of contacts made of Al(2%Cu)–TiW films on amorphized (100) silicon, **176**, 131
Thermal degradation of $TiSi_2$/poly-Si gate electrodes, **168**, 325
Thermal stability of TiN films deposited onto silicon substrates, **176**, 7
Ti/Ni bilayers on silicon: sputter-induced intermixing, rapid thermal annealing and ternary silicide formation, **177**, 263
Titanium nitridation in N_2 and NH_3 high frequency plasma, **173**, 83

X-ray analysis of heat-treated titanium nitride films, **170**, 201
Transient currents
Transient currents in conditions of continuous injection in thin insulating layers with spatially non-homogeneous trap distribution, **167**, 13
Transistors
Characteristics of hydrogenated amorphous silicon thin film transistors fabricated by d.c. magnetron sputtering, **175**, 37
0.8 μm wavelength integrated photoreceiver: improvement using a special heteroepitaxy suitable for high electron mobility transistor fabrication, **172**, L59
Transition metals
Reversible optical recording on rare-earth–transition-metal disks, **175**, 261
Temperature dependence of the critical radius of domains in rare earth transition metal alloys for magnetic media, **175**, 305
Transmission electron microscopy
Aluminium metallization of polyester and polypropylene films: properties and transmission electron microscopy microstructure investigations, **174**, 155
Transmission electron microscopy examination of ultramicrotomed sections of tantalum and its anodic oxide films, **173**, 263
A transmission electron microscopy study of the crystallization of ion-beam-mixed $Pd_{80}Si_{20}$ amorphous thin films, **167**, 141
A transmission electron microscopy study on the crystallization of amorphous Ni–P electroless deposited coatings, **166**, 273
Transparent films
Transparent thin film thermocouple, **176**, 73
Trap distribution
Transient currents in conditions of continuous injection in thin insulating layers with spatially non-homogeneous trap distribution, **167**, 13
Tricosenoic acid
Disclination recombination kinetics in water–surface monolayers of 22-tricosenoic acid, **178**, 81
A reflection high energy electron diffraction analysis of the orientation of the monoclinic subcell of 22-tricosenoic acid Langmuir–Blodgett bilayers as a function of the deposition pressure, **172**, 149
The sticking of magnesium on ω-tricosenoic acid multilayers deposited by the Langmuir–Blodgett technique, **167**, 261
Trough design
Aspects of Langmuir trough design in relation to the study of molecular monolayers of polymers and condensed films, **178**, 17
Design of a new Langmuir–Blodgett trough with the zone-heating mechanism above the water surface, **178**, 183
A convection-free monolayer trough for fluorescence microscopic monitoring of ultrathin organic films, **178**, 115
Fabrication of copoly(methacrylic acid-methylacrylate) Langmuir–Blodgett films using a moving-wall-type Langmuir–Blodgett trough, **178**, 175
Tungsten
Comparison of the diffusion barrier properties of tungsten films prepared by hydrogen and silicon reduction of tungsten hexafluoride, **171**, 343
Crystallization of β-WC_{1-x} in W–C multilayers, **176**, L177
The deposition mechanisms and microstructures of tungsten films produced by silicon reduction of WF_6, **166**, 37
Effect of heat treatment on the structure, composition and electrochromic properties of evaporated tungsten oxide films: I, **169**, 257
Elliptical blue patches growing in obliquely deposited WO_3 films, **172**, L71
Epitaxial growth of WO_3 thin films on MgO and Al_2O_3, **168**, 133
Experimental and thermodynamical investigation of selective low pressure chemical vapour deposition of tungsten using WCl_6 as tungsten source, **176**, 263
Interface analysis of sputtered W–C, Rh–C and Ni–C multilayers for soft X-ray applications, **175**, 161
Magnetron-sputtered WO_3 films for electrochromic devices, **175**, 227
Mechanism for photosensitization of peroxopolytungstic acid film by substitution of niobium or tantalum for a part of the tungsten, **172**, L97
A mechanistic study of SF_6 reactive ion etching of tungsten, **176**, 289
Observations of aluminium diffusion and its effect on the specific contact resistance of Al/W/Si ohmic contact, **176**, 91
Plasma spraying of WO_3: structural characterization of the coatings, **166**, 249
Plasma-enhanced chemical vapor deposition of tungsten, **170**, 91
Quantitative comparison of a tungsten and a

tantalum cracker cell for epitaxy with arsine, **174**, 75
Reaction kinetics in tungsten/barrier metal/silicon systems, **166**, 1
The reliability of integrated circuits protected with Ti–W/Au bumps, **166**, 113
Selective low pressure chemical vapour deposition of tungsten: deposition kinetics, selectivity and film properties, **175**, 55
The structure and composition of contacts made of Al(2%Cu)–TiW films on amorphized (100) silicon, **176**, 131
Tungsten silicide barrier layers in aluminium ohmic contact systems, **177**, 9

U

Urea
Langmuir–Blodgett films of polyallylamine modified with long perfluoroalkyl chains by urea bonds, **178**, 373

V

Vacancy redistribution
On the kinetics of redistribution of vacancies in f.c.c. metal films under high rate heating, **168**, 363
Vacuum deposition
Fluorescence characteristics, formation mechanism and chromophore association of ω-(1-pyrenyl)alkanoic acid films prepared by vacuum deposition, **169**, 323
Vanadium
Chemical stability of vanadium boride with aluminum, **166**, 29
Dislocation mechanisms of epitaxial strain relaxation in Ta/V multilayer films, **173**, 225
Effect of V–O barriers in Cr–Si–O/V–O/Al thin film system, **177**, 315
Frequency-dependent conductivity in vanadium pentoxide gel, **167**, 67
Preparation of amorphous thin films of $(Ti,V)O_2$ and $(Ti,Nb)O_2$ by r.f. sputtering, **176**, 111
Vaporization
Column growth in layers produced by vaporization, **167**, 281
Vapour phase epitaxy
Metal–organic vapour phase epitaxy: a thin film technology for large-scale production of high power GaAs/GaAlAs laser diodes, **175**, 213
Vertical dipping method
Vertical dipping method as a means of controlling the in-plane molecular orientation in Langmuir–Blodgett films, **178**, 157

W

van der Waal's fluid
Phase transitions in adsorbed layers. XII: a two-dimensional van der Waal's fluid with softened repulsive interactions, **173**, 287
Waveguides
Depth profiling of magnesium and titanium-doped $LiNbO_3$ waveguides, **175**, 235
Work-function spectroscopy
Work function spectroscopy as a tool for thin film analysis, **174**, 149

X

X-ray analysis
X-ray analysis of heat-treated titanium nitride films, **170**, 201
X-ray diffraction
Structural studies of Langmuir–Blodgett multilayers by means of soft X-ray diffraction, **170**, 309
X-ray diffraction studies on thin palladium films epitaxially grown on Ag(1111), **174**, 105
X-ray mirrors
Layered synthetic X-ray mirrors: fabrication, tests and applications, **175**, 151
X-ray photoelectron spectroscopy
Influence of anion incorporation and argon implantation of substrate on ionic transport through anodic Nb_2O_5 films studied by X-ray photoelectron spectroscopy measurements, **168**, 21
X-ray photoelectron spectroscopy and Rutherford backscattering spectrometry study of anion incorporation in anodically grown films, **167**, 245
X-ray photoelectron spectroscopy study of lipid-free multilayer systems of copper phthalocyanine tetrasulphonate, **178**, 221
X-ray photoelectron spectroscopy study of the synthesis of copper sulphide in Langmuir–Blodgett films, **178**, 535
X-ray reflection
Determination of the thickness and distribution of a Langmuir–Blodgett film using a soft X-ray reflection, **178**, 519

Y

Ytterbium
Preparation and optical and electrical properties of co-evaporated $Pb_{1-x}Yb_xTe$ films, **175**, 221
Yttrium
Characterization of a plasma-sprayed YBaCuO superconductor, **168**, 231

Characterization of ion-beam- and magnetron sputtered $YBa_2Cu_3O_{7-x}$ high T_c superconducting films by secondary neutral mass spectrometry depth profiling, **174**, 255
Effects of deposition conditions on the superconducting properties of r.f. and d.c. magnetron sputter-deposited $YBa_2Cu_3O_{7-x}$ films, **166**, 181
Growth and properties of $YBa_2Cu_3O_{7-x}$ superconducting thin films, **166**, 171
Optimization of rapid thermal processing to prepare superconducting Y–Ba–Cu–O thin films, **174**, 185
Physical and electrical properties of yttria-stabilized zirconia epitaxial thin films deposited by ion beam sputtering on silicon, **175**, 23
Reactions of $YBa_2Cu_3O_{7-x}$ thin films on silicon substrates, **174**, 5
Superconducting properties of irradiation-induced effects in epitaxial YBaCuO thin films, **174**, 179
Thermal cyclic response of yttria-stabilized zirconia/CoNiCr–AlY thermal barrier coatings, **172**, 185
Thermally sprayed coatings of $YBaCu_3O_{6+x}$, **166**, 163
Yttrium oxide based metal–insulator–semiconductor structures on silicon, **170**, 185
Yttrium oxides in vacuum-plasma-sprayed CoNiCrAlY coatings, **173**, 99

Z

Zinc
Electrical properties of copper-doped ZnTe films, **176**, L183
An electrochemical study of sprayed CdS and CdZnS films, **170**, 171
Growth and characterization of ZnO films deposited on a monolithic Si_3N_4–SiO_2–Si configuration, **168**, 291
Heat treatment in hydrogen gas and plasma of transparent conducting oxide films such as ZnO, SnO_2 and indium tin oxide, **176**, 277
Influence of substrate and target temperatures on properties of transparent and conductive doped ZnO thin films prepared by r.f. magnetron sputtering, **171**, 307
A microstructural study of oriented polymer-zinc diethyldithiocarbamate thin films, **168**, 353
On the use of zinc acetate as a novel precursor for the deposition of ZnO by low-pressure metal-organic chemical vapour deposition, **173**, 95
Optical properties of ZnO films deposited by r.f. sputtering on sapphire substrates, **176**, L167
Preparation and properties of diodes on low-resistivity zinc phosphide films, **176**, 13
Structural properties of ZnO films prepared by r.f. sputtering for optical applications, **175**, 255
Structure and properties of metallic Sn–Zn alloy films prepared by plasma-enhanced metal-organic chemical vapor deposition, **177**, 271
Zirconium
Deposition and characterization of $ZrTe_x$ thin films, **174**, 289
On spinodal decomposition in magnetron-sputtered (Ti,Zr) nitride and carbide thin films, **174**, 51
Physical and electrical properties of yttria-stabilized zirconia epitaxial thin films deposited by ion beam sputtering on silicon, **175**, 23
Properties of d.c. magnetron-sputtered lead zirconate titanate thin films, **172**, 251
Solid state reaction in crystalline and amorphous Co–Zr multilayers, **174**, 45
Thermal cyclic response of yttria-stabilized zirconia/CoNiCr–AlY thermal barrier coatings, **172**, 185

DIAMOND FILMS '90

First European Conference on Diamond and Diamond-like Carbon Coatings

September 17-19, 1990, CRANS-MONTANA, Switzerland

The invited lectures and contributed papers will review the latest developments in:

- Diamond, Diamond-like and other Carbon-based Films
- Coating processes (plasma, ion, directed beam, new hybid systems)
- Properties and Applications (optical, opto-electronic, electronic, mechanical, chemical)
- Characterization and Evaluation methods
- Novel Applications and Emerging Issues

Under the guidance of the International Scientific Steering Committee, consisting of 30 world leading experts, the Programme Committee, lead by Chairman Prof. Allan Matthews (University of Hull), has composed a programme which fully reflects the fast pace of research on Diamond and Diamond-like carbon coatings and the widening range of applications.

The following invited speakers are included in the programme:

J.C. Angus, U.S.A.	Y. Hirose, Japan	D.R. McKenzie, Australia
P.K. Bachmann, F.R.G.	S. Holly, U.S.A.	S. Söderberg, Sweden
C.A. Brookes, U.K.	P.V. Huong, France	B.V. Spitsyn, U.S.S.R.
R.F. Bunshah, U.S.A.	M. Kamo, Japan	V.P. Varnin, U.S.S.R.
J.T. Glass, U.S.A.	B. Lux, Austria	

A one-day Intensive Course will be held on Sunday, September 16, 1990, for newcomers to the field. Instructors are: Dr. Thomas R. Anthony, Prof. John C. Angus and Prof. Jeffrey T. Glass.

Registration Fees:

Conference Registration Fees: Sfr. 550.- (before May 31, 1990), Sfr. 700.- (from June 1 1990); Authors Sfr. 425.-; Students Sfr. 350.-

Course Registration Fees: Sfr. 805.- (before May 31, 1990), Sfr. 895.- (from June 1 1990) ; Students Sfr. 450.-

Please return to COMST

☐ I would like to be kept informed on Diamond Films '90
☐ I plan to attend
☐ I plan to attend the one-day intensive course
☐ Rent a Technology Transfer Display Board, please send details for rental.

Conference Organizers in Medicine, Science and Technology

P.O. Box 415
1001 Lausanne 1, Switzerland
Tel.: (021) 23 48 86
Fax: (021) 234 972
Tlx: 454 539 coms ch

Name:_____ Initials:_____

Company:_____ Title:_____

Function:_____

Address & P.O. Box:_____

Town:_____ Postal Code:_____

Country:_____

Dislocations in Solids

Volume 8

Basic Problems and Applications

edited by **F.R.N. Nabarro,** *University of the Witwatersrand, Johannesburg, South Africa*

This series offers a comprehensive review of the entire study of dislocations. Attention is focused on the influence of dislocations on all physical and metallurgical properties. Whereas, formerly, it was possible to assemble the entire knowledge of dislocations into a single volume, the current scope of knowledge has increased to such an extent as to make a series of books a matter of necessity.

"This series is surely the best in its field and will be essential to materials scientists, solid-state physicists and other research workers who deal with the fundamentals of mechanical behavior." (Trans Tech S.A.)

It was fashionable at one time to say that, while dislocations were pleasant playthings for physicists and could explain some long-established technological observations, their study did not contribute to the advance of technology and the economy. The chapters in Volume 8 remind us that a knowledge of esoteric topics, such as interfacial dislocations and the detailed structure of the cores of dislocations in unusual crystal structures, has been essential in the development of semiconductor devices and of superalloys.

Contents: 38. Line Defects in Interfaces *(R.C. Pond)*. 39. The Dislocation Core and Plasticity *(M.S. Duesbery)*. 40. Conduction Electron Scattering in Dislocated Metals *(B.R. Watts)*. 41. The Prediction of Critical Misfit and Thickness in Epitaxy *(W.A. Jesser, J.H. van der Merwe)*. 42. Microstresses and the Mechanical Properties of Crystals *(P.J. Jackson)*. 43. The Electroplastic Effect in Metals *(H. Conrad, A.F. Sprecher)*. Author Index. Subject Index. Cumulative Index.

1989 842 pages
US$ 173.75 / Dfl. 330.00
Subscr. Price: US$ 147.25 / Dfl. 280.00
ISBN 0-444-70515-5

NORTH-HOLLAND
(an imprint of Elsevier Science Publishers)

P.O. Box 103, 1000 AC Amsterdam, The Netherlands
P.O. Box 882, Madison Square, New York 10159, USA

408/B/020

SUBMISSION OF PAPERS

Three copies of **letters** or **full papers** should be sent to Editorial Office (U.K.) of Elsevier Sequoia, Mayfield House, 256 Banbury Road, Oxford OX2 7DH, Gt. Britain.

All the authors of a paper or letter should sign the covering letter.

SECTIONS

The journal is divided into the following sections.

A—Electronics and Optics: galvanomagnetic phenomena, superconductivity, electro-optics and non-linear optics, electromagnetic interactions. Fundamental studies and those related to electronic and optical devices.

B—Metallurgical and Protective Layers: preparation, erosion and wear resistance, diffusion and diffusion barriers, mechanical properties.

C—Preparation and Characterization: nucleation, growth and fabrication of condensed matter films, X-ray and electron diffraction, and electromagnetic, electron beam, ionic and electron microscope characterization.

D—Langmuir–Blodgett and Related Films: preparation methodologies, chemical, biochemical and biological properties, physical and optical properties, other characteristics and device applications.

E—Condensed Matter Film Behaviour: multidisciplinary topics not covered above or those that cannot be easily defined as falling in one category.

A pamphlet containing more detailed instructions on the preparation of manuscripts for THIN SOLID FILMS may be obtained from the publishers.

ELSEVIER SEQUOIA S.A. (1990) 0040-6090/90/$3.50

All rights reserved. No part of this publication may be reproduced, stored in a retrieval system or transmitted in any form or by any means, electronic, mechanical, photocopying, recording or otherwise, without the prior written permission of the publisher, Elsevier Sequoia S.A., P.O. Box 564, 1001 Lausanne 1, Switzerland.

Submission of an article for publication implies the transfer of the copyright from the author(s) to the publisher and entails the author(s)' irrevocable and exclusive authorization of the publisher to collect any sums or considerations for copying or reproduction payable by third parties.

Upon acceptance of an article by the journal, the author(s) will be asked to transfer copyright of the article to the publisher. This transfer will ensure the widest possible dissemination of information under the U.S. Copyright Law.

For Material Subject to U.S. Copyright Law

Special regulations for readers in the U.S.A.

This journal has been registered with the Copyright Clearance Center, Inc. Consent is given for copying of articles for personal use, or for the personal use of specific clients.

This consent is given on the condition that the copier pays through the Center the per-copy fee stated in the code on the first page of each article for copying beyond that permitted by Sections 107 or 108 of the U.S. Copyright Law. The appropriate fee should be forwarded with a copy of the first page of the article to the Copyright Clearance Center, Inc., 21 Congress Street, Salem, MA 01970. If no code appears in an article, the author has not given broad consent to copy and permission to copy must be obtained directly from the author. All articles published prior to 1982 may be copied for a per-copy fee of US$2.50, also payable through the Center. This consent does not extend to other kinds of copying, such as for general distribution, resale, advertising and promotion purposes or for creating new collective works. Special written permission must be obtained from the publisher for such copying.

No responsibility is assumed by the Publisher for any injury and/or damage to persons or property as a matter of products liability, negligence or otherwise, or from any use or operation of any methods, products, instructions or ideas contained in the material herein.

Printed in The Netherlands

CONTENTS

Cumulative Author Index for Vols. 166–178 1
Cumulative Subject Index for Vols. 166–178 13

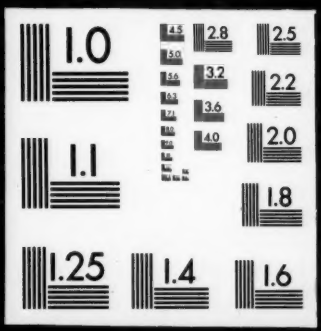
1.0
1.1
1.25
1.4
1.6
2.8
3.2
3.6
4.0
2.5
2.2
2.0
1.8